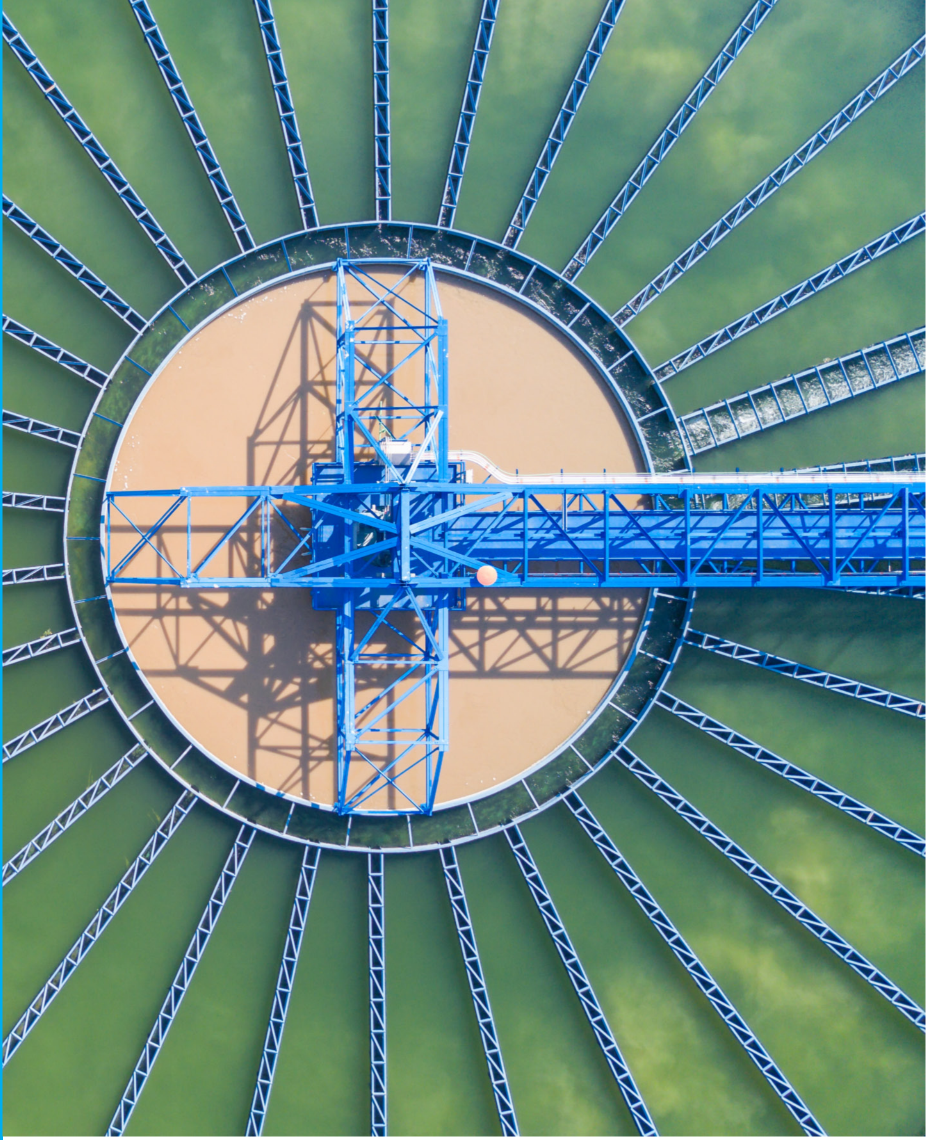

TECHNOLOGY • RESEARCH HIGHLIGHTS • VISIONS • SCIENCE •
321

Industrial and mine water chemistry

Advanced aqueous database for modelling industrial processes

Risto Pajarre | Pertti Koukkari | Petteri Kangas

VTT TECHNOLOGY 321

Industrial and mine water chemistry

Advanced aqueous database for modelling industrial processes

Risto Pajarre, Pertti Koukkari & Petteri Kangas

VTT Technical Research Centre of Finland Ltd

ISBN 978-951-38-8622-6 (Soft back ed.)
ISBN 978-951-38-8620-2 (URL: http://www.vttresearch.com/impact/publications)

VTT Technology 321

ISSN-L 2242-1211
ISSN 2242-1211 (Print)
ISSN 2242-122X (Online)
http://urn.fi/URN:ISBN:978-951-38-8620-2

JULKAISIJA – UTGIVARE – PUBLISHER

Teknologian tutkimuskeskus VTT Oy
PL 1000 (Tekniikantie 4 A, Espoo)
02044 VTT
Puh. 020 722 111, faksi 020 722 7001

Teknologiska forskningscentralen VTT Ab
PB 1000 (Teknikvägen 4 A, Esbo)
FI-02044 VTT
Tfn +358 20 722 111, telefax +358 20 722 7001

VTT Technical Research Centre of Finland Ltd
P.O. Box 1000 (Tekniikantie 4 A, Espoo)
FI-02044 VTT, Finland
Tel. +358 20 722 111, fax +358 20 722 7001

Cover image: Shutterstock

Juvenes Print, Tampere 2018

Preface

During recent decades, computational methods have been established as key design tools for accurate and secure process engineering. Finland has been one of the leading countries in applying these methods especially when tools and databases related to rigorous multi-phase chemistry are considered. Thermodynamic software created by VTT (ChemSheet) as well within industry such as Outotec (HSC) are state-of-the-art tools in the world.

One of the most interesting and challenging topics has been multi-phase chemistry of aqueous solutions. The pioneering studies in using thermodynamic software in simulation of hydrometallurgical processes was conducted by Koukkari et al. (Koukkari et al., 1994), where sulfuric acid treatments in titania pigment production and NPK fertiliser manufacturing were studied. The early work was based on critical assessment of available non-ideality data including the Bromley, Meissner, Pitzer, Chen and NRTL models. At the time, it was concluded that Pitzer formalism was the most promising to be used for further development. The chosen Pitzer technique has become perhaps the most widespread of the excess Gibbs energy (activity) formalisms used for aqueous process simulations during recent years. At VTT the development of process simulation software for aqueous process solutions commenced in 1996 and in 1998 ChemSheet software was published together with its first Pitzer non-ideality database applications focussed on redox processes that are frequently encountered both in pulp bleaching and aqueous metallurgy (Salminen et al., 2015).

The next extensive development of this aqueous Pitzer database was conducted around the year 2000 (Koukkari et al., 2001). The database was then extended with an additional aqueous phase representing the fibre within the pulp suspension (Pajarre et al., 2006). This extension was successfully utilised both for metal cation control in pulp bleaching and washing (Räsänen, 2003; Sundquist, 2016) and when the neutral conversion of paper machines was studied: calcium carbonate was introduced as filler and thus the pH of paper machine waters was elevated from the acidic region to the neutral region (Kalliola et al., 2012).

The third phase of development efforts was conducted during the years 2014-2016 within the *Handling and recycling of multicomponent process concentrates* (Multirec) project. Here the application areas were related to the process concentrates that also appear within power production as well as in mining and hydrometallurgical industries. This project also summarises the development efforts of the aqueous Pitzer database conducted over the course of two decades within VTT.

The authors would like to acknowledge Tekes – the Finnish Funding Agency for Innovation, the VTT Technical Research Centre of Finland, Outotec, Metsä Fibre, Andritz and Valmet for funding this Multirec project. In addition, the support within the expert group from Process Flow Solution, KBR Ecoplanning and Wetend Technologies is also acknowledged.

Summing up, the best process model is a successfully applied process model. The authors wish that this report and a related database would be a start-up point for many successful development efforts conducted by scholars and experts within the industry

January 2018

Risto Pajarre, Pertti Koukkari and Petteri Kangas

Contents

Appendices

Abstract

List of symbols

AMD	Acidic mine drainage
ANDRA	French National Radioactive Management Agency
a	aqueous phase
aq	aqueous phase
BAT	Best Available Technology
BET	Brunauer-Emmett-Teller adsorption model
ESP	Electro-static precipitation
g	gaseous phase
HKF	Helgeson-Kirkham-Flowers
M	cation
N	cation
NEA	Nuclear Energy Agency
NRTL	Non-random two-liquid model
OECD	Organisation for Economic Co-operation and Development
redox	Reduction–oxidation
REE	Rare Earth Element
s	Solid phase
SME	Small and medium-sized enterprises
THEREDA	Thermodynamic Reference Database
UNIQUAC	*UNI*versal *QUA*si*C*hemical
UrFU	Ural Federal University
USGS	U.S. Geological Survey

VTT	VTT Technical Research Centre of Finland
X	anion

a_i	activity
A^{ϕ}	Debye-Hückel limiting slope
$\mathbb{A}$	Affinity
c_n	Fitting parameter of BET model or HKF model
C_{Mx}	Pitzer parameter
C, C_p	Heat capacity
$C_p(T)$	Temperature-dependent heat capacity at constant pressure
d_n	Parameters of temperature dependent Pitzer parameters
${}^{E}\theta_{ij}(I)$	Function of ionic strength and the charge of the two species
EH	Reduction potential
G	Gibbs free energy
$\Delta_f G^{\circ}$	Gibbs free energy of formation
H	Enthalpy
$\Delta_f H^{\circ}$	Enthalpy of formation (at 25 °C)
I	Ionic strength of solution
K_{eq}	Solubility product
λ	Donnan distribution coefficient
n	Amount of substance
n_{ca}	Amount of salt *ca* in the liquid mixture
n_i^{α}	Amount of species *i* in phase α
N	Total amount
m_i	Molality
pH	pH-value
P	Pressure
Q	Ion activity product in the solution
r	Number f adsorption sites in a solute molecule

r_{ca}	Number of adsorption sites for each salt *ca* molecule
R	Gas constant
S	Entropy
S°	Entropy (at 25 °C)
$S_{cc'a}$/ $S_{caa'}$	Empirical parameters of BET-model
SI	Saturation index
T_{ijk}	Mixture parameter of BET-model
T	Temperature
U	Negative internal energy of monolayer adsorption
U_L	Internal energy of liquefaction
$\nu_{M(X)}$	Number of cations
V	Volume
w	Molar mass of solvent water
x_{ca}^{*}	Dry mole fraction of *ca*
x_i	Mole fraction
Y_{ca}	Amount of the solvent adsorbed onto salt ca
Y^T	Total amount of solvent
z_i	charge of solute i;
β_{MX}	Pitzer parameter
ε	Dielectric constant of water
λ_{ni}	Pitzer parameter
θ_{Ij}	Pitzer parameter
ϕ	Osmotic coefficient
Ψ_{ijk}	Pitzer parameter
μ_i^0	Standard chemical potential (molar Gibbs energy) of species *i*
μ_i^{α}	Chemical potential of species *i* in phase α
γ_i	Activity coefficient
ω	Born coefficient
ω_{MX}	Pitzer parameter (Archer modification)

1. Introduction

Industrial concentrates and mine waters are usually a complex mixture of metal ions, anions, gases and precipitates within aqueous media. Typical metals found in these waters are sodium, potassium, iron, calcium, magnesium, manganese, zinc, copper and nickel. Corresponding anions are those associated with e.g. carbon, sulfur and chlorine. In a practical (multiphase) system, the respective gaseous components will also affect the solvent-solute interactions. In industrial applications temperatures will vary, most typically from ambient 20 °C up to 95 °C in atmospheric systems. In some cases, the solutions are rather concentrated and in many cases wanted or unwanted precipitates occur. Thus these mixtures can be considered as true multi-phase chemical systems which need to be properly understood in order to design, engineer and operate these processes successfully.

Concentrates and solutions descending from industrial side streams still form a challenge for designing environmentally sustainable processes. The problem is common for many industries ranging from mining and minerals processing to chemical and forest industries. The changes in BAT requirements as well as the opportunities to develop new international Cleantech businesses increase the need to develop proactive methods for recycling chemicals and for elimination of environmental hazards. The necessary techniques frequently contain technological solutions and conditions that are very different from those in the main product line. Examples of practical industrial processes are i) handling of mine waters and neutralisation sediments, ii) recovery and recycling of chemicals within metal, chemical and forest industries, iii) scrubbing techniques of flue gasses (so called 'wet cleantech'-applications), iv) in-line precipitation and crystallisation technologies, v) new energy technologies exploiting concentrates and vi) different material recycling technologies.

Plant design by necessity includes thorough analysis of mass and energy balances, often devised for complex and multi-stage processes. The task can be supported in great detail, if appropriate data and software tools for simulation of the multiphase treatments are available. During the last few decades computational methods have been established as key design tools for accurate and secure process engineering particularly in the chemical industry. They are also used widely for analysis of alternative chemistry concepts, scale-up and for removing bottlenecks.

Yet, in other fields of process industry, the uses of computational methods for multistage process simulation has remained more limited, often covering but the bulk mass and energy balances. Within the conventional chemical industry, one most often deals with a limited number of phases which has allowed for accurate calculations by using thermodynamic equations of state in combination with mechanistic reaction rate models, other processes, such as those occurring in pulp and papermaking, hydrometallurgy and water treatment, by necessity must deal with processes that include saturated solutions, slurries and suspensions as well as brines. With such true multiphase problems, the conventional methodology used in widespread process-simulating software has been rendered somewhat insufficient, and techniques allowing for multiphase and multicomponent analysis are needed.

Thermodynamic simulation has thus become a tool of great importance in the development of aqueous multi-phase systems. Advanced computational techniques can be used for balance and speciation analysis including design and control of existing processes as well as for the generation of new chemistry concepts. Thermodynamic models can accurately describe the behaviour of aqueous solutions over wide ranges of temperature, pressure, and concentration. With improving heat capacity and activity data, they may also predict the solution properties up to saturation levels in the varying conditions.

In order to describe the interaction between different cations, anions and neutral species within the aqueous media, an activity model is required. Within this study, the so called Pitzer formalism for solute interactions is utilised. The Pitzer technique is perhaps the most widespread of the activity formalisms used for aqueous process simulations and has been widely adapted, e.g., for academic geochemical studies. In this report, such data has been assessed for the key solute species present in typical industrial concentrates in the aforementioned conditions of moderately elevated temperatures (up to 100 °C at atmospheric conditions).

Chapters 2 and 3 of this booklet give a short introduction to the chemical system and the calculation of thermodynamic equilibrium by utilising the Gibbs' free energy method. The Pitzer formalism and some additional amendments are described in Chapter 4. Chapter 5 introduces an optional adsorption (BET) model which is one possible solution for describing activities in very concentrated solutions where the Pitzer parameters are not applicable anymore. Other possible ways for modelling concentrated solutions are listed in Chapter 6. Practical ways of extrapolating data are described in Chapter 7 and references to thermodynamic data sources and databanks are listed in Chapter 8. Cases where sufficient thermodynamic data is not available are discussed in Chapter 9. Selected thermodynamic data with Pitzer parameters is described in Chapter 10 and validation of the assessed data is conducted in Chapter 11. Some special cases related to over- and undersaturated systems are listed in Chapter 12 as well as discussion of Redox potential is given in Chapter 13. Ion exchange phenomena is reviewed in Chapter 14. Practical application examples within the process industry are given in Chapter 15. Finally, the results are concluded in Chapter 16. The appendices list the database parameters and illustrate additional aspects related to the topics studied.

The results reported in this document can be utilised by the academia, process industries, technology companies and their SME subcontractors. As shown in some of the examples, the adaptation of advanced thermodynamic techniques can lead to ground breaking new solutions both in process technologies and their related services.

2. Description of the applied chemical system

In the models of this work, the chemical systems are described by means of chemical thermodynamics. The systems are divided into phases and their constituent species. Phases may either be mixtures of multiple species (gas phase, aqueous phase and solid mixture phases) or pure phases of stoichiometric invariant composition (Solids of fixed composition such as $Ca_2SO_4*2H_2O$). Stoichiometry of each invariant phase and species in a mixture phase are defined in terms of chemical system components, typically elements such as C, H, N and O, or electronic charge, but it is also possible for set components to be stoichiometric combinations of elements. The gaseous phase in the models is generally assumed to be an ideal mixture, while the species in the aqueous phase and solid mixture are affected by composition and temperature-dependent interaction energies. Each species and phase is characterised by its amount expressed by molar or mass units as well as by its thermodynamic properties (activities, chemical potentials, enthalpies, volumes, etc.) dependent on the system temperature, pressure and for mixture phases on system composition, i.e., the interaction between the phase constituents.

3. Equilibrium calculation using Gibbs energy minimisation

The thermodynamic models have been applied using the Chemsheet program (Koukkari et al., 2005), and the data has been collected in the compatible ChemApp/ChemSage (Petersen and Hack, 2007) format. With ChemSheet, the chemical reactions taking place in multiphase systems are calculated with the Gibbs energy minimisation method. As a result of minimisation, the equilibrium composition of the system is obtained. The method requires that temperature, pressure and initial composition (initial amounts of species as listed in Table 2) are known and given as input parameters. Temperature or pressure inputs can be replaced by given constraints on volume or enthalpy.

The Gibbs energy minimisation method does not entail assumptions of exact reaction paths between the chemical species. The chemical species are yet linked together by their elemental composition, i.e., the components they are composed of. The equilibrium concentrations are obtained as the composition that gives the minimum Gibbs energy without violating the elementary mass balances (mole number of each component in equilibrium composition must be the same as it was in its initial composition). Thus the equilibrium calculation corresponds to the mathematical problem of finding the global minimum of the constrained free energy function.

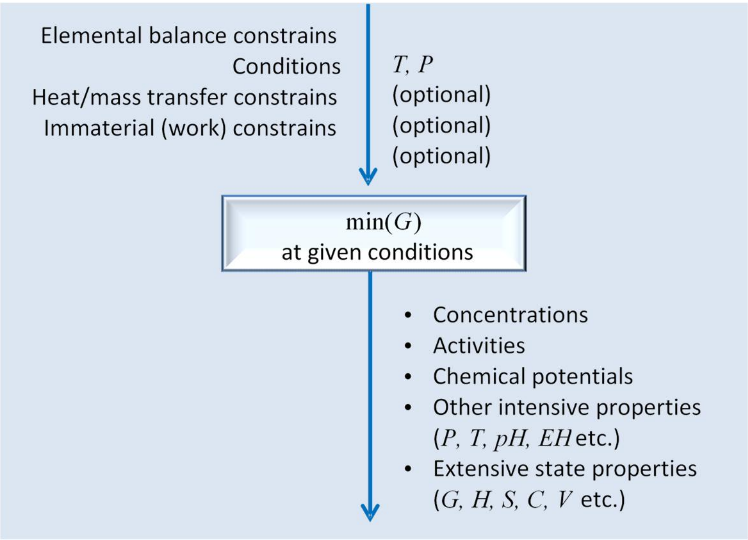

Figure 1. A block diagram for the Gibbs'ian thermochemical method. With the Gibbs energy simulation, all the thermodynamic state quantities can be systematically derived from the fundamental relations.

The Gibbs energy is a function of temperature, pressure and composition. Gibbs energy for a multiphase system can be given as:

$$G = \sum_{\alpha}\sum_{i} n_i^{\alpha}\mu_i^{\alpha} \qquad (1)$$

where n_i^{α} is the amount of species *i* in phase α and μ_i^{α} is its chemical potential. The chemical potential can be separated into ideal and non-ideal terms:

$$\mu_i = \mu_i^0 + RTlna_i = \mu_i^0 + RTln(\gamma_i x_i) \qquad (2)$$

where μ_i^0 is the standard chemical potential (molar Gibbs energy) of species *i,* R is the gas constant, T is the temperature, a_i, γ_i and x_i are the activity, activity coefficient and mole fraction of species *i*. For aqueous solutions instead of a mole fraction-based scale, a molality-based scale is typically used:

$$\mu_i = \mu_i^0 + RTlna_i = \mu_i^0 + RTln(\gamma_i m_i) \qquad (3)$$

where m_i is the molality of the species in question.

In this work, the standard chemical potential is calculated and tabulated via expression of enthalpy of formation at 25 °C ($\Delta_f H^{\circ}$), temperature-dependent heat capacity at constant pressure ($C_p(T)$), and entropy at 25 °C (S°). The heat capacity is collected to fit the form of function

$$C_p = a + bT + cT^2 + d/T^2 \qquad (4)$$

ChemApp also enables entering the needed thermodynamic data in the form of Gibbs energy function

$$\Delta_f G_i^{\circ} = \mu_i^0 = A + BT + CTlnT + DT^2 + ET^3 + F/T \qquad (5)$$

It should be noted though that when using enthalpy, entropy, heat capacity formalism, the molar Gibbs energy function is calculated by the program as

$$G = H - ST \qquad (6)$$

where H and S are the given enthalpy and entropy values in the data file. When the previously mentioned values $\Delta_f H^{\circ}$and S°used the resulting value is

$$G = \Delta_f H^{\circ} - S^{\circ}T \qquad (7)$$

which differs from the most commonly tabulated Gibbs free energy of formation value $\Delta_f G^{\circ}$ by

$$\Delta_f G^{\circ} - \left(\Delta_f H^{\circ} - S^{\circ}T\right) = (S^{\circ} - \Delta_f S^{\circ})T \qquad (8)$$

The term in brackets in equation (8) equals the sum elemental entropies of the species. It is a temperature invariant constant dependent only on the stoichiometry of the species. Calculated equilibrium compositions are not affected as long as the same convention is used for all species in the system, but care should be taken when combining data from different data sources with different data formats.

The applied Gibbs energy minimisation routines allow a number of ways for the user to describe the non-ideality of the mixture phase, generally in terms of the excess Gibbs energies. The number of excess energy models included in ChemApp is extensive (Eriksson and Königsberger, 2008) and is continuously being updated. The applicability of chemical equilibrium solvers for various environmental problems is wide. In particular, speciation models for aquatic geochemical systems, calculation of solubilities of gases and minerals, analysis of the effect of pH on the dissolution of a mineral, investigation of water-gas-rock effects during carbon storage in geological formations, and radioactive waste disposal modelling are all examples of problems that may benefit form multicomponent equilibrium calculations. For such purposes, a large amount of multicomponent software as well as extensive databases has been developed. Among the more commonly used software are the following:

- HSC (Outotec, 2015)
- PhreeqC [US Geological Survey] (Parkhurst and Appelo, 2013)
- EQ3/EQ6 [Lawrence Livermore National laboratory] (Wolery, 1992, 1994; Wolery and Daveler, 1992)
- Factsage/ChemApp/ChemSheet product family [GTT technologies and CRCT] (Bale et al., 2002, 2009; Koukkari et al., 2005; Petersen and Hack, 2007)
- Minteq [originally US Environmental Protection Agency] (Allison et al., 1991; HydroGeoLogic Inc and Allison Geoscience Consultants Inc., 1998; VISUAL MINTEQ, 2013)
- Geochemists workbench [originally University of Illinois, now Aqueous Solutions LLC] (Aqueous Solutions LLC, 2015; Bethke and Yeakel, 2015)
- CHESS [Chemical Equilibrium of Species and Surfaces, MINES ParisTech] (van der Lee and DeWindt, 2002; CHESS, 2015)
- GEMS [Paul Scherrer Institut] (Kulik et al., 2013; Gems Development Team, 2015)
- WATEQ4F [US Geological Survey] (Ball and Nordstrom, 1991)
- MINEQL + (currently Enviromental Research Software)(Environmental Research Software, 2015)
- JESS (Joint Expert Speciation System, Murdoc University) (Joint Expert Speciation System, 2015; May, 2015)
- OLI Studio (OLI Systems Inc, 2015)
- HCh(Shvarov, 2008)

4. Pitzer equations

4.1 Original model

The activity coefficient of a species is typically a function of temperature and phase composition. Aqueous solutions are typically strongly non-ideal and realistic calculations of solution equilibrium necessitating the modelling of excess thermodynamic properties of the system as a function of solution composition within the temperature range of operation.

In an aqueous solution, the activity coefficients (using a molality-based scale) can be estimated using the ion interaction model of Pitzer. A fairly generalised version of the equation, compatible with many of the extensions, is given below (Clegg et al., 1994)

$$\begin{aligned} ln\gamma_M &= z_M^2 F + \sum_{a=1}^{N_a} m_a(2B_{Ma} + ZC_{Ma}^T) + \sum_{c=1}^{N_c} m_c \left(2\Phi_{Mc} + \sum_{a=1}^{N_a} m_a \Psi_{Mca} \right) \\ &+ \sum_{a=1}^{N_a-1} \sum_{a'=a+1}^{N_a} m_a m_{a'} \Psi_{aa'M} + |z_M| \sum_{c=1}^{N_c} \sum_{a=1}^{N_a} m_c m_a C_{ca} + \sum_{n=1}^{N_n} m_n \, (2\lambda_{\mathrm{nM}}) \end{aligned} \tag{9}$$

$$\begin{aligned} ln\gamma_X &= z_X^2 F + \sum_{c=1}^{N_c} m_c(2B_{cX} + ZC_{cX}^T) + \sum_{a=1}^{N_a} m_a \left(2\Phi_{Xa} + \sum_{c=1}^{N_a} m_c \Psi_{Xac} \right) \\ &+ \sum_{c=1}^{N_c-1} \sum_{c'=c+1}^{N_c} m_c m_{c'} \Psi_{cc'X} + |z_X| \sum_{c=1}^{N_c} \sum_{a=1}^{N_a} m_c m_a C_{ca} + \sum_{n=1}^{N_n} m_n \, (2\lambda_{\mathrm{nX}}) \end{aligned} \tag{10}$$

and

$$ln\gamma_N = \sum_{c=1}^{N_c} m_c(2\lambda_{nc}) + \sum_{a=1}^{N_a} m_a(2\lambda_{na}) \tag{11}$$

while the activity of the water, expressed by osmotic coefficient ϕ , is obtained as

$$\begin{aligned}\sum_i m_i(\phi - 1) = 2\Bigg(&-A^{\phi} I^{3/2}/\left(1 + 1.2I^{1/2}\right) + \sum_{c=1}^{N_c}\sum_{a=1}^{N_a} m_c m_a \left(B_{ca} + ZC_{ca}^{T\phi}\right) \\ &+ \sum_{c=1}^{N_c-1}\sum_{c'=c+1}^{N_c} m_c m_{c'} \left(\Phi_{cc'}^{\phi} + \sum_{a=1}^{N_a} m_a \Psi_{cc'a}\right) \\ &+ \sum_{a=1}^{N_a-1}\sum_{a'=a+1}^{N_a} m_a m_{a'} \left(\Phi_{aa'}^{\phi} + \sum_{c=1}^{N_c} m_c \Psi_{aa'c}\right) \\ &+ \sum_{n=1}^{N_n}\sum_{a=1}^{N_a} m_n m_a \lambda_{na} + \sum_{n=1}^{N_n}\sum_{c=1}^{N_c} m_n m_c \lambda_{nc}\Bigg)\end{aligned} \tag{12}$$

where

$$\begin{aligned}F = -A^{\phi}\left(\frac{I^{1/2}}{(1 + 1.2I^{1/2})} + \frac{2}{1.2}\ln\left(1 + 1.2I^{1/2}\right)\right) \\ + \sum_{c=1}^{N_c}\sum_{a=1}^{N_a} m_c m_a \left(B'_{ca} + \tfrac{1}{2}ZC_{MX}^{T'}\right) + \sum_{c=1}^{N_c-1}\sum_{c'=c+1}^{N_c} m_c m_{c'} \Phi'_{cc'} \\ + \sum_{a=1}^{N_a-1}\sum_{c'=a+1}^{N_a} m_a m_{a'} \Phi'_{aa'} + \sum_{c=1}^{N_c-1}\sum_{c'=c+1}^{N_c} m_c m_{c'} \Phi'_{cc'} \\ + \sum_{a=1}^{N_a-1}\sum_{c'=a+1}^{N_a} m_a m_{a'} \Phi'_{aa'} + \sum_{c=1}^{N_c-1}\sum_{c'=c+1}^{N_c} m_c m_{c'} \Phi'_{cc'} \\ + \sum_{a=1}^{N_a-1}\sum_{c'=a+1}^{N_a} m_a m_{a'} \Phi'_{aa'}\end{aligned} \tag{13}$$

$$Z = \sum_i |z_i| m_i \tag{14}$$

$$B_{MX} = \beta_{MX}^{(0)} + \beta_{MX}^{(1)} g\left(\alpha_{MX}^{(1)}\sqrt{I}\right) + \beta_{MX}^{(2)} g\left(\alpha_{MX}^{(2)}\sqrt{I}\right) \tag{15}$$

$$B'_{MX} = \beta_{MX}^{(1)} g'\left(\alpha_{MX}^{(1)}\sqrt{I}\right)/I + \beta_{MX}^{(2)} g'\left(\alpha_{MX}^{(2)}\sqrt{I}\right)/I \tag{16}$$

$$B_{MX}^{\phi} = \beta_{MX}^{(0)} + \beta_{MX}^{(1)} e^{-\alpha_{MX}^{(1)}\sqrt{I}} + \beta_{MX}^{(2)} e^{-\alpha_{MX}^{(2)}\sqrt{I}} \tag{17}$$

$$C_{MX}^{T} = C_{MX}^{(0)} + 4C_{MX}^{(1)} h\left(\omega_{MX}\sqrt{I}\right) \tag{18}$$

$$C_{MX}^{T'} = 4C_{MX}^{(1)} \frac{h'\left(\omega_{MX}\sqrt{I}\right)}{I} \tag{19}$$

$$C_{MX}^{T\phi} = C_{MX}^{(o)} + C_{MX}^{(1)} \exp\left(-\omega_{MX}\sqrt{I}\right) \tag{20}$$

$$g(x) = 2(1 - (1 + x)e^{-x})/x^2 \tag{21}$$

$$g'(x) = -2\left(1 - \left(1 + x + \frac{x^2}{2}\right) e^{-x}\right)/x^2 \tag{22}$$

$$h(x) = \{6 - [6 + x(6 + 3x + x^2)] \exp(-x)\}/x^4 \tag{23}$$

$$h'(x) = \exp(-x)/2 - 2h(x) \tag{24}$$

$$\Phi_{ij}^{\phi} = \theta_{ij} + {}^{E}\theta_{ij}(I) + I\,{}^{E}\theta'_{ij}(I) \tag{25}$$

$$\Phi_{ij} = \theta_{ij} + {}^{E}\theta_{ij}(I) \tag{26}$$

and

$$\Phi'_{ij} = {}^{E}\theta'_{ij}(I) \tag{27}$$

where

$C_{Mx}^{(0)}$, $C_{Mx}^{(1)}$, $\beta_{MX}^{(0)}$, $\beta_{MX}^{(1)}$, $\beta_{MX}^{(2)}$, θ_{Ij}, Ψ_{ijk} and λ_{ni} are model parameters, which may be temperature dependent, fitted to experimental data
m_i is the molality;
z_i is the charge of solute i;
I is the ionic strength of solution;
A^{ϕ} (≈ 0.39 at 298K) is the Debye-Hückel limiting slope; and
${}^{E}\theta_{ij}(I)$ is a function of ionic strength of the solution and the charge of the two species in question (details given, e.g., by Pitzer (1995)).

In the most commonly used formulation by Harvie et al, (Harvie et al., 1984), the parameter $C_{Mx}^{(1)}$ is omitted (assumed to be zero). Parameter $\alpha_{MX}^{(1)}$ is set to 2.0 if at least one of the ions in the interacting pair are univalent, and to a value of 1.4 otherwise, while $\alpha_{MX}^{(2)}$ has a value of 12.0 for cation-anion pairs. The C_{MX}^{T} parameter is then often tabulated as

$$C_{MX}^{T} \equiv C_{MX}^{(0)} \equiv C_{MX} = C^{\phi} / \left(2\sqrt{|z_M z_X|}\right) \tag{28}$$

Pitzer's equation for the aqueous phase is a virial coefficient expansion of Debye–Hückel's theory and is capable of describing the ionic activities of aqueous species in concentrated solutions, usually up to a strength of 6 M. The use of Pitzer's equation is restricted by the amount of existing data in the solutions. For interactions that no parameters are known or cannot be fitted, the missing values are usually assumed to equal zero and the model reduces to a Davies equation like non-ion specific electrostatic description, valid for solutions $\lesssim$ 0.1 M.

Table 1 shows an example thermodynamic system that has been used and validated in multicomponent equilibrium calculations. It contains a gas phase that uses ideal mixing or Tsonopoulos model for non-ideal gas (for high pressure conditions if required), an aqueous water phase that uses the Pitzer electrolyte model, and pure solid phases that are mainly used to input various acidic and basic salts and oxides into solution pools.

Table 1. Example thermodynamic system.

Phase	Constituent	Element													
		B	C	Cl	Cs	H	I	Li	N	Na	O	P	e-	H2O	HNO3
Gas	H2O(g)					2					1			1	
	N2(g)								2						
	O2(g)										2				
	H2(g)					2									
	CO(g)		1								1				
	CO2(g)		1								2				
	CH4(g)		1			4									
	HI(g)					1	1								
	I2(g)						2								
	HCl(g)			1		1									
	HNO3(g)					1			1		3				1
	CsI(g)				1		1								
	CsOH(g)				1	1					1				
	H3BO3(g)	1				3					3				
Water	H2O(a)					2					1				
	B(OH)3(a)	1				3					3				
	B(OH)4(-a)	1				4					4		1		
	Cl(-a)			1									1		
	Cs(+a)				1								-1		
	CsOH(a)				1	1					1				
	H(+a)					1							-1		
	I(-a)						1						1		
	I2(a)						2								
	Na(+a)									1			-1		
	OH(-a)					1					1		1		
	N2(a)								2						
	HNO3(a)					1			1		3				1
	NH3(a)					3			1						
	NH4(+a)					4			1				-1		
	NO2(-a)								1		2		1		1
	NO3(-a)								1		3		1		1
	H2PO4(-a)					2					4	1	1		
	HPO4(-2a)					1					4	1	2		
	PO4(-3a)										4	1	3		
	H3PO4(a)					3					4	1			
	CO2(a)		1								2				
	CO3(-2a)		1								3		2		
	HCO2(-a)		1			1					2		1		
	HCO3(-a)		1			1					3		1		
	NaCO3(-a)		1							1	3		1		
	Li(-a)							1					1		
Solids	CsI(s)				1		1								
	CsOH(s)				1	1					1				
	H3BO3(s)	1				3					3				
	LiCl(s)			1				1							
	LiOH(s)					1		1			1				
	Na2O*2B2O3*10H2O(s)	2				20				2	17				
	Na2O*5B2O3*10H2O(s)	5				20				2	26				
	NaCl(s)			1					1	1					
	NaOH(s)					1			1	1	1				
	Na3PO4(s)									3	4	1			
	Na2HPO4(s)					1				2	4	1			
	NaH2PO4(s)					2			1	1	4	1			
	HCl(s)			1		1									
	HNO3(s)					1			1		3				
Constraints	H2O(g)+													1	
	H2O(g)-													-1	

As an example case, the modelled and experimental osmotic coefficients of aqueous NaOH solution are shown in Figure 2. The osmotic coefficient is plotted as a function of the square root of molality. On the left side, the experimental data (Hamer and Wu, 1972) extends to 29 mol/kg, while on the right side only the concentration range up to 1 mol/kg is shown. The exact values and parameter fits are specific to each individual system, but schematically the results are similar for other salts soluble up to sufficiently high concentrations. In addition to a regular Pitzer parameter fit of the system, also the model curves with $\beta_{MX}^{(0)}$, $\beta_{MX}^{(1)}$ and C^{ϕ} have either half or double their regular values shown. $\beta_{MX}^{(2)}$ parameter is not normally used for 1:1 electrolytes, but the effect of its inclusion are shown for values -10 and 10. Also shown are the results using an unparametrised Pitzer model (all ion interaction parameters set to zero) and the Debye–Hückel limiting law. The second virial coefficient-based term $\beta_{MX}^{(0)}$ effects the results in all concentrations, while the exponentials in equation (17) make parameters $\beta_{MX}^{(1)}$ and $\beta_{MX}^{(2)}$ significant only at moderately low concentrations. The third virial coefficient related term C^{ϕ} becomes more important only at higher concentrations. The experimental on modelled values start to deviate when molality increases above 6 mol/kg and the correspondence between the two gets rapidly worse with concentrations above 10 mol/kg.

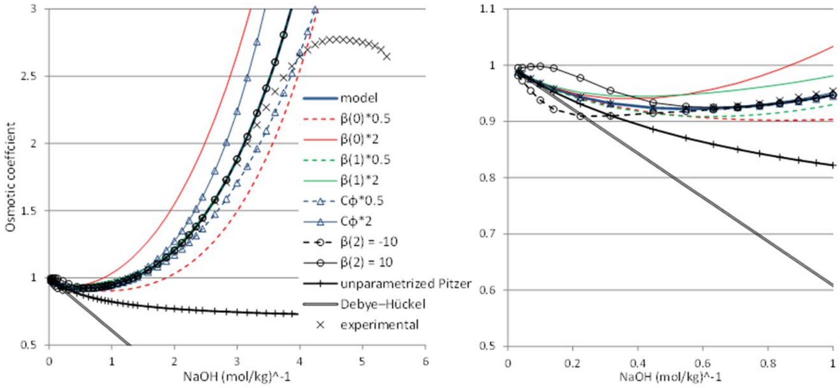

Figure 2. The osmotic coefficient in NaOH as a function of the square root of molality at 25 °C. The effect of various model parameters is shown.

4.2 Archer modification

The validity of the Pitzer model (with parameters fitted to experimental data of the relevant binary and ternary systems typically extends typically to molalities of approximately 6 mol/kg. Various modifications to the Pitzer model have been proposed that offer to extend the validity range of the model or improve it in cases where the fit between the parametrised model and the experimental results has been found not completely satisfactory even with concentrations below 6. Not all of the proposed extensions are mutually compatible.

In the modification proposed by Archer (D. G. Archer, 1991; Clegg et al., 1994) an ionic strength dependence is included with the third virial coefficient C by applying both $C^{(0)}$ and $C^{(1)}$ parameters. Also, a (possibly charge-dependent) value for the ω_{MX} parameter needs to be chosen (often 2.5). Example systems where work has been published with the Archer modification applied include the following:

- NaBr up to 9.5 mol/kg when ω_{MX} = 1.7 (Rard and Archer, 1995)
- NaCl up to 11 mol/kg with ω_{MX} = 2.5 (Archer, 1992)
- H_2SO_4, up to 6.1 mol/kg with ω_{MX} = 2.5 (Clegg et al., 1994)
- (NH4)2SO4 up to 7.5 mol/kg with ω_{MX} = 2.5 (Clegg et al., 1996)
- Sea water / ammonia with ω_{MX} = 2.5 (Clegg and Whitfield, 1995)

4.3 Non-standard values of α_{MX} parameters

Another fairly often applied modification is to change the ion strength dependency of the virial parameter B by applying values for the exponential parameter $\alpha_{MX}^{(1)}$ and/or $\alpha_{MX}^{(2)}$ that differ from the most commonly used ones. This feature has also been implemented (for interaction-specific but fixed $\alpha_{MX}^{(1)}$ and $\alpha_{MX}^{(2)}$ values) in the ChemApp thermodynamic code and used in the THEREDA database (AF Colenco et al., 2011). Other published evaluations using non-standard α_{MX} parameters have been made for, e.g.,

- $CuCl_2$ where $\alpha_{MX}^{(2)}$= 1, (Christov, 1994)
- $MnCl_2$, $CoCl_2$, $NiCl_2$ with $\alpha_{MX}^{(2)}$=-1 (Christov, 1994)
- Na_2SO_4 with $\alpha_{MX}^{(1)}$=1.7 (Hovey et al., 1993), with $\alpha_{MX}^{(1)}$=1.4 (Holmes and Mesmer, 1986)
- $Ca(B(OH)_4)_2$ and $Mg(B(OH)_4)_2$ with $\alpha_{MX}^{(2)}$ = 6 (Simonson et al., 1988)
- $Ca_3(Fe(CN)_6)_2$, $Ba_3(Fe(CN)_6)_2$, $La_2(SO_4)_3$, $Mg_2Fe(CN)_6$, $Ca_2Fe(CN)_6$ and $Sr_2Fe(CN)_6$ with $\alpha_{MX}^{(2)}$= 50 (Pitzer and Silvester, 1978)

Temperature-dependent α_{MX} parameter values have been applied for

- $MgSO_4$ with $\alpha_{MX}^{(2)}$ being proportional to A^{Φ} (Phutela and Pitzer, 1986)
- $CaCl_2$ (Holmes et al., 1994)

4.4 Modified molality scale

In the model presented by, e.g., Sippola (2012, 2015), the original on-molality-scale-presented Pitzer equations are transformed into what are then called ‘modified’ or ‘reduced’ molalities, which are effectively based on mole fractions, scaled so that they coincide with a molality scale at low concentrations. The reduced molalities and ionic strengths are defined by

$$m_i^r = \frac{n_i}{M_w \sum_j n_j} \tag{29}$$

where the summation goes over all solution species, including the solvent, and

$$I_r = \frac{1}{2}\sum_i m_i^r z_i^2 \tag{30}$$

The expressions for osmotic coefficients and activities are

$$\begin{aligned}
\sum_i m_r\left(\phi - \sqrt{x(H_{2O})}\right) \\
&= 2\left(-A^{\phi} I^{3/2}/\left(1 + 1.2I^{1/2}\right)\right. \\
&+ \sum_{c=1}^{N_c}\sum_{a=1}^{N_a} m_c^r m_a^r\left(B_{ca} + ZC_{ca}^{T\phi}\right) \\
&+ \sum_{c=1}^{N_c-1}\sum_{c'=c+1}^{N_c} m_c^r m_{c'}^r\left(\Phi_{cc'}^{\phi} + \sum_{a=1}^{N_a} m_a \Psi_{cc'a}\right) \\
&+ \sum_{a=1}^{N_a-1}\sum_{a'=a+1}^{N_a} m_a^r\, m_{a'}^r\left(\Phi_{aa'}^{\phi} + \sum_{c=1}^{N_c} m_c^r \Psi_{aa'c}\right) \\
&\left.+ \sum_{n=1}^{N_n}\sum_{a=1}^{N_a} m_n^r m_a^r \lambda_{na} + \sum_{n=1}^{N_n}\sum_{c=1}^{N_c} m_n^r m_c^r \lambda_{nc}\right)
\end{aligned} \tag{31}$$

$$\begin{aligned}
ln\gamma_M = z_M^2 F + \sum_{a=1}^{N_a} m_a^r(2B_{Ma} + ZC_{Ma}^T) + \sum_{c=1}^{N_c} m_c^r\left(2\Phi_{Mc} + \sum_{a=1}^{N_a} m_a^r \Psi_{Mca}\right) \\
+ \sum_{a=1}^{N_a-1}\sum_{a'=a+1}^{N_a} m_a^r m_{a'}^r \Psi_{aa'M} + |z_M|\sum_{c=1}^{N_c}\sum_{a=1}^{N_a} m_c^r m_a^r C_{ca} + \sum_{n=1}^{N_n} m_n^r(2\lambda_{\mathrm{nM}})
\end{aligned} \tag{32}$$

and

$$\begin{aligned}
ln\gamma_X = z_X^2 F + \sum_{c=1}^{N_c} m_c^r(2B_{cX} + ZC_{cX}^T) + \sum_{a=1}^{N_a} m_a^r\left(2\Phi_{Xa} + \sum_{c=1}^{N_c} m_c^r \Psi_{Xac}\right) \\
+ \sum_{c=1}^{N_c-1}\sum_{c'=c+1}^{N_c} m_c^r m_{c'}^r \Psi_{cc'X} + |z_X|\sum_{c=1}^{N_c}\sum_{a=1}^{N_a} m_c^r m_a^r C_{ca} + \sum_{n=1}^{N_n} m_n^r(2\lambda_{\mathrm{nX}})
\end{aligned} \tag{33}$$

The osmotic coefficient in equation (31) is defined in normal fashion by the equation

$$\phi = -ln a_{H_2O} \frac{1}{w \sum_i m_i} \tag{34}$$

where w is the molar mass of solvent water (0.01801528 kg/mol) and summation goes over all regular (non-reduced) solute molalities, while the other terms in equations (31)-(33) follow those given earlier in equations (9)-(27), except that all the molalities and ionic strengths in them are replaced by the corresponding reduced values.

As a part of this work, the application of a model based on a reduced molality scale was also considered. For any benefit, the modified Pitzer equations should be refitted directly to experimental data. The advantage from using a scale where the concentration variable does not approach infinity with highly concentrated solutions (as it does with the regular molality scale) seems intuitive. However, calculation tests done during this work indicated, that no direct better extrapolation to higher molalities of the earlier thermodynamic parameters is achieved by adapting the new scale. The typical behaviour of the osmotic coefficient over wide concentration range (experimental versus one obtained from a regular Pitzer model with fitted parameters) is as shown in Figure 3. In the reduced scale, the right end of the sigmoid curve is further compressed, making better direct extrapolativity of the relatively straight section of the model curve unlikely.

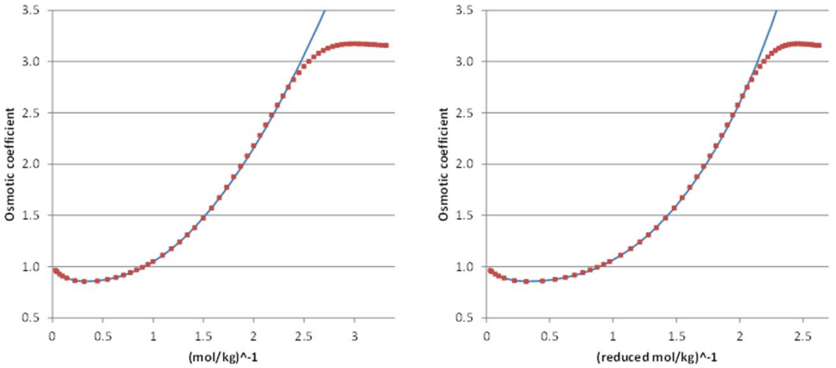

Figure 3. The osmotic coefficient of $CaCl_2$ solution at 25 °C. Experimental data from Rard and Clegg (1997). Model parameters as applied in this work. On the left side, the regular molaity scale is used, on the right side, the reduced molalites of Sippola (2015).

4.5 Additional complexes

In most Pitzer equation applications, the non-idealities of the aqueous solution are modelled with few if any explicit complex species. For example, in the work of Harvie et al. (1984) for the Na-K-Mg-Ca-H-Cl-SO_4-OH-CO_3-CO_3-CO_2 –system, the only associated aqueous species are HCO_3(-aq), HSO_4(-aq), MgOH(-), $CaCO_3$(aq) and $MgCO_3$(aq). Inclusion of complex species would enable calculations at higher concentrations, but adds many additional fitting parameters to the data assessment. A model for aqueous $CaCl_2$ system up to the saturation level has been published by Sterner et al. (1998) by applying CaCl(+aq) and $CaCl_2$(aq) complexes and extending to the solubility limit within a wide temperature range (Figure 4).

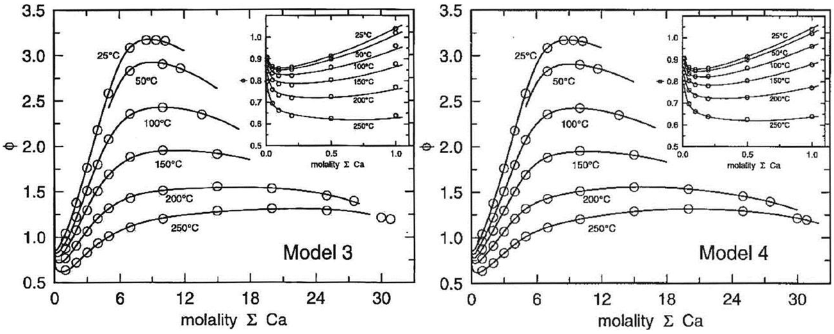

Figure 4. Osmotic coefficient in the $CaCl_2$ solution as a function of molality and temperature. Experimental data points compared to the Pitzer model with complex species by the Sterner et al. model (at left, “Model 3”) with interaction energy equations as presented by Harvie et al. (1984). The model on the right (“Model 4”) with the extended interaction energy equations by Archer (1991). While the match with experiments is excellent with both models, the one with the original interaction energy equations may predict a second, false, free energy minimum at very high concentrations that the Archer modification avoids. Figure from the work by Sterner et al. (1998).

While the obtained match between model and experiments is excellent, the number of additional fitted parameters is large (two equilibrium coefficients and four interaction parameters with CaCl(-aq) and $CaCl_2$(aq) species. Additional complexes at least potentially interfere with other equilibria with Ca(+2aq) and Cl(aq) ions in a multicomponent system. Because of an error in how self-interactions of neutral species in the Pitzer model are handled in ChemApp, the test implementation of the model could not be properly carried out during this work.

5. Brunauer-Emmett-Teller (BET) adsorption model for highly concentrated solutions

Stokes and Robinson (1948) first proposed the use of the Brunauer-Emmett-Teller (BET) adsorption isotherm for representing the water activities of very concentrated salt solutions, and demonstrated its application to a series of pure electrolytes. The basic model equation for a pure salt solution is given by

$$\frac{m_i a_{H_2O}}{55.51\left(1-a_{H_2O}\right)} = \frac{1}{cr} + \frac{c-1}{cr} a_{H_2O} \tag{35}$$

where formally

$$c = \exp(-\epsilon / RT) \tag{36}$$

and

$$\epsilon = U - U_L \tag{37}$$

with U being the negative internal energy of monolayer adsorption of water onto the solute and U_L the internal energy of liquefaction of pure water and r is the number f adsorption sites in a solute molecule, though in practice both c and r are considered adjustable fitting parameters. According to equation (35), the quantity $m_i a_{H_2O} / \left(55.51\left(1-a_{H_2O}\right)\right)$ should be linear function of a_{H_2O}. This is typically the case for water activities below about 0.3 (Stokes and Robinson, 1948; Ally, 1999) or molalities above about 10 M (Ally and Braunstein, 1996).

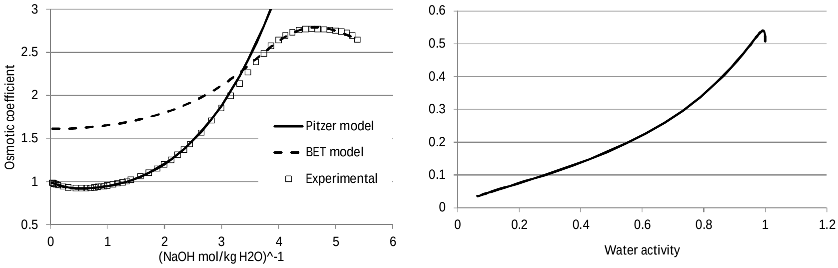

Figure 5. Example of an osmotic coefficient of a highly soluble salt (NaOH) over a wide concentration range. On the left side, the osmotic coefficient is shown as a function of the square root of molality. The Pitzer model works well with dilute and moderately concentrated solutions, while the BET model works well with highly concentrated solutions. On the right side, the expression from the left hand equation (35) is plotted as a function of experimental water activity. The BET model is valid in the linear range. Water activity of 0.3 corresponds approximately to a molality of 13 (square root 3.7) mol/kg, and an activity of 0.5 to molality of 10 mol/kg.

Later the BET equation has been extended to common-ion mixtures with a mixing rule (Sangster et al., 1978) and expressions for salt activities have been determined

(Abraham, 1981; Voigt, 1993). The model has also been applied for calculating molar enthalpies and volumes (Ally and Braunstein, 1993). Ally and Braunstein (1998) have determined that the BET expressions for solvent and salt activities in a two-salt single-solvent system by using statistical mechanics. The parameters r and c have accordingly been extended for the more complex systems, yet with basic notation following the original approach of Stokes and Robinson.

For practical applications, it is desirable to be able to calculate activities of arbitrarily complex mixtures containing many ionic solutes. Such an extension for the BET-model was presented by Clegg and Simonson (2001) and their representation for ternary interactions is reviewed in this report. They derived equations for ionic and solvent activities in a single-solvent, multi-ion mixture based on the Gibbs free energy of the mixed solution model formerly derived by Ally and Braunstein (1998). The equations were extended to include ternary (three-ion) mixture effects, and were used to model salt solubilities in one ternary aqueous mixture and water activities in common ion and reciprocal salt systems. As the results further show fairly good agreement with experimental data, particularly in high ionic strengths, their approach was documented in this work as one key option for modelling such solution conditions.

Using the adsorption model approach, the Gibbs energy (G) containing arbitrary numbers of cations (c) and anions (a) is written by Clegg and Simonson (2001) as follows:

$$\frac{G}{RT} = \sum_{c}\sum_{a} n_{ca}\left[\ln x^{*}_{ca} + r_{ca}\ln\left(1 - Y_{ca}/(r_{ca}n_{ca})\right)\right] + Y^{T}\ln\left(1 - \sum_{c}\sum_{a} {}^{Y_{ca}}\!/_{Y^{T}}\right) \tag{38}$$

where

Y^T is the total amount of solvent (mol)
Y_{ca} the amount of the solvent adsorbed onto salt *ca* (mol)
n_{ca} the amount of salt *ca* in the liquid mixture (mol)
x^*_{ca} the dry mole fraction of *ca* (amount of salt ca divided by the total amount of all salts in the mixture)
r_{ca} model parameter, describing the number of adsorption sites for each salt *ca* molecule

For complex solutions, at least three-ion interactions should be included and thus the adsorption site parameter has been extended by using the interaction parameters *cc'a* and *caa'*, yielding

$$r_{ca} = r^{0}_{ca} + \frac{1}{2}\sum_{c'} x^{*}_{c'a}S_{cc'a} + \frac{1}{2}\sum_{a'} x^{*}_{ca'}S_{caa'} \qquad ;\ (c \neq c'; a \neq a') \tag{39}$$

The hydration parameter r^0_{ca} is determined from data for single-salt solutions. The interaction coefficients $S_{cc'a}$ and $S_{caa'}$ are empirical parameters whose values are received by fitting to activity data for ternary mixtures. The dependence of hydratation on adsorption energy is given by Clegg and Simonson (2001) as

$$lnc_{ca} = \left(r_{ca}^{0} lnc_{ca} + \tfrac{1}{2}\sum_{c'} x_{c'a}^{*} T_{cc'a} + \tfrac{1}{2}\sum_{a'} x_{ca'}^{*} T_{caa'} \right) \cdot \frac{1}{r_{ca}} \quad ; \ (c \neq c'; a \neq a') \tag{40}$$

where $T_{cc'a}$ and $T_{caa'}$ are the empirical mixture parameters, and c_{ca}^{0} is a pure solution parameter for the single salt.

The theoretical assumption underlying the presented equations, which were originally also suggested by Stokes and Robinson (1948), is that the solvent activity in a solution of finite concentration is reduced by the adsorption of the solvent onto the dissolved salts. Model parameters are then deduced from the numbers of adsorption sites and adsorption energies on a salt, instead of hydratation on an ionic basis. The restriction of overall charge neutrality for solutions further means that ion parameters cannot be individually determined.

The composition of a salt solution containing only a single cation or anion, and two or more ions of the opposite charge type, can be unambiguously defined in terms of the salts present. Accordingly, an aqueous solution containing the cations M and N and anion X has a unique composition in terms of the salts M+X− and N+X−. For systems containing two or more ions of both charge types, a generalised expression taking into account all possible salt combinations is adopted. The amount of each salt in the solution is determined from the numbers of equivalents of each cation and anion ($n_c z_c$, $n_a|z_a|$) in the mixture[1] . The expression for amount (n_{MX}) of salt $M_{\nu^+}X_{\nu^-}$ is then

$$n_{MX} = 2 n_M n_X \left\{ z_M |z_X| \Big/ \left(\nu_{M(X)} \nu_{X(M)} \right) \right\}^{½} \Big/ \left\{ \sum_{c} n_c z_c + \sum_{a} n_a |z_a| \right\} \tag{41}$$

Here prefix *n* indicates the amount of each ion (*i*), z_i is its charge and $\nu_{M(X)}$ is the number of cations M in one molecule of the salt $M_{\nu^+}X_{\nu^-}$ ($\nu_{X(M)}$ giving the number of respective anions). The summations go over all cations (*c*) and anions (*a*).

The dry mole fraction of salt $M_{\nu^+}X_{\nu^-}$ is then:

---

[1] The example given by Clegg and Simonson (2001) is as follows: A solution containing 2 mol of cation M^{2+}, 3 mol of cation N^{+}, 2 mol of anion X^{-}, and 2.5 mol of anion Y^{2-}. The total adsorption of solvent by such a combination of ions is attributed to the salts MX_2, MY, NX, and N_2Y. In order to take account of differing charges on the ions, the various dry mole fractions in equations (1)–(3) are calculated on the basis of equivalent fractions. The equivalent fraction of M^{2+} in the mixture is $(2 \cdot 2)/(2 \cdot 2 + 3 \cdot 1) = 4/7$. Deducing form the total counterion charge, then, of the 4 equivalents of M^{2+} present, 2/7 will be paired with anion X^{-} and 5/7 paired with Y^{2-}. Similarly, 3 equivalents of N^{+} are present, of which with 2/7 are assumed to be paired with X^{-} and 5/7 with Y^{2-}, The total amount of salts MX_2, MY, NX, and N_2Y can then be deduced.

$$x^*_{MX} = n_M n_X \left\{ {z_M|z|_X} \Big/ {\left(\mathrm{v}_{M(X)}\mathrm{v}_{X(M)}\right)} \right\}^{½} \Big/ \sum_c \sum_a n_c n_a \{z_c|z_a|/(\mathrm{v}_{c(a)}\mathrm{v}_{a(c)})\}^{½} \tag{42}$$

Using the above equations for n_{MX} and x^*_{MX} in the Gibbs energy equation (1) and differentiating with respect to the amount of cations and anions the activities of the ions are obtained:

$$\begin{aligned} lna_M = {} & \sum_c \sum_a n'_{ca}[lnx^*_{ca} + r_{ca}ln\{1 - Y_{ca}/(r_{ca}n_{ca})\}] \\ & + \sum_c \sum_a n_{ca}r'_{ca}ln\{1 - Y_{ca}/(r_{ca}n_{ca})\} \\ & - \sum_c \sum_a c'_{ca}(r_{ca}n_{ca} \\ & - Y_{ca})\Bigg(Y^T - \sum_c \sum_a Y_{ca}\Bigg) \Bigg/ \Bigg(\sum_c \sum_a Y_{ca}\Bigg) \end{aligned} \tag{43}$$

$$\sum_c \sum_a c'_{ca}(r_{ca}n_{ca} - Y_{ca})\Bigg(Y^T - \sum_c \sum_a Y_{ca}\Bigg) \Bigg/ \Bigg(\sum_c \sum_a Y_{ca}\Bigg)$$

The summations are over all cations and anions while the prime indicates differentiation of the particular quantity with respect to the amount of cation M (n_M). As noted by Clegg and Simonson (2001) the additional differentiation term $\sum_c \sum_a x^{*\prime}_{ca} n_{ca} / x^*_{ca}$ is left out, as when determining the mean activity of the salt by combining with the respective anion activity such terms will cancel. The anion activity lna_X is identical to the cation activity sentence, except that the primes refer to differentiation with respect to n_X.

The equation of the activity of solvent is

$$lna_s = ln\Bigg(Y^T - \sum_c \sum_a Y_{ca}\Bigg) - lnY^T \tag{44}$$

The differentials that occur in the formulas of lna_M and lna_X will have the following form. The differential of the amount of salt n_{Ma} with respect to the amount of cation *M* is:

$$\begin{aligned} n'_{Ma} = {} & 2n_a\left\{\frac{z_M|z_a|}{\left(\mathrm{v}_{M(a)}\mathrm{v}_{a(M)}\right)}\right\}^{½} \Bigg/ \Bigg(\sum_c n_c z_c + \sum_a n_a|z_a|\Bigg) \\ & - 2z_M n_M n_a\left\{\frac{z_M z_a}{\left(\mathrm{v}_{M(a)}\mathrm{v}_{a(M)}\right)}\right\}^{½} \Bigg/ \Bigg(\sum_c n_c z_c + \sum_a n_a z_a\Bigg)^2 \end{aligned} \tag{45}$$

The differential of n_{ca} with respect to amount of cation *M* (*c*≠*M*) is:

$$n'_{ca} = -2z_M n_c n_a \left\{ \frac{z_c z_a}{\left(\nu_{c(a)}\,\nu_{a(c)}\right)} \right\}^{½} \Bigg/ \left(\sum_c n_c z_c + \sum_a n_a z_a \right)^2 \quad ; \ (c \neq M) \tag{46}$$

and the differential of the dry mole fraction x^*_{Ma} with respect to the amount of cation *M*:

$$\begin{aligned} x^{*\prime}_{Ma} = n_a \left\{ \frac{z_M z_a}{\left(\nu_{M(a)}\nu_{a(M)}\right)} \right\}^{½} /F \\ - n_M n_a \left\{ \frac{z_M z_a}{\left(\nu_{M(a)}\nu_{a(M)}\right)} \right\}^{½} \sum n_a \left\{ \frac{z_M z_a}{\left(\nu_{M(a)}\nu_{a(M)}\right)} \right\}^{½} \Big/ F^2 \end{aligned} \tag{47}$$

Where

$$F = \sum_c \sum_a \left\{ \frac{z_c z_a}{\left(\nu_{c(a)}\,\nu_{a(c)}\right)} \right\}^{½} n_c n_a \tag{48}$$

Respectively, the differential of x^*_{ca} with respect to n_M when *c* ≠ *M* is given by:

$$x^{*\prime}_{ca} = -n_c n_a \left\{ \frac{z_c z_a}{\left(\nu_{c(a)}\,\nu_{a(c)}\right)} \right\}^{½} \times \sum n_a \left\{ \frac{z_M z_a}{\left(\nu_{M(a)}\,\nu_{a(M)}\right)} \right\}^{½} /F^2 \tag{49}$$

As the mixture parameters S_{ijk} and T_{ijk} are constant, the derivatives of r_{ca} and c_{ca} with respect to amount of cation M are (from equations (2) and (3)):

$$r'_{ca} = \tfrac{1}{2}\sum_{c'} x^{*\prime}_{c'a} S_{cc'a} + \tfrac{1}{2}\sum_{a'} x^{*\prime}_{ca'} S_{caa'} \qquad ; \ (c \neq c'; a \neq a') \tag{50}$$

and

$$c'_{ca} = c_{ca} \left[\frac{K'_1}{r_{ca}} - \{ r^0_{ca} ln c^0_{ca} + K_1 \} r'_{ca}/r^2_{ca} \right] \tag{51}$$

where

$$K_1 = \tfrac{1}{2}\sum_{c'} x^*_{c'a} T_{cc'a} + \tfrac{1}{2}\sum_{a'} x^*_{ca'} T_{cca'} \qquad ; \ (c \neq c'; a \neq a') \tag{52}$$

and

$$K'_1 = \tfrac{1}{2}\sum_{c'} x^{*\prime}_{c'a} T_{cc'a} + \tfrac{1}{2}\sum_{a'} x^{*\prime}_{ca'} T_{cca'} \qquad ; \ (c \neq c'; a \neq a') \tag{53}$$

With this treatment, the calculation of solvent and solute activities from the equations above requires the solution of N simultaneous equations for the amounts of solvent adsorbed by each salt ca in the mixture, where N is the total number of salts.

The BET treatment is developed around a limiting law for mixtures that are infinitely dilute in respect to the mixture component water, this is the opposite of most treatments that, as a limiting case, include the Debye–Hückel law for solutions that infinitely dilute in respect to solutes in water. As a consequence, the BET model works best for highly concentrated solutions and is unusable for dilute solutions. A model applicable for all solutions would therefore need to be able to combine the BET approach with another model that can be used for dilute, moderately concentrated solutions, such as the Pitzer model.

6. Other approaches for concentrated electrolyte solutions

Among other thermodynamic models for concentrated electrolyte solutions, the more important ones include the, Electrolyte NRTL model (Chen and Song, 2004) the OLI systems Mixed Solvent electrolyte model (Wang et al., 2002) and the extended UNIQUAC model developed at Technical University of Denmark (DTU) (Thomsen, 2005). A comparison of these approaches has been presented by, e.g., Lin et al. (2009). All of these models connect the long- or long- and medium-range electrostatic interaction into a short-range local composition (NRTL or UNIQAC) model. The Electrolyte NRTL model has been incorporated to Aspentech in the Aspen Plus engineering suite, The OLI model is used in the OLI stream analyser and flowsheet Electrolyte Simulation Programs and can be linked to Aspen Plus, gPROMS, IDEAS, PIPESIM, PRO/II and UniSim simulation programs (OLI Systems Inc., 2016).

The benefit of these approaches is also the ability to handle mixed electrolyte aqueous organic solutions, while in the Pitzer model it is assumed that the solvent is always water. On the other hand, the amount of openly published parameter data for specifically aqueous solutions is scarce compared to the Pitzer model evaluations.

7. Data extrapolations for systems at elevated temperatures

7.1 Approximations when high temperature data is not available

In many cases the experimental thermodynamic determinations for aqueous solutions have been made only at 25 °C, or in temperatures that are considerably lower than those that are being modelled. Correlations and estimation methods have been presented for such cases for extrapolation.

7.2 Correlations for standard heat capacity data for aqueous species.

The most extensive published set of heat capacity data for aqueous ions and complexes are the ones based on the modified Helgeson-Kirkham-Flowers (HKF) model (Shock and Helgeson, 1988), applying equations of state and correlations to parametrised representations of infinite dilution heat capacities for aqueous ions and neutral species at high temperatures. The full set of thermodynamic equations (including volumetric) is presented by Shock and Helgeson. For the present work holding the most relevance is the equation for heat capacity

$$
\begin{aligned}
c_p = c_1 + \frac{c_2}{(T-\theta)^2} - \left(\frac{2T}{(T-\theta)^3}\right)\left(a_3(P-P_r) + a_4 \ln\left(\frac{\psi+P}{\psi-P_r}\right)\right) + \omega T X \\
+ 2TY\left(\frac{\partial\omega}{\partial T}\right)_P - T\left(\frac{1}{\varepsilon}-1\right)\left(\frac{\partial^2\omega}{\partial T^2}\right)_P
\end{aligned}
\tag{54}
$$

where c_1, c_2, a_3 and a_4 are ion specific parameters, T and P are temperature and pressure (in units of K and bar), ε is the dielectric constant of water, θ, ψ and P_r are constant model or reference parameters of 228 K, 2600 bar and 1 bar respectively. ω is the temperature and pressure dependent Born coefficient and Y and X functions defined by equations (55)-(56)

$$
Y = -\left(\frac{\partial(1/\varepsilon)}{\partial T}\right)_P \tag{55}
$$

$$
X = \left(\frac{\partial Y}{\partial T}\right)_P \tag{56}
$$

A simplification of the heat capacity equation valid to about 170 °C and low pressures has been given by Hämäläinen et al. (1991). In these conditions, the Born function can be considered a constant, so in reference pressure the heat capacity equation simplifies to:

$$
c_p = c_1 + \frac{c_2}{(T-\theta)^2} + \omega T X \tag{57}
$$

7.3 Pitzer parameter extrapolations for higher temperatures

Guidelines for estimation of Pitzer parameters at the elevated temperatures when the experimental data is limited has been given by Königsberger (2001). He proposed applying a constant heat capacity model whereby the Pitzer parameters are expected to follow the functional form of Eq. (58)

$$X(T) = X_0 + a\left(\frac{1}{T} - \frac{1}{T_0}\right) + b \cdot ln(T/T_0) \tag{58}$$

If no heat excess capacity data is available (only the value of the interaction parameter at a reference temperature, typically 298.15 K, and its first temperature derivative are known), b in equation (58) is zero. While the direct application of equation (58) for systems with fitted data to only one temperature (no heat capacity or enthalpy data,) would lead to applying a constant interaction parameter value, it is the recommendation of Königsberger then to instead use the temperature dependency given by equation (59):

$$X(T) = X_0\left(\frac{T_0}{T}\right) \tag{59}$$

8. Common thermodynamic data sources

There exists several collections of thermodynamic data for aqueous solution systems with various backgrounds and corresponding strengths and weaknesses.The SUPCRT92 database (Johnson et al., 1992) applies the HKF model (Shock and Helgeson, 1988), which contains data for about 250 solid minerals, 35 gaseous species and nearly 1750 aqueous species, mostly inorganic or organic complexes with metal cations (GEOPIG - Arizona State University, 2015). The database has been developed for give reasonable results for geochemical process at high temperatures and pressures.

There are several database projects for nuclear safety. The OECD NEA (Nuclear Energy Agency) database project aims to be comprehensive, internally consistent and quality-assured for selected elements (Guillaumont et al., 2003; Grenthe et al., 2004; OECD, 2014). The NAGRA database (Paul Scherrer Institut, Switzerland) (Thoenen et al., 2014) aims to be more comprehensive by accepting data by somewhat less stringent standards. The ThermoChimie database (Giffaut et al., 2014; Andra, 2015) by ANDRA (French National Radioactive Management Agency) draws heavily on SUCRT92, NBS, USGS and NEA databases. The American Yucca Mountain Project extended the OECD NEA and SUPCRT92 data (Mariner, 2003; Wolery and Sutton, 2011, 2013) with a Pitzer interaction-based model.

The Thermoddem database by Bureau de Recherches Géologiques et Minères (French Geological Survey) (Blanc et al., 2012). The data is available, e.g., in Phreeqc, Chess, Geochemist’s workbench formats. It has been constructed for geochemical modelling for environmental studies, especially for chemical systems involving waste materials.

THEREDA (Thermodynamic Reference Database) is a Germany-based project dedicated to the creation of a comprehensive, internally consistent thermodynamic reference database to be used with suitable codes for the geochemical modelling of aqueous electrolyte solutions up to high concentrations (AF Colenco et al., 2011; Moog et al., 2015). The project is being collectively planned and executed by the most relevant research institutions that work in the field of final disposal of radioactive waste. The THEREDA database is used for the geochemical modelling of processes in the near- and far-field of different host rock types, featuring high-saline solutions, which are envisaged as potential sites for final repositories in Germany.

The aqueous species data in the HSC database draws heavily on the work Shock and co-workers SUPCRT92 database, while the solid phase has been collected from a great number of sources. The database is extensive, for solubility calculations - the drawback is the often limited accuracy of calculations done on data combined form several sources (Diakonov et al., 1998). The OLI SYSTEM has advanced in-house models for aqueous and mixed electrolyte solutions (Kosinski et al., 2007).

IVTANTHERMO for Windows is developed by the Thermocenter of the Russian Academy of Sciences. It contains several programs including a free energy minimiser and database for some 3200 substances formed by 96 chemical elements, but no specific model for an aqueous system is reported (Belov et al., 1999; IVANTHERMO, 2004).

9. Modelling of systems with insufficient interaction data

A typical approach while doing industrial thermochemical models is to ignore the interaction parameters that are not readily available and set them to zero with the implicit assumption that zero is a reasonable default value for the unknown parameters. This is not the case with the Pitzer model when applied to interactions between ions that are not both univalent (Figure 6):

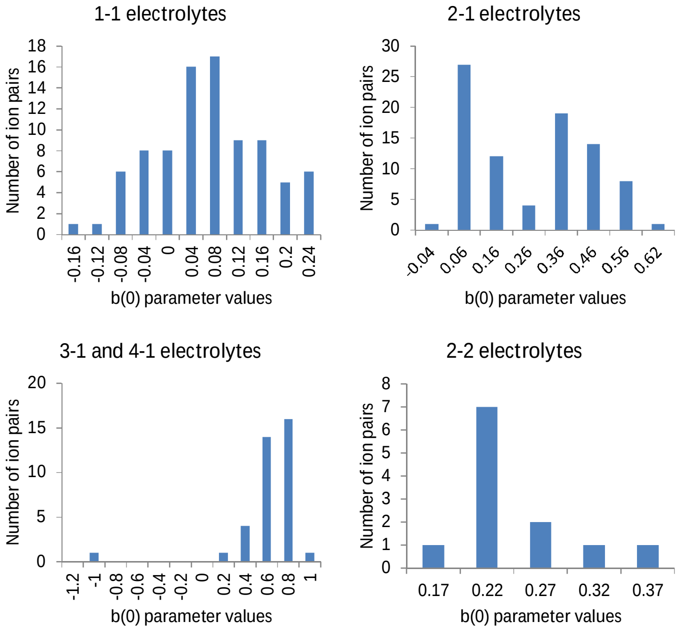

Figure 6. Distribution of the $\beta_{MX}^{(0)}$ interaction parameter values (at 25 °C) for different types of salts based on the ionic charges. Only in the case of 1:1 electrolytes are the values at least approximately evenly distributed around zero. Parameter dataset from Pitzer (1995).

In the case when no interaction parameter is specified for a cation—anion pair, application of the Pitzer model leads to calculation of ionic and water activities based on the first terms of equations (9), (10) and (12) (or the corresponding equations for the reduced molality scale). As it contains contribution to the logarithmic activity coefficient that is proportional to the square of ionic charge, the activity coefficients calculated in this fashion easily get exceedingly small for concentrated or moderately concentrated solutions.

The problem has been reviewed in relation to actinides by Felmy and Rai (1999). Within a project done at VTT (Chapter 15), the parametrisation was noted to be unsatisfactory when applied to Rare Earth Element (REE) solutions rich in sulphate that were considerably more concentrated than those studied by Felmy and Rai. A better practical result was obtained following Christov (2004), by applying a parameter set previously determined and tested for interactions of Al(+3aq) and Fe(+3aq) cation with sulphate ion.

In general, when applying the Pitzer model, the applied interaction parameters and speciation should have been determined simultaneously. When this is not possible, known parameters for species of similar chemistry (especially charge) should be used. Applying highly charged multinuclear complexes with an insufficiently parametrised Pitzer model is best avoided.

10. Selected thermodynamic data

Thermodynamic data including H, S and C_p as well as interaction coefficients were mostly taken from existing literature. In some cases parameter values were adjusted for a better fit as noted in text and in the Appendices. All the validation calculation examples are done with the same data set as shown in Appendices A-C.

While the international research interest has focussed on geochemical processes often related with environmental nuclear waste repository problems, VTT has extended experience developing pioneering simulation routines such as ChemSheet and BALAS to provide a quantitative tool for hydrometallurgical engineering problems. The multicomponent reactors are connected to modular process modelling software typically used in chemical and process engineering.

For complex industrial solutions appearing in a variety of pH ranges and in changing temperatures, it is important to take into account the non-ideality of the solutions to gain reliable results with engineering calculations. The VTT Pitzer database allows for reliable predictive simulations of the metal cations commonly occurring in aqueous sulphate, carbonate and chloride systems. In Table 2, the key cations in the Pitzer database are listed. ’Major species’ refers to ionic species with more thoroughly evaluated solubility equilibria also suitable for simulations at higher-temperature industrial processes up to 95 °C. The minor species are those species present with more tentative and limited activity data. REE refers to Rare Earth Elements. The actual database includes not only these key species but also their most common solute combinations

Table 2. Key ionic species in the VTT Pitzer activity database.

	Cation	Anion
Major species	Na^+, K^+, Ca^{2+}, Mg^{2+}, H^+	Cl^-, SO_4^{2-}, OH^-, CO_3^{2-}
Minor species	Al^{3+} ,Fe^{3+}, Cu^{2+}, Mn^{2+}, REE^{3+}	SiO_4^{4-}

The database can also incorporate solubility data of complex salts and mineral compounds from major international geochemical databases described above in Chapter 8, then also including less commonly occurring cationic species. Thus, e.g,. use of alternative pH and solubility-controlling chemicals as well as optional connections in a multi-stage hydrometallurgical plant or within a set of water treatment units can be simulated with fair accuracy.

10.1 H, S and C_p values for gaseous and aqueous species and solid stoichiometric phases

The gaseous, solid and aqueous species derived from the key elements in Table 2 were selected for further thermochemical studies and are given in Appendix A. Listed are enthalpy of formation and entropy at 298.15 K and coefficients for heat capacity according to the equation

$$c_p \,/(J \cdot mol^{-1}) = a_1 + a_2(T/K) + a_3(T/K)^2 + a_4(T/K)^{-2} \qquad (60)$$

The heat capacity equation coefficients are typically given for multiple temperature intervals with the maximum temperature T_{max} for each interval given with a coefficient set. The REE data has been excluded in this listing.

10.2 Pitzer parameter values

The speciation model given above is chosen to work with the following Pitzer parameter set. In Appendix B are given the type of the interaction, interacting species and coefficients for the temperature-dependent parameter equation

$$X = d_1 + d_2(T/K)^{-1} + d_3 ln(T/K) + d_4(T/K) + d_5(T/K)^2 + d_6(T/K)^{-2} \qquad (61)$$

The formalism applied is the one supported by the ChemApp ‘PIMZ’ model, where the $\alpha_{MX}^{(1)}$ and $\alpha_{MX}^{(2)}$ parameters (equations (15)-(17)) can be defined for each cation-anion pair separately.

10.3 Data for solid mixture phases

The data for the non-stoichiometric burkeite phase is given in Appendix C. The data for glaserite phase was taken from (Lindberg et al., 2006, 2007).

11. Validation examples of the Pitzer database

The data for aqueous solution and related solid phases has been validated comparing the calculation results with experimental salt solubility. Mostly the calculations have been done at temperatures 25 °C, 50 °C and 100 °C, but following available experimental data, sometimes other temperatures have also been used.

11.1 Hydroxide systems

Solubility limits of alkali hydroxides are beyond the typical application range of the Pitzer model. Systems with two anions, one of which is hydroxide are grouped with another anion.

Solubility in Na/Ca/OH is shown at left in Figure 7. Experimental results are from Duchesne and Reardon (1995), Konno et al. (2002) and Pallagi et al. (2011) for 25 °C and Konno et al. for 50 °C and 75 °C. Solubility $Al(OH)_3$ in an NaOH solution is shown at right in Figure 7. Experimental results are from Königsberger et al. (2006) quoting Russell et al. (1955).

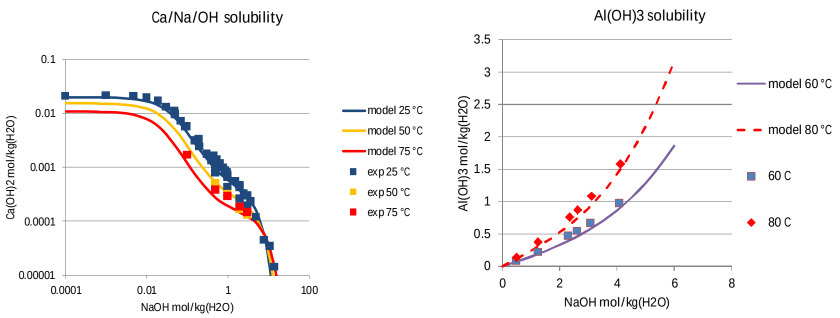

Figure 7. Solubility in Na/Ca/OH system (left) and in Na/Al/OH system (right)

11.2 Carbonate and hydrogen carbonate systems

Solubility of Na2CO3 in water as a function of temperature given left in Figure 8. The model results are compared to experimental results from Carter et al. (2014) quoting Linke (1965) for Na_2CO_3*$10H_2O$, Na_2CO_3*$7H_2O$ and Na_2CO_3*$1H_2O$, and Shi and Rousseau (2001) for Na_2CO_3*$1H_2O$ and Na_2CO_3. The solubility products of Na_2CO_3*$1H_2O$ and Na_2CO_3 have been fitted to the solubility data and chosen interaction parameter values. Solubility in the K/Na/CO3 system is shown on the right in Figure 8. Experimental data points are from Hill and Miller (1927) for 25 °C and 50 °C and from Ervin et al. (1944) for 100 °C. The solubility of K_2CO_3 is quite high for the Pitzer model to handle and no attempt was made to make the solubility at 100 °C fit the model.

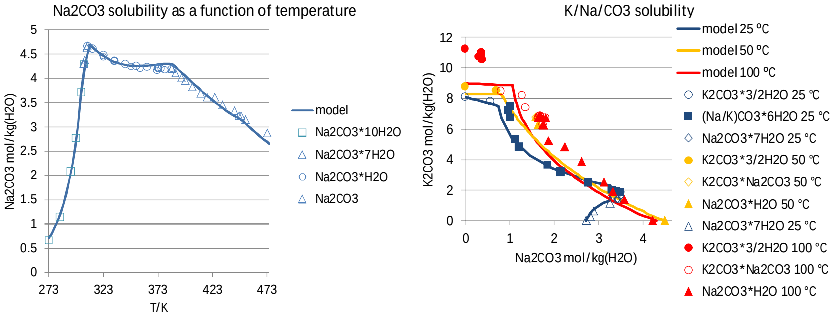

Figure 8. Solubility of Na_2CO_3 as a function of temperature (left) and solubility at K/Na/CO_3 system (right).

Solubility in a Na_2CO_3/$NaHCO_3$ system is shown right in Figure 9. Experimental data points are from Freeth (1923) and Hill and Bacon (1927) for 25 °C and 50 °C and from Waldeck et al. (1934) for 100 °C.

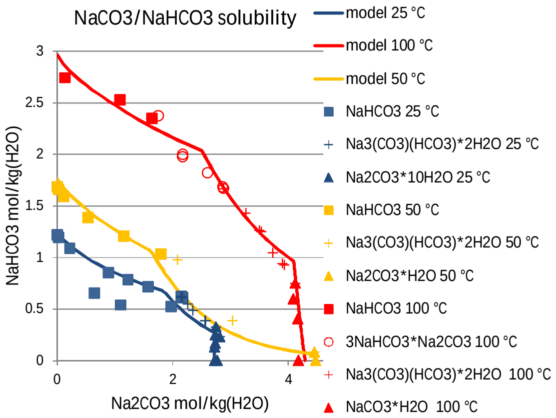

Figure 9. Solubility in the Na/CO_3/HCO_3 system.

11.3 Chloride systems

Solubility in the K-Na-Cl system is shown in Figure 10. Experimental data points are from Moučka et al. (2012) for 25 °C and Pabalan and Pitzer (1987) both quoting Linke (1965) and Greenberg and Møller (1989) quoting Bukshtein et al. (1953) for 100 °C.

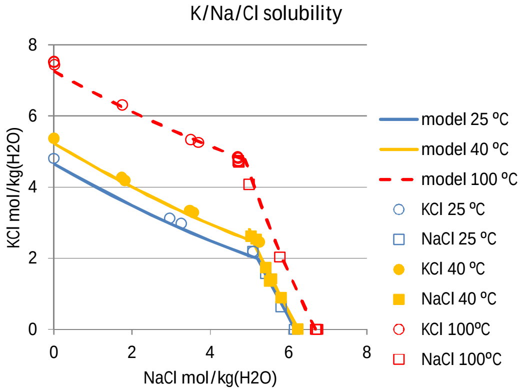

Figure 10. Solubility in K/Na/Cl system.

11.4 Sulphate systems

The solubility of calcium sulphate in water as a function of temperature is shown in Figure 11. Experimental data points are as collected by Møller (1988). For a better fit, the solubility product (thermodynamic values for the solid) were adjusted for $CaSO_4$ (in temperatures below 50 °C) and for $CaSO_4$*$2H_2O$ (for temperatures above 100 °C)

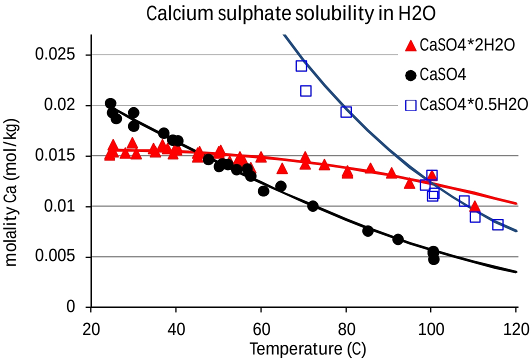

Figure 11. Solubility of $CaSO_4$ in water as a function of temperature.

Solubility of gypsum in sulphuric acid as a function of acid composition within temperature range 25-90 °C is shown in Figure 12. A linear concentration scale is used on the left and a logarithmic scale is used on the right. The experimental data points are from Marshall and Jones (1966). One of the deficiencies of the existing thermodynamic compilations was a lack of Pitzer model-based datasets that could be used with $CaSO_4$-containing systems both in near neutral conditions and together with H_2SO_4. The parameter set by Greenberg an Moller, which applied Ca(+2aq)-HSO_4(-aq), was adjusted in this work for this purpose.

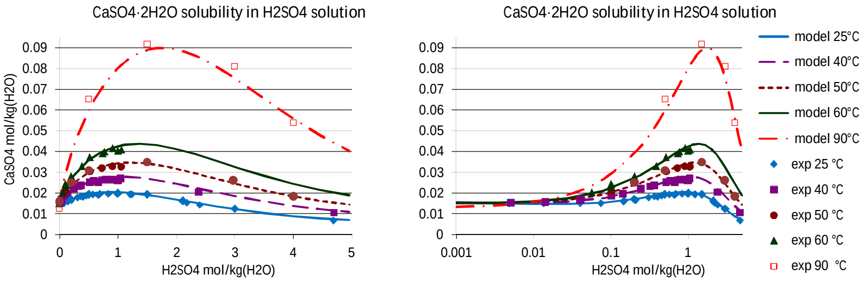

Figure 12. Solubility of gypsum in sulfuric acid. Linear concentration scale used in left and logarithmic scale in right.

Solubility in the Ca-K-SO4 system is shown at left in Figure 13. Dotted lines show various calculated metastable states (Chapter 12). The experimental data points are from Wang et al. (2013) and Greenberg and Møller (1989) quoting Bukshtein et al. (1953) and Stephen & Stephen (1963). Solubility in the Ca-Na-SO4 system is shown on the right in Figure 13. The experimental data points are from Block and Waters (1968).

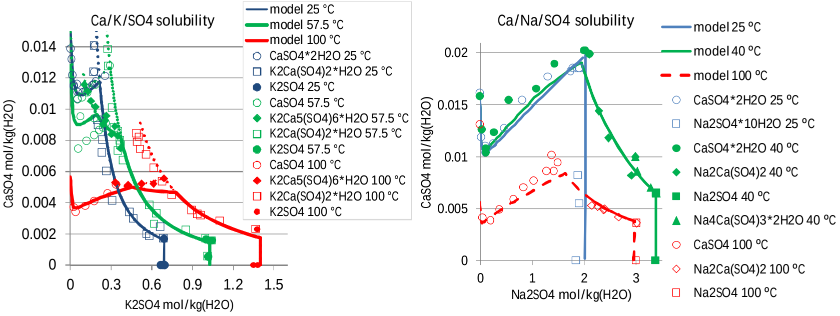

Figure 13. Solubility in the Ca/K/SO_4 system (left) and in the Ca/Na/SO_4 system (right).

Solubility in the K-Na-SO4 system is shown on the left in Figure 14. The experimental data points for the K-Na-SO4 system are from Popović et al. (2013) quoting Linke (1965) and Filippov and Cheremnykh (1983) for 25 °C, Bhattacharia et al. (2015) quoting Deng et al. (2013) for 50 °C and Freyer and Voigt (2004) quoting Yanateva et al. (1963) for 100 °C.

Solubility of the Na-OH-SO4 system is shown on the right in Figure 14. Experimental data points are from Harvie et al. (1984) quoting Windmaisser and Stöckl

(1950) and Itkina and Kokhova (1953) for 25 °C, Seidell et al. (1952) for 50 °C and Green and Frattali (1946) for 100 °C.

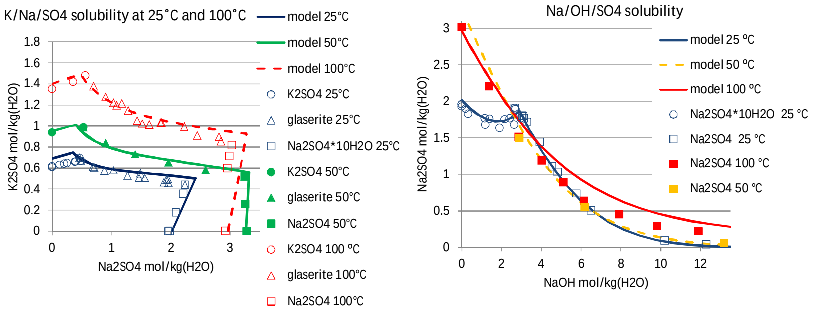

Figure 14. Solubility in the K/Na/SO_4 system (left) and in the Na/OH/SO_4 system (right).

Solubility in the Al-Ca-SO_4 and Al-Mg-SO_4 systems at 25 °C are shown in figure Figure 15. Experimental data from Reardon (1988), quoting Mosgovykh et al. (1984) for the Al-Ca-SO_4 system and Moshinskii and Chibizov (1975) and Bassett and Watt (1950) for an Al-Mg-SO_4 system.

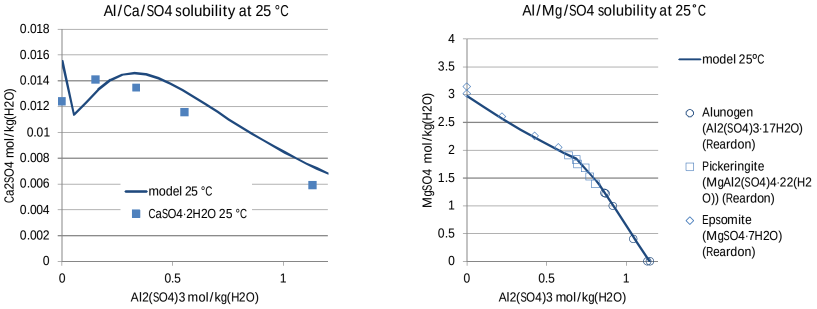

Figure 15. Solubility in Al/Ca/SO_4 and Al/Mg/SO_4 systems

Solubility in the Al-Na-SO_4 system is shown in Figure 16. Experimental data is from Christov (2002)

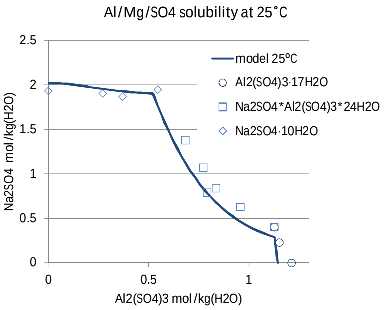

Figure 16. Solubility in Al/Na/SO_4 system at 25 °C.

11.5 Mixed anion systems

Solubility in the K-Cl-SO4 system is shown on the left in Figure 17. Experimental data points are for 25 °C and 50 °C from Bhattacharia et al. (2015) quoting Deng et al. (2013) and for 100 °C from Greenberg and Møller (1989) quoting Bukshtein et al. (1953).

Solubility in a $CaSO_4$-NaCl system is shown on the right in Figure 17. Experimental data points are from Bock (1961) for 25 °C, Bock and Marshall et al. (1964) for 40 °C and Marshall et al., Block and Waters (1968) and Freyer and Voigt (2004) for 100 °C.

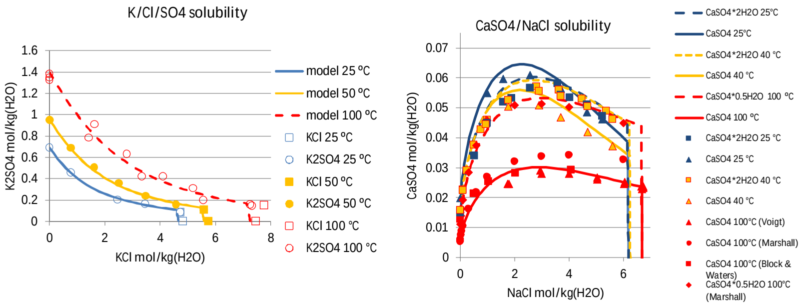

Figure 17. Solubilities in KCl-K_2SO_4 (left) and $CaSO_4$-NaCl (right) systems.

Solubility in Na-CO3-SO4 system is shown on the left in Figure 18. Experimental data points are from Harvie et al. (1984) for 25 °C, Makarov and Blidin (1938) and Teeple (1929) for 50 °C and Green and Frattali (1946) for 100 °C. The points for solubility at 0 °C is as presented by Marion (2001).

Solubility in a Na-Cl-CO3 system is shown on the right in Figure 18. The experimental data points are from Freeth (1923).

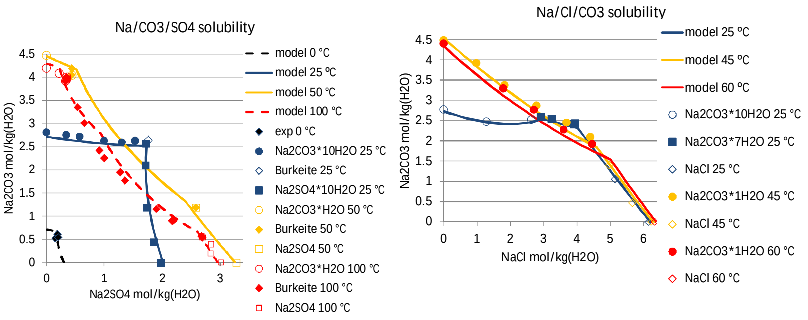

Figure 18. Solubilities in Na/CO_3/SO_4 and Na/Cl/CO_3 (right) systems.

11.6 Mixed salts as solid solutions

Two solid mixtures are included in the database, the non-stoichiometric sodium sulphate carbonate or burkeite and potassium sodium sulphate or glaserite.

11.7 Burkeite ($Na_6(SO4)_{2+x}(CO3)_{1-x}$)

For a description of a non-stoichiometric burkeite, a regular solution of Na_2SO_4 and Na_2CO_3 was adopted. The interaction parameter was fitted to the data presented by Picot et al. (2012) regarding salt composition as a function of the solution composition (Figure 19).

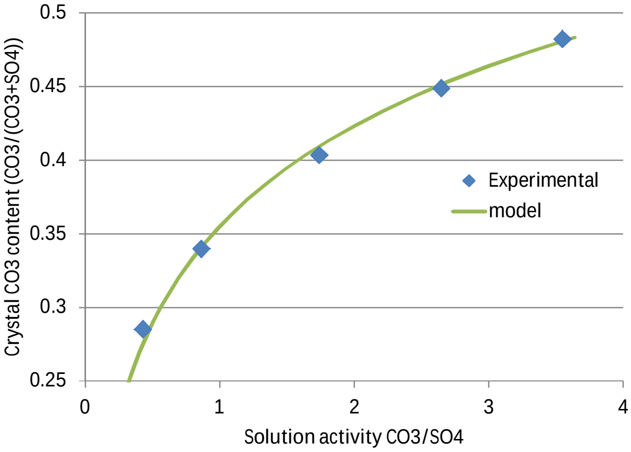

Figure 19. Burkeite crystal composition as a function of aqueous solution composition at 100 °C.

Comparison of the composition of the solid as function of liquid composition according to model at 100 °C and 115 °C is compared to various experimental results as collected by Bialik et al. (2008) is shown in Figure 20.

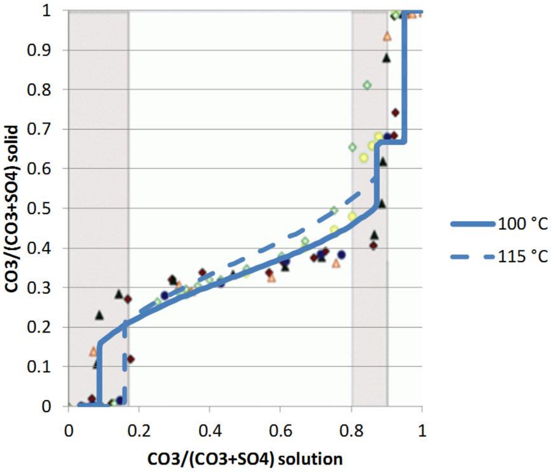

Figure 20. Composition of the solid phase as function of aqueous composition. Model curves compared with various experimental data points as presented by Bialik et al. (2008)

A diagram of the most stable solid phases in the aqueous Na2CO3-Na2SO4 system is shown in Figure 21 with a comparison to the data of Makarov and Blidin (1938).

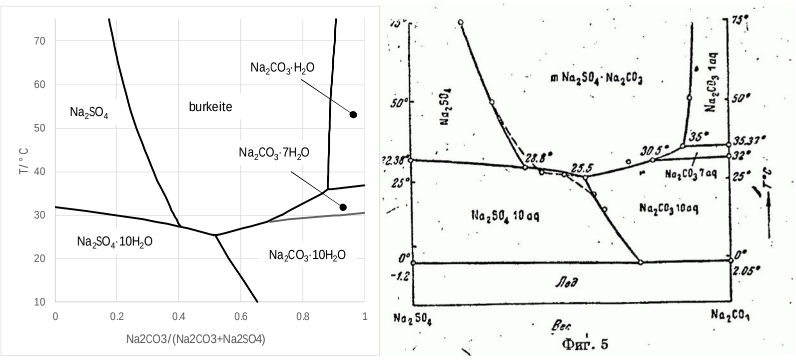

Figure 21. Phase stability diagram in an aqueous Na_2CO_3-Na_2SO_4 system. Experimental diagram by Makarov and Blidin (1938) is shown for comparison.

11.8 Glaserite ($K_{3-x}Na_{1+x}(SO_4)_2$)

For the glaserite salt, the data from Lindberg et al. (2006, 2007) has been adopted. While the data evaluation there was conducted mostly for higher temperatures, the resulting model also seems to work satisfactorily around 100 °C. A comparison of the model results to the experimental ones from Freyer and Voigt (2004) was shown in Figure 14.

12. Modelling of metastable and other non-equilibrium systems

One of the main strengths of VTT's thermochemical models is the ability to directly perform directly calculations in systems that are displaced from equilibrium or are controlled by the kinetics of slow reactions such as precipitation dissolution or oxidation. Aspects of these kinds of calculations most relevant to aqueous systems are discussed briefly in this section and in Appendix D. Further information can be found in the referenced publications.

12.1 Over- and under-saturated systems

Generally thermochemical calculation codes (including ChemApp and ChemSheet) allow solving thermodynamic equilibrium with specified phases excluded from calculations. This can be used, for example for solubility precipitation calculations where the solid phase present is not the most stable one thermodynamically. The Constrained Free Energy (CFE) method also enables the application of specific quantitatively set deviations from equilibrium. A commonly used quantity to describe such non-equilibrium systems is the saturation index (SI) defined as

$$SI = \log\left(\frac{Q}{K_{eq}}\right) \tag{62}$$

where K_{eq} is the thermodynamic solubility product for the salt and Q the corresponding ion activity product in the solution. Thermodynamically, for a salt M_aX_b dissolving as

$$M_aX_b(s) = aM^{z+}(aq) + bX^{z-}(aq) \tag{I}$$

the saturation index is related to the affinity ($\mathbb{A}$) of the dissolution reaction as well as activity (Eriksson, 1975) of the under- or over-saturated salt (a_{salt})

$$SI \cdot \ln(10) = \ln\left(\frac{Q}{K_{eq}}\right) = \frac{\Delta G_{diss}}{RT} = -\frac{\mathbb{A}}{RT} = -\ln(a_{salt}) \tag{63}$$

Theory and computational methods of setting affinities for non-equilibrium reactions has been discussed in detail in, e.g., Pajarre et al. (2016).

An example of a metastable states that can be modelled and with suitable conditions measured were illustrated by the binary $CaSO_4$-H_2O system shown in Figure 11. Depending on temperature the stable solid phase in equilibrium with the solution is either the dehydrate (gypsum), monohydrate or the anhydride. The equilibrium solubility is given by the lowest curve but also the various metastable states corresponding to the equilibrium of a higher energy solid phase with the solution are shown. As the formation of a solid not present in the system is often a slow process the various metastable states can also be experimentally explored and measured.

12.2 Thermodynamic calculations combined with reaction kinetics

Non-equilibrium constraints can also be used to control the advancement of individual reactions based on known rate equations within partial thermodynamic equilibrium. The theory of this has been discussed in, e.g., Pajarre et al. (2016) while an application to calcium carbonate (PCC) precipitation is shown in Koukkari et al. (2011). From the overall practical point of view, the most valuable models are usually those where the reaction of kinetic effects can be deduced form 1—3 reaction rates, while thermodynamic controls' side reactions and equilibration are over a longer time scale.

A detailed example of a kinetically controlled reactive system is presented in Appendix D with a $CaCO_3$ precipitation model.

13. Redox systems

A special kind of partial-equilibrium system are those reduction—oxidation reactions. While in a redox equilibrium system, the redox potential can be linked to the chemical potential of electron in the system, in practice in a multicomponent system with multiple redox pairs, rarely even in an approximate sense can a single common redox potential value be determined (Lindberg and Runnells, 1984). An identified redox pair can be included in a multicomponent model with or without kinetic constraints, while the ionic activities can then be applied to deduce the redox potential (Eh) and be compared with measurement (Koukkari and Liukkonen, 2002). Multiple redox pairs can also be controlled by the CFE method, but there is no straightforward connection between the varying species-specific redox potentials and any particular measured Eh value.

14. Ion exchange phenomena with aqueous solutions including pulp suspensions

Electrochemical systems consisting of two parts separated by a semipermeable membrane were first investigated by Frederick Donnan (1911) in the early 20th century. The equilibrium condition for such systems is the equality of the electrochemical potential in the parts of the system

$$\mu_i^{0'} + RTlna_i' + z_iF\psi' = \mu_i^{0''} + RTlna_i'' + z_iD\psi'' \qquad (64)$$

Assuming the same solvent is present on both sides and molar volumes of solutes can be ignored, this leads to

$$\left(\frac{a_i''}{a_i'}\right) = \left(\exp\left(\frac{F(\psi'-\psi'')}{RT}\right)\right)^{z_i} \equiv \lambda^{z_i} \qquad (65)$$

where λ is the so-called Donnan distribution coefficient. An example calculation with corresponding experimental results for aqueous pulp system is shown in Figure 22. Here the the fiber wall effectively works as the membrane separating the two aqueous volumes, while non-mobile ions are the acidic groups in the pulp that are chemically bound to it.

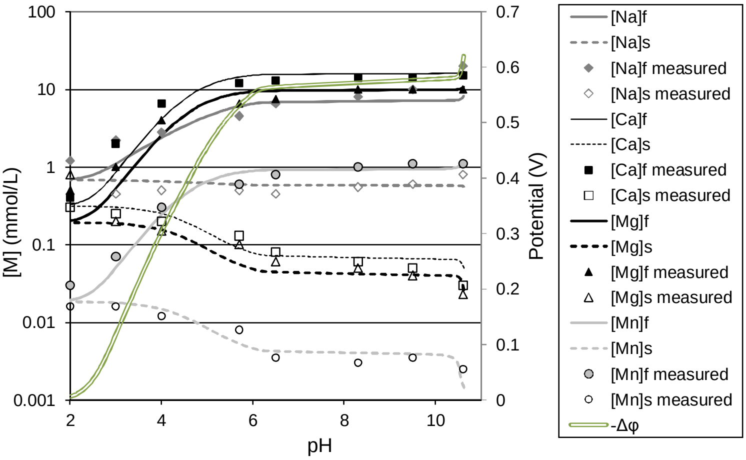

Figure 22. Donnan potential and model curves for concentrations inside and outside the pulp susepnsion undergoing ion-exchange shown together with corresponding experimental data points. From Pajarre et al. (2016).

The ion exchange model can be supplemented with typical complex forming agents such as EDTA and DTPA, which are common in industrial applications. The complexation modelling results for a 4.8% consistency pulp suspension treated with EDTA chelating agent are shown in Figure 23. At very low pH, the organic acids are not deprotonated and the metal concentrations would be expected to be roughly equal in the fibres and in the surrounding solution. With increasing pH, the negatively charged fibres will attract cations, with the effect as described by equation (65) being stronger for divalent than monovalent ions. The formation of negatively charged complexes with EDTA explains why a larger fraction of Ca than Mg remains in the solution with pH values greater than 4.

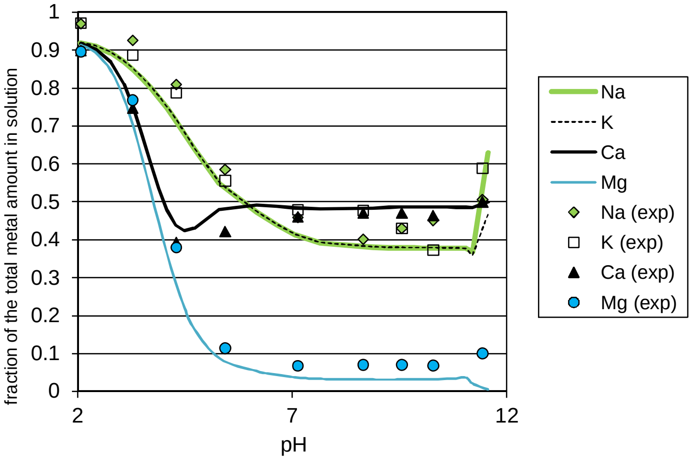

Figure 23. Comparison of simulated and experimentally determined metal ion contributions in an EDTA containing pulp suspensions. Based on Pajarre et al. (2006)

The application of the Donnan equilibrium within a multiphase Gibbs energy model has been discussed by, e.g., Pajarre et al. (2016) with practical application within paper industries in, e.g., Koukkari et al. (2007), Pajarre et al. (2008), Kalliola et al. (2012), Kangas et al. (2012) and Sundquist (2016).

For cases where the Donnan model alone is not sufficient to describe the interactions of the bound charged groups and mobile ions, an application of a Gibbs energy minimisation-compatible Donnan model with specific complexation interaction added has been presented by Sundman et al. (2008).

15. Application examples

In order to illustrate the applicability of the presented Pitzer database, practical examples, a number of computational studies of hydrometallurgical processes were performed. The key emphasis was to use published data on processes. The chosen examples were:

- The leaching process for alkaline (soda) ash
- Neutralisation treatment of acidic mine water (AMD)
- Simulation of a mining water sulphate treatment cycle
- Recovery of rare earth compounds from acidic leachate

While the ash and AMD problems typically consist of a limited number of metal cations, the rare earth recovery process studied was more complicated due to its very nature of including a large number of both metal cations and their both neutral and charged hydrocomplexes.

The practical modelling work was conducted by combining i) a flowsheet process simulator capable of solving mass and energy balances with ii) a thermodynamic equilibrium solver applicable for modelling the multi-phase chemistry related to aqueous solutions. A similar approach has been previously applied for the modelling of the calcium chemistry in pulp and paper industry (Kalliola et al., 2012; Sundquist, 2016) where it has been shown that this methodology is well adapted for large industrial systems with several multiphase reactors. The basic technique applied here was a combination of a Balas steady-state process simulator by VTT and ChemApp by GTT Technologies. Balas is particularly apt for mass and energy balance calculations (VTT - Technical Research Centre of Finland, 2013), yet its former connection with the ChemApp multicomponent-multiphase thermochemical engine (Bale et al., 2002) is used for calculations of thermodynamic equilibrium in several unit processes (mixing, flash, separation).

The additional tool used for process modelling was HSC Sim by Outotec Oyj. While using HSC Sim, the aqua module complemented with the Pitzer activity database could be utilised as part of the flow sheet simulation. An aqua module is then in parallel with the Balas-ChemSheet combination based on the minimisation of Gibbs free energy and can be used for solving the chemistry of a water solution.

The practical details vary between two process simulation approaches (HSC Sim vs. Balas/ChemApp), but the general principle of operation is very similar. The typical operation mode of process simulation is that of sequential equilibrium and distribution units, as coupled with stream vectors. The stream vector can be defined to include the same constituents and phases that are used for calculating the thermodynamic equilibrium. Thus, each stream represents a multicomponent entity in the simulation. The reactors are either distributors (also called splitters or separators) or true equilibrium reactors. The distributors must include user-defined fractionation parameters, while equilibrium reactors will perform Gibbs free energy minimisation to yield the equilibrium composition. Reactor temperature and pressure are typical input data for each unit, but may also be calculated from the thermochemical specifications of the process.

The advantage of the thermodynamic approach in calculation of aqueous processes is that by providing the ionic activities, the software can be used for predictive and/or validating pH-calculations for cases, where solubilities and ionic strengths are known and pH as an independent intensive property can be measured from different locations of the process. In addition, the measured pH values can be used as feedback while controlling the chemical dosage of chemicals suitable for adjusting solution conditions.

15.1 The ash leaching process

The first example of aqueous processes where thermodynamic modelling can be applied is the ash-leaching process. It is utilised for example in the pulp mills where the kraft recovery boiler ESP (electrostatic precipitator) ash is treated. The aim is to remove chlorine and potassium from the ash while simultaneously recycling the sodium and sulfur compounds back to the pulping processes. This technology is based on the solubility of different species. The aim is that potassium and chlorine compounds with higher solubility will dissolve. Compounds containing sodium and sulfur have lower solubility and they will remain in the solid phase. After the leaching reactor, the phases are separated and the solids will be recycled to process while the bleed is removed from the process. A flowsheet of the ash-leaching process is developed with an HSC Sim process simulator and is given in Figure 24. The chemical system applied for this process model is given in Table 3.

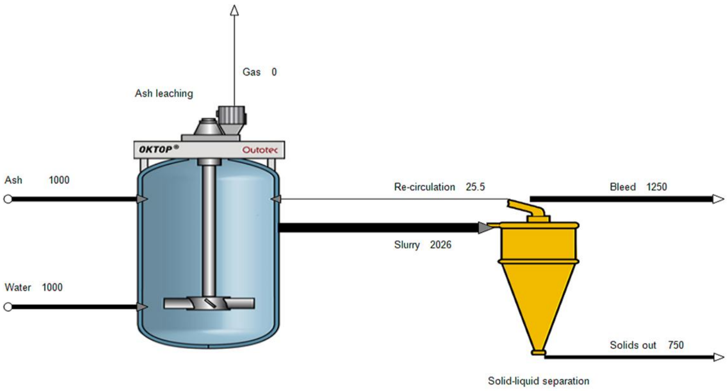

Figure 24. The ash leaching process for removing chlorine and potassium from the ESP ash of the recovery boiler while recycling the sodium and sulfur back to process. Figures are given per 1000 kg of treated water.

Table 3. Chemical system applied for modelling the ash leaching process.

Gaseous	Aqueous		Pure	
$H_2O(g)$	H_2O		NaCl	KCl
$CO_2(g)$	$H^+(aq)$	$OH^-(aq)$	Na_2CO_3	K_2CO_3
$N_2(g)$	$Na^+(aq)$	$Cl^-(aq)$	Na_2SO_4	K2SO4
$O_2(g)$	$K^+(aq)$	$SO_4^{-2}(aq)$	NaOH	KOH
$SO_3(g)$		$HSO_4^-(aq)$	$Na_2CO_3\cdot 10H_2O$	$Na_2CO_3\cdot 7H_2O$
		$CO_3^{-2}(aq)$	$Na_2CO_3\cdot H_2O$	$Na_2CO_3\cdot \mathrm{NaHCO3}\cdot 2H_2O$
		$HCO_3^-(aq)$	Na_2O	$Na_2\mathrm{SO4}\cdot 10H_2O$
		$CO^2(aq)$	$NaHCO_3$	$Na_6(CO_3)(SO_4)_2$
			H_2SO_4	

The evaluation of this example is conducted against literature data. The composition of incoming ESP ash is: Na 30.5%, K 6.1%, Cl 7.7%, SO_4 54.3% and CO_3 1.5%. The water-to-ash rate is 1:1 and the recycling rate is 2% (Gonçalves et al., 2008). The liquid content of solids flow is 25% (Larsson, 2012).

The process model built with the HSC Sim process simulator is able to predict the ash-leaching process with reasonable accuracy (Figure 25). The sodium recovery rate and potassium removal rate is close to those reported in the literature. There is more variation in the sulfur recovery rate as well as the chlorine removal rate. The literature data is obtained from the Aracruz pulp mill (Gonçalves et al., 2008) and its average values during a longer period. The values calculated here with the process model represent a single operational point of the process. The other possible source of errors is the dry content of solids flow. If more solution is introduced with the solids, the removal rates will be decreased.

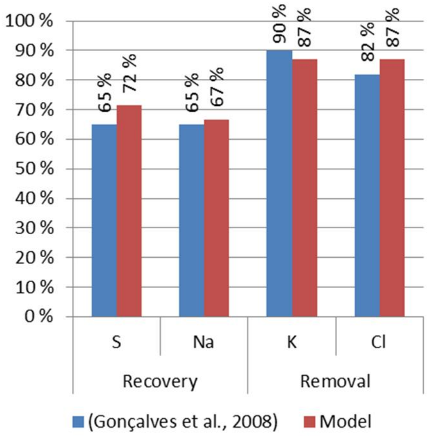

Figure 25. The ash leaching process. Literature data is from the Aracruz pulp mill given as average values Gonçalves et al. (2008).

The chemical system presented in Table 3 is simplified illustration of the actual chemical system. For example, the co-precipitation is not included here. In reality, the compounds such as glaserite and burkeite are present in the ash leaching systems. In addition, the feasibility of the presented model should also be evaluated in cases where the potassium or carbonate content of ESP ash is high.

15.2 Neutralisation of acid mine drainage

Acidic mine water effluents form a common problem, both in operating and abandoned mining sites. Various techniques of treating such streams either chemically or biochemically are being developed both in Finland and elsewhere. As the chemical conditions are highly variable on each site, a multicomponent model could be used to support the choice of alternative treatments.

Geldenhuys et al. (Geldenhuys et al., 2003) have published a three-stage experimental and pilot setup for neutralising acidic, sulphate-containing mine waters in Upper Olifants River Catchment in the Mpumalanga area of South Africa. Their pilot plant consisted of treatment of 10 m3/day and was used for on-site treatment of the mine water. The process consisted of three stages, including 1) Limestone ($CaCO_3$) neutralisation with CO_2-production to raise the pH to 7; 2) lime ($Ca(OH)_2$) treatment to pH 12 for $Mg(OH)_2$ precipitation and gypsum ($CaSO_4 \cdot 2H_2O$) crystallisation; 3) pH adjustment with CO_2 recovered from stage 1 and $CaCO_3$ precipitation. With varying retention times in stages 1-3, the sulphate level could be reduced from ~3000 mg/l to close to 1,094 mg/l. The process flowsheet is presented in Figure 26.

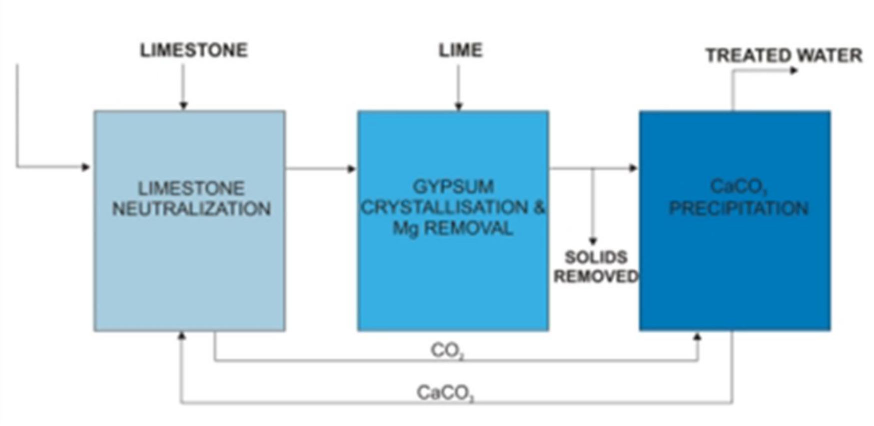

Figure 26. Oliphant River AMD treatment (Geldenhuys et al., 2003; INAP, 2003).

According to Geldenhuys et al. the main cations of the Olifants river AMD are Ca^{+2}, Na^{+}, Mg^{+2} and Mn^{+2}. The respective anions are SO_4^{-2} and Cl^{-}. Thus, a thermodynamic system presented in Table 4 is composed for the modelling of this aqueous solution.

Table 4. A chemical system applied for modellingthe acidic mine drainage of Olifants River. The system applied to HSC is somewhat more limited. Species applied in the HSC Sim model are marked with *.

Gaseous	**Aqueous**		**Pure**	
$N_2(g)^*$	H_2O^*		burkeite	$Na_2Ca(CO_3)_2{\cdot}2H_2O^*$
$CO_2(g)^*$	$H^+(aq)^*$	$OH^-(aq)^*$	$Ca(OH)_2^*$	$Na_2Ca(SO_4)_2$
$H_2O(g)^*$	$Ca^{+2}(aq)^*$	$Cl^-(aq)^*$	$CaCl_2^*$	$Na_2CO_3^*$
	$Mg^{+2}(aq)^*$	$CO_3^{-2}(aq)^*$	$CaCO_3^*$	$Na_2CO_3{\cdot}10H_2O^*$
	$MgOH^+(aq)$	$HCO_3^-(aq)^*$	CaO	$Na_2CO_3{\cdot}7H_2O^*$
	$Mn^{+2}(aq)^*$	$SO_4^{-2}(aq)^*$	$CaSO_4^*$	$Na_2CO_3{\cdot}H_2O^*$
	$Mn_2(OH)_3^+(aq)$	$HSO_4^-(aq)^*$	$CaSO_4{\cdot}0.5H_2O^*$	$Na_2CO_3{\cdot}NaHCO_3{\cdot}2H_2O^*$
	$Mn_2OH^{+3}(aq)$	$MnO_2^{-2}(aq)$	$CaSO_4{\cdot}2H_2O^*$	$Na_2CO_3(beta)$
	$MnHCO_3^+(aq)$	$MnO_2H^-(aq)$	$H_2SO_4^*$	Na_2O^*
	$MnHSO_4^+(aq)$		$Mg(OH)_2^*$	$Na_2SO_4^*$
	$MnOH^+(aq)$		$Mg_2(OH)_2CO_3{\cdot}3H_2O^*$	$Na_2SO_4(I\_Hexag)$
	$Na^+(aq)^*$		$MgCl_2^*$	$Na_2SO_4{\cdot}10H_2O^*$
			$MgCO_3^*$	$Na_2SO_4(IV)$
	$CO_2(aq)^*$		$MgCO_3{\cdot}3H_2O^*$	$NaCl^*$
	$CaCO_3(aq)$		$MgSO_4^*$	$NaHCO_3^*$
	$MgCO_3(aq)$		$MgSO_4{\cdot}7H_2O^*$	$NaOH^*$
	$MnO(aq)$		$Mn(OH)_2^*$	
			$MnCO_3$	
			$MnSO_4^*$	

*Species applied in HSC Sim model.

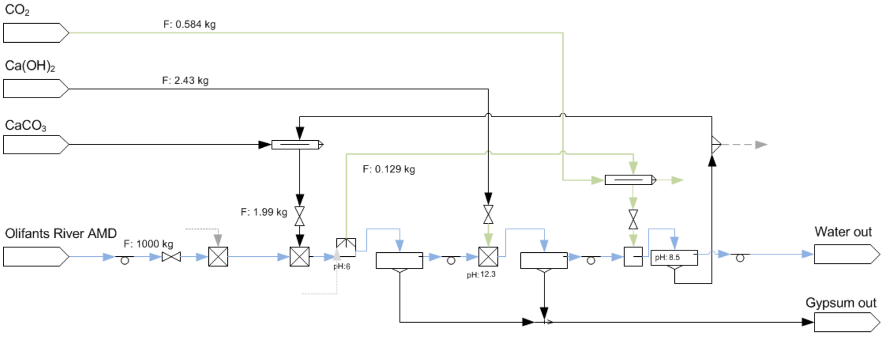

Figure 27. The BALAS/ChemSheet model of the Oliphant River AMD treatment process. Figures are given per 1000 kg of treated water.

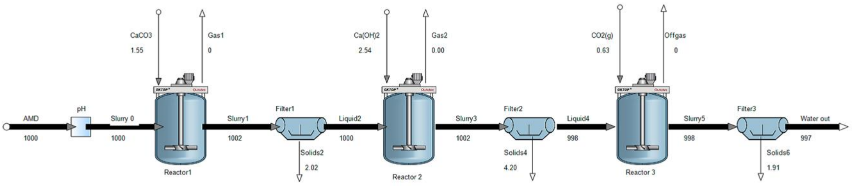

Figure 28. The HSC Sim model of the Oliphant River AMD treatment process. Figures are given per 1000 kg of treated water.

Two process simulators capable of describing aqueous systems software were used for modelling the Oliphant river AMD: i) The Balas process simulator combined with the ChemSheet and ii) HSC Sim with an aqueous module. Thermodynamic equilibrium of aqueous solutions was solved in three stages of the process (limestone, lime and carbon dioxide treatment) in both cases by minimising Gibbs' free energy of the aqueous system. The process itself was modelled either with the BALAS process simulator or HSC Sim-Developed process models are presented as a flowsheet in Figure 27 and Figure 28.

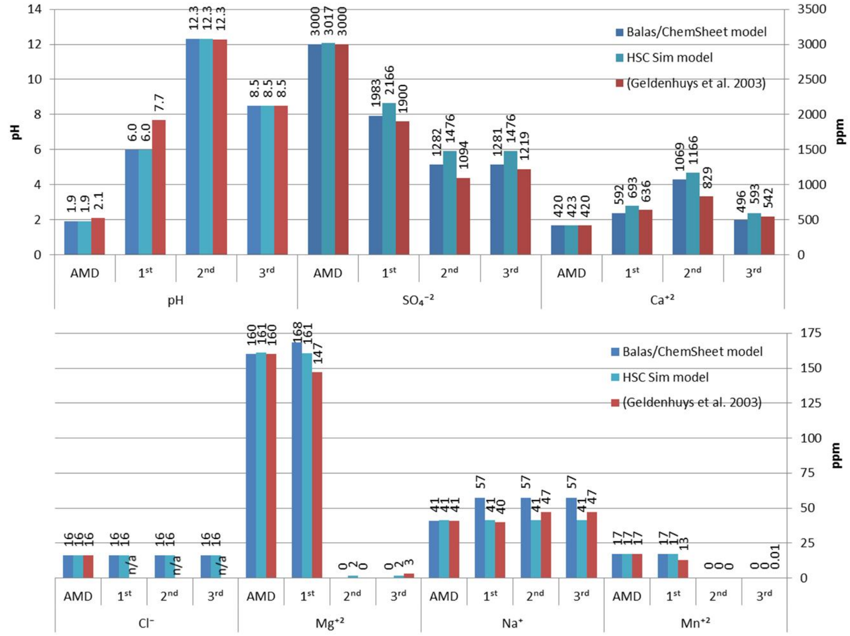

Figure 29. Composition of Olifants river AMD before treatment (AMD), after limestone treatment (1st), after lime treatment (2nd), and after CO^2 treatment (3rd). Validation data by Geldenhuys et al. (Geldenhuys et al., 2003).

Input parameters for the process models were i) the composition of Olifants river AMD and ii) the pH values of the three precipitation stages. The input composition of the water is presented in Figure 29. The pH value for the 1st limestone stage was set to 6.0, for the 2nd lime stage 12.3 and 8.5 for the 3rd CO_2 precipitation stage. Respective experimental values by Geldenhuys et al. were 7.7, 12.3 and 8.5. The lower value was applied in the models for the first precipitation stage was due to the model restrictions: higher pH values than 6.3 were, however, not reachable with the mere addition of limestone. The charge of three precipitation chemicals, limestone, lime and CO_2 were controlled based on the pH value of the corresponding stage.

The compositions of Olifants River AMD before treatment and after three precipitation stages are given in Figure 29. The respective values from both process models are shown in the same figure. The agreement between the simulation model and the observed values is satisfactory, in general verifying the assumed equilibrium process.

Small deviations can be observed for the Mg, Ca and Na. According to Geldenhuys et al. there is a small fraction of Mg and Na in limestone. This could result small some variations related to these species. The pH-based charging of chemicals causes some deviations when two different process models are compared. A somewhat different chemical system and thermodynamic data could also cause these differences. The pH-based charging of chemicals could also cause a higher flow of $Ca(OH)_2$ to the 2nd stage and thus a higher level of Ca at this stage. The lower pH value at the 1st stage in the model could cause a difference in the solubility of Mn. Both models give qualitatively good results when modelling the cleansing of AMD water.

15.3 Talvivaara mine leachate and water treatment

Hietala and Härmä (Hietala and Härmä, 2012) have described the process of the metal fractionation and waste water treatment at the Talvivaara nickel mine. The fractionation of metals from the ore itself is conducted based on biochemical heap leaching. The collected leachate will be treated with hydrogen sulfide in order to recover metals, mainly copper, zinc and nickel as respective sulfides. Lime and limestone are used for the waste water treatment and caustic soda for the pH control. The design capacity of the metal recovery plant is 1200 m^3 leachate per hour corresponding to 24 000 t of nickel annually.

In this study, a four stage process for the recovery of metals and the treatment of waste water is modelled, see Figure 30. The following stages are included: i) preneutralisation where limestone is applied for the pH control (pH 3.0), ii) the precipitation of nickel and cobalt with hydrogen sulfide at pH 4.0 (caustic soda is applied for neutralising the formed acid), iii) precipitation of iron with limestone at pH 6.0, and iv) final neutralisation with lime at pH 10.5.

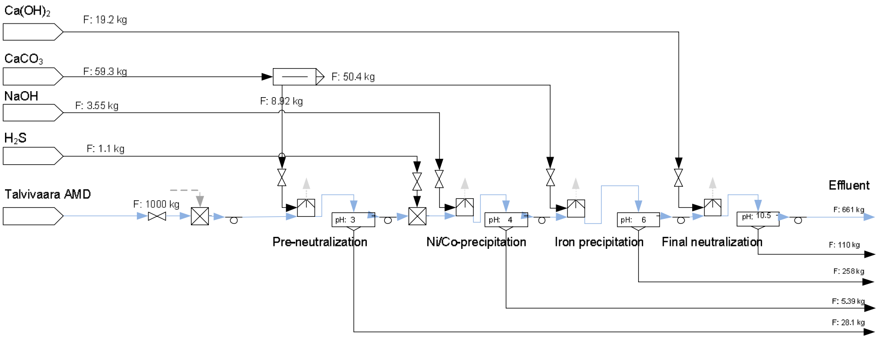

Figure 30. BALAS/ChemSheet model of the Talvivaara metal recovery and waste water treatment. Figures are given per 1000 kg of treated water.

The key cations in the presented process are Ni^{+2}, Co^{+2}, Fe^{+3}, Al^{+3}, Ca^{+2}, Mg^{+2}, Mn^{+2} and Na^{+}. The respective anions are SO_4^{-2}, OH^{-}, and CO_3^{-2}. When modelling this case, the following assumptions are made: Ni^{+2} and Co^{+2} are excluded from the thermodynamic model and the sulfide precipitation is modelled as stoichiometric reactions. However, the counter-ion, SO_4^{-2}, of these species is included for modelling the acidity. Iron is modelled as Fe^{+3}. Hietala and Härmä reported that there are both ferric and ferro iron present. However, the actual distribution is not reported. Thus in the model, it is assumed that all iron is Fe^{+3} and a modified material properties of $Fe(OH)_3$ are applied in order to avoid iron precipitation at yearly stages of the process. Thermodynamic system applied for modelling Talvivaara case is given in Table 5.

Here again, a combination of Balas and ChemSheet programs were utilised for modelling the process. The thermodynamic equilibrium of aqueous solutions was solved in five stages of process with the ChemApp thermodynamic solver. The process itself was modelled with the BALAS process simulator and a flowsheet can be seen in Figure 30.

Composition of the leachate before pre-neutralisation (Hietala and Härmä, 2012) was used as an input composition. In addition, the pH-levels from processing steps reported in the same literature were used to calculate the chemical dosage to various stages where data was available. The input composition and pH set points are illustrated in Figure 31.

The metals and sulfate concentrations (as mg/l) are reported in Figure 31. Here all particular metal constituents are considered to be respective ions. Similarly, all sulfur is reported as sulfate in the solution.

Table 5. Chemical system applied for modelling Talvivaara leachate and waste water treatment.

Gaseous	Aqueous		Pure	
H_2O(g)	H_2O		$Fe(OH)_3$	$Na_2Ca(SO_4)_2$
CO_2(g)	H^+(aq)	OH^-(aq)	$Fe_2(SO4)_3$	Na_2CO_3
	Fe^{+3}(aq)	HCO_3^-(aq)	$Al(OH)_3$(amorphous)	$Na_2CO_3 \cdot 10H_2O$
	$Fe_2(OH)_2^{+4}$(aq)	CO_3^{-2}(aq)	$Al2(SO4)_3$	$Na_2CO_3 \cdot 7H_2O$
	$Fe3(OH)4^{+5}$(aq)	HSO_4^-(aq)	$Al_2(SO4)_3 \cdot 17H2O$	$Na_2CO_3 \cdot H_2O$
	FeO^+(aq)	SO_4^{-2}(aq)	$Ca(OH)_2$	$Na_2CO_3 \cdot NaHCO_3 \cdot 2H_2O$
	$FeOH^{+2}$(aq)	FeO_2^-(aq)	$CaCO_3$	Na_2SO_4
	Al^{+3}(aq)	MnO_2^{-2}(aq)	CaO	$NaHCO_3$
	$Al(OH)^{4-}$(aq)	MnO_2H^-(aq)	$CaSO_4$	NaOH
	AlO^+(aq)	$MnOH^+$(aq)	$CaSO_4 \cdot 0.5H_2O$	H_2SO_4
	Ca+2(aq)		$CaSO_4 \cdot 2H_2O$	burkeite
	Mg+2(aq)		$Mg(OH)_2$	M_4AH_{10}
	MgOH+(aq)		$Mg_2(OH)_2CO_3 \cdot 3H_2O$	
	Mn^{+2}(aq)		$MgAl_2(SO_4)_4 \cdot 22H_2O$	
	$Mn_2(OH)_3$+(aq)		$MgCO_3$	
	$Mn2OH^{+3}$(aq)		$MgCO3 \cdot 3H_2O$	
	$MnHCO_3^+$(aq)		$MgSO_4$	
	$MnHSO_4$+(aq)		$MgSO_4 \cdot 7H_2O$	
	Na^+(aq)		$Mn(OH)_2$	
		MnO(aq)	$MnCO_3$	
	CO_2(aq)	AlO_2H(aq)	$MnSO_4$	
	$CaCO_3$(aq)	$MgCO_3$(aq)	$Na_2Ca(CO_3)_2 \cdot 2H_2O$	

The results of the Talvivaara leachate model show clear agreement with observed Ca^{+2}, Al^{+3} and SO_4^{-2} concentrations. The sulfate concentrations are higher at the beginning of the process as the mass balance reported in Hietala and Härmä did not fully agree. Thus an additional amount of sulfate is used as model input. When observing the iron concentration, the unwanted early precipitation of Fe^{+3} is avoided as the formation enthalpy of $Fe(OH)_3$ is slightly adjusted when compared to standard values (e.g., -830 kJ/mol in HSC and -817 kJ/mol in this study). With this adjustment, the behaviour of ferric and ferro iron is fitted into the model. The precipitation of manganese is occurring earlier in the model than in the real process. An explanation could be the two different oxidation states of manganese, +2 and +3. Even the Hietala and Härmä (2012) report indicated all manganese as Mn^{+2}. The model further predicts that magnesium will precipitate later at the final process stage, when the pH is elevated with lime. In the real process, magnesium is constantly precipitating from the aqueous solution. Co-precipitation of magnesium should be studied in order to evaluate this tendency better. Finally, it can be seen that the sodium concentration is lower in the model than in the real process. This will also have an effect on the sulfate concentration after the final stage. In the model, the sodium is added at the Ni/Co-precipitation for controlling pH. It is obvious that in the actual process there might be additional sources of sodium that have not been reported by Hietala and Härmä (2012).

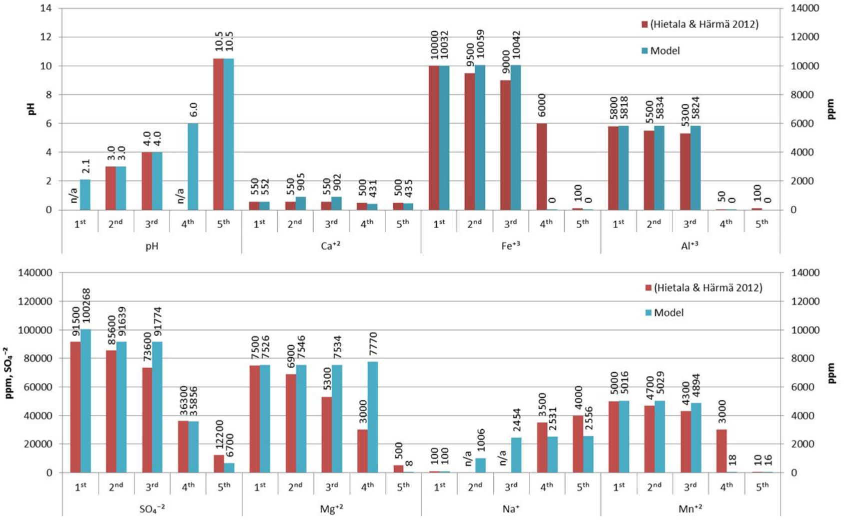

Figure 31. Composition of Talvivaara leachate before treatment pre-neutralisation (1st), after pre-neutralisation with limestone (2nd), after Ni/Co-precipitation (3rd), and after iron precipitation (4th), and after final neutralisation (5th). Validation data by Hietala and Härmä (2012).

15.4 Models for hydrometallurgical precipitations

Most metal ions form specific stoichiometric compounds once the pH of the solution exceeds a compound-specific threshold, making it possible to selectively separate metals by controlling the pH. Thus, the potentiometric fractionation of metals is conventional practice in hydrometallurgy. Combined with multi-component speciation models, the potentiometric (pH) titration curves may also be used to support a more detailed understanding of the metal-infused solution and its pH buffering properties, e.g., in the presence of various amounts of CO_2 containing gas in the system (Figure 32).

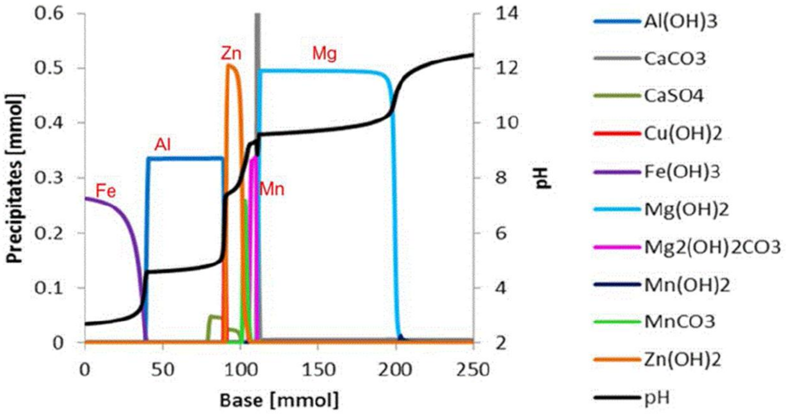

Figure 32. Order, identity, and magnitude of precipitates formed during titration according to ChemSheet simulation. The amount of carbon dioxide in the model has been adjusted to fit the experimental findings. From Salminen et al. (2015).

As an example of a more challenging multicomponent process, the recovery of rare earth compounds from an in-situ-leaching system was considered. While the AMD problems typically consist of a rather simple, 3 or 4-stage pH-dependent precipitation processes with a limited number of metal cations, a rare earth recovery process that has also been studied is more complicated due to the very nature of its including a large number of both metal cations and both their neutral and charged hydrocomplexes.

Ural Federal University (UrFU) and VTT have performed joint research on the development of industrial technologies for the extraction of Rare Earth Elements (REE) and scandium from phosphogypsum and Uranium ISL leachate solutions (Mashkovtsev et al., 2016). Leaching-absorption experiments at UrFU have been supported with a multicomponent solution modelling by VTT. The simulations have been performed with VTT's ChemSheet and Balas programs.

Thermodynamic equilibrium calculations were used in the model wherever possible (precipitation-clarification modules). The thermodynamic data system was for this purpose also extended to include aqueous and solid rare earth (RE) species. For the adsorption, washing and desorption stages with an ion exchange resin however, the equilibrium approach could not be used and the distribution coefficients were deduced and applied based on experimental data (Figure 33).

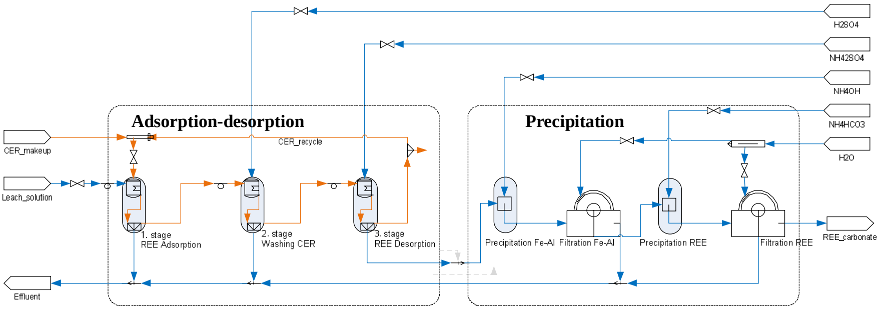

Figure 33. The process for recovering rare earth compounds. Thermodynamic model of aqueous suspension applied for the precipitation process steps.

The final stage of the process model contains precipitation of the RE carbonates. The RE concentrations in the solution before precipitation are typically below 1 mM, but the sulphate concentrations are around 2 M. The initial model attempt ignored the RE-sulphate interactions within the Pitzer formalism and was unable to predict the precipitation behaviour both in laboratory test and in the full extraction model.

With the RE-SO_4 interactions included (based on Al_3+/Fe_3+-SO_4^{2-} data (Christov, 2004)), the model was able to give a reasonable match for both laboratory experiments on RE carbonate precipitation and within the flowsheet model of the extraction process. An alternative published parameter set determined for Am^{3+}-SO_4^{2-} system (Rai et al., 1995), but not tested for high concertation solubility calculations, predicted far lower activity coefficients and did not match the observed RE-CO_3^{2-} precipitation behaviour.

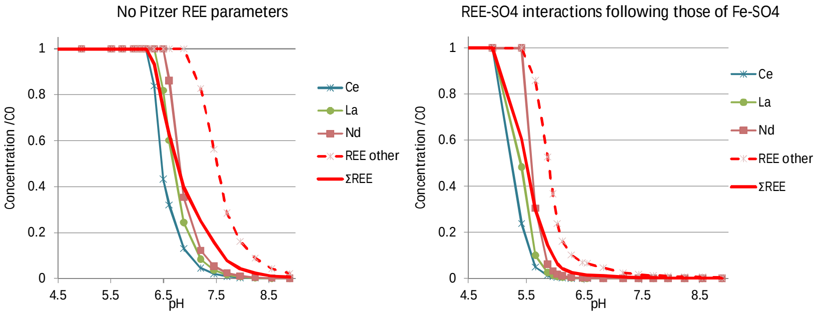

Figure 34. Effect of the applied Pitzer parameters based on Fe-SO_4^{2+} interactions shown for RE- CO_3^{2} precipitation in a sulphate rich solution.

15.5 Summary of application examples

The systems as explained above have been developed for various hydrometallurgical and ‘wet cleantech’ applications. The need for improved chemistry and pH control is common for all these applications, which occur in aqueous media and focus on treatment of gases, salts, brines and metalliferous ores. The up-to-date status of digitalised solubility data (including the values of the necessary activity parameters) together with the Gibbs free energy solvers allows for the solution of the ionic state and pH of such systems with reasonable accuracy. Due to their their rigorous thermodynamic background, the models can be also used for mass and energy balances and prediction of improved and new chemistry concepts.

The industrial applications range from the control of mine water effluents to metal management in ion-exchanging pulp suspensions, thus covering both many processes in hydrometallurgy as well as those of pulp bleaching and paper-making, including the lime recirculation. Novel solutions are being developed for the recovery of alkali and sulfur chemicals in both forest and mining industries. A challenging new field is the application of advanced hydrometallurgical models in both complex waste water treatment (such as precipitation processes based on usage of aluminium or barium chemicals). In developing hydrometallurgical precipitation processes, the multicomponent multiphase models may also open new possibilities by providing additional know-how of pH and redox conditions and serving as a rail-guide for optional fractionation methods.

16. Conclusions

Within this report, a basic theory of modelling concentrated aqueous solutions based on thermodynamic approach is given. For complex industrial solutions appearing in a variety of pH ranges and in changing temperatures, it is important to take into account the non-ideality of the solutions to gain reliable results with engineering calculations. The primary emphasis has been given to the well-known Pitzer formalism for describing the activity coefficients in the concentrated aqueous solutions. An extended database of Pitzer parameters, as collected and assessed during ~15 years of research have been enlisted. The distinct feature is the incorporation of temperature-dependent parameters ranging from 25°C to 95°C. The database then allows for reliable, predictive simulations of the major metal cations commonly found in industrial sulphate, carbonate and chloride solutions. The database can also incorporate solubility data of complex salts and mineral compounds from selected international geochemical databases.

The data is used in multicomponent reactor modules, which are are connected to modular process modelling software typically used in chemical and process engineering. Alternative dosage for neutralisation, pH control and solubility controls, as well as optional connections in a multi-stage hydrometallurgical plant or within a set of water treatment units, can be simulated with reasonable accuracy. Model-based experimentation helps to reduce the costs of process development and allows for significant savings in time and resources when new chemistry options are evaluated. The models thus provide a fast and inexpensive tool for both troubleshooting and problem solving as well as for developing new economical and environmentally benign approaches for industrial and mine water management.

References

Abraham, M., 1981. L'activité d'un sel à hautes concentrations dans l'eau pure. J. Chim. Phys. 78, 57–59.

AF Colenco, GRS, HZDR-IRC, KIT-INE, TU-BAF, 2011. Thermodynamische Referenz-Datenbasis.

Allison, J.D., Brown, D.S., Novo-Gradac, K.J., 1991. MINTEQA2/PRODEFA2, A Geographical Assessment Model For Environmental Systems: Version 3.0 User's Manual. Athens, Georgia.

Ally, M.R., 1999. Solute and Solvent Activities of CaCl2(aq) Solutions from the Adsorption Isotherm Treatment. J. Chem. Eng. Data 44, 792–797. doi:10.1021/je980296c

Ally, M.R., Braunstein, J., 1993. BET model for calculating activities of salts and water, molar enthalpies, molar volumes and liquid-solid phase behavior in concentrated electrolyte solutions. Fluid Phase Equilib. 87, 213–236. doi:10.1016/0378-3812(93)85028-K

Ally, M.R., Braunstein, J., 1996. Activity coefficients in concentrated electrolytes: a comparison of the Brunauer-Emmett-Teller (BET) model with experimental values. Fluid Phase Equilib. 120, 131–141. doi:10.1016/0378-3812(95)02977-X

Ally, M.R., Braunstein, J., 1998. Statistical mechanics of multilayer adsorption: electrolyte and water activities in concentrated solutions. J. Chem. Thermodyn. 30, 49–58. doi:10.1006/jcht.1997.0278

Andra, 2015. Thermo-Chimie (version applicative 4.3.0) [WWW Document].

Aqueous Solutions LLC, 2015. The Geochemist's Workbench [WWW Document].

Archer, D.G., 1991. Thermodynamic Properties of the NaBr + H2O System. J. Phys. Chem. Ref. data 20, 509–555.

Archer, D.G., 1991. Thermodynamic Properties of the NaBr+H2O System. J. Phys. Chem. Ref. Data 20, 509. doi:10.1063/1.555888

Archer, D.G., 1992. Thermodynamic Properties of the NaCl+H2O System. II. Thermodynamic Properties of NaCl(aq), NaCl□2H2O(cr), and Phase Equilibria. J. Phys. Chem. Ref. Data 21, 793. doi:10.1063/1.555915

Baes, C., Mesmer, R., 1986. The Hydrolysis of Cations. Krieger publishing company, Malabar, Florida.

Bale, C.W., Bélisle, E., Chartrand, P., Decterov, S. a., Eriksson, G., Hack, K., Jung, I.-H., Kang, Y.-B., Melançon, J., Pelton, a. D., Robelin, C., Petersen, S., 2009. FactSage thermochemical software and databases — recent developments. Calphad 33, 295–311. doi:10.1016/j.calphad.2008.09.009

Bale, C.W., Chartrand, P., Degterov, S.A., Eriksson, G., Hack, K., Ben Mahfoud, R., Melançon, J., Pelton, A.D., Petersen, S., 2002. FactSage thermochemical software and databases. Calphad 26, 189–228. doi:10.1016/S0364-5916(02)00035-4

Ball, J.W., Nordstrom, D.K., 1991. User â€™ S Manual for Wateq4F , With Revised Thermodynamic Data Base and Test Cases for Calculating Speciation of Major , Trace , and Redox Elements in Natural Waters.

Bassett, H., Watt, W., 1950. 289. Pickeringite and the system MgSO4 –Al2(SO4)3-H2O. J. Chem. Soc. 1408–1414. doi:10.1039/JR9500001408

Belov, G., Iorish, V., Yungman, V., 1999. IVTANTHERMO for Windows—database on thermodynamic properties and related software. Calphad 23, 173–180.

Bethke, C.M., Yeakel, S., 2015. The Geochemist'sWorkbench® Release 10.0 - Reference Manual.

Bhattacharia, S.K., Hossain, N., Chen, C.C., 2015. Thermodynamic modeling of aqueous Na^+-K^+-Cl^--SO<inf>4</inf>$^{2-}$ quaternary system with electrolyte NRTL model. Fluid Phase Equilib. 403, 1–9. doi:10.1016/j.fluid.2015.05.045

Bialik, M.A., Theliander, H., Sedin, P., Verrill, C.L., Demartini, N., 2008. Solubility and Solid-Phase Composition in Na2CO3-Na2SO4 Solutions at Boiling Temperature : A Modeling Approach. Ind. Eng. Chem. Res. 47, 3233–3238. doi:10.1021/ie071436r

Biedermann, G., Chow, J.T., 1966. Studies on the hydrolysis of metal ions. Acta Chem. Scand. 20, 1376–1388.

Blanc, P., Lassin, A., Piantone, P., Azaroual, M., Jacquemet, N., Fabbri, A., Gaucher, E.C., 2012. Thermoddem: A geochemical database focused on low temperature water/rock interactions and waste materials. Appl. Geochemistry 27, 2107–2116. doi:10.1016/j.apgeochem.2012.06.002

Block, J., Waters, O.B., 1968. Calcium sulfate-sodium sulfate-sodium chloride-water system at 25.deg. to 100.deg. J. Chem. Eng. Data 13, 336–344. doi:10.1021/je60038a011

Bock, E., 1961. ON THE SOLUBILITY OF ANHYDROUS CALCIUM SULPHATE AND OF GYPSUM IN CONCENTRATED SOLUTIONS OF SODIUM

CHLORIDE AT 25 °C, 30 °C, 40 °C, AND 50 °C. Can. J. Chem. 39, 1746–1751. doi:10.1139/v61-228

Bukshtein, V.M., Valyashko, M.G., D., P.A. (Eds.), 1953. Spravochnik po rastvorimosti solevykh sistem (A reference book of solubilities of salt systems) Vols. I and II. Izdatelstvo Vsesujuznuvo Nauchnovo-Issledstvono Instituta Goz., Goskhimizdat., Moscow-Leningrad.

Caiani, P., Conti, G., Gianni, P., Matteoli, E., 1989. Apparent molar heat capacity and relative enthalpy of aqueous sodium hydroxoaluminate between 323 and 523 K. J. Solution Chem. 18, 447–461. doi:10.1007/BF00657332

Carter, R., Pierson, K.L., Reynolds, J.G., 2014. Binary Pitzer Model Parameters for Predicting the Solubility of Key Electrolytes in Hanford Waste, in: Waste Management Symposium. Phoenix.

Chen, C.-C., Song, Y., 2004. Generalized electrolyte-NRTL model for mixed-solvent electrolyte systems. AIChE J. 50, 1928–1941. doi:10.1002/aic.10151

CHESS, 2015. Home — Chess [WWW Document].

Christov, C., 1994. Thermodynamic study of (b1RbCl + b2MeCl2)(aq), where b denotes molality and Me denotes Mn, Co, Ni, or Cu, at the temperature 298.15 K, on the basis of Pitzer's model. J. Chem. Thermodyn. 26, 1071–1080. doi:10.1006/jcht.1994.1125

Christov, C., 2002. Thermodynamics of formation of ammonium, sodium and potassium alums and chromium alums. Calphad 26, 85–94. doi:10.1016/S0364-5916(02)00026-3

Christov, C., 2004. Pitzer ion-interaction parameters for Fe(II) and Fe(III) in the quinary {Na+K+Mg+Cl+SO4+H2O} system at T=298.15 K. J. Chem. Thermodyn. 36, 223–235. doi:10.1016/j.jct.2003.11.010

Christov, C., Dickson, A.G., Møller, N., 2007. Thermodynamic Modeling of Aqueous Aluminum Chemistry and Solid-Liquid Equilibria to High Solution Concentration and Temperature. I. The Acidic H-Al-Na-K-Cl-H2O System from 0 to 100 °C. J. Solution Chem. 36, 1495–1523. doi:10.1007/s10953-007-9191-9

Clegg, S.L., Milioto, S., Palmer, D.A., 1996. Osmotic and Activity Coefficients of Aqueous (NH4)2SO4 as a Function of Temperature, and Aqueous (NH4)2S 4 −H2SO4 Mixtures at 298.15 K and 323.15 K. J. Chem. Eng. Data 41, 455–467. doi:10.1021/je950289d

Clegg, S.L., Rard, J. a., Pitzer, K.S., 1994. Thermodynamic properties of 0?6 mol kg?1 aqueous sulfuric acid from 273.15 to 328.15 K. J. Chem. Soc. Faraday Trans. 90, 1875–1894. doi:10.1039/ft9949001875

Clegg, S.L., Simonson, J.M., 2001. A BET model of the thermodynamics of aqueous multicomponent solutions at extreme concentration. J. Chem. Thermodyn. 33, 1457–1472. doi:10.1006/jcht.2001.0869

Clegg, S.L., Whitfield, M., 1995. A chemical model of seawater including dissolved ammonia and the stoichiometric dissociation constant of ammonia in estuarine water and seawater from −2 to 40°C. Geochim. Cosmochim. Acta 59, 2403–2421. doi:10.1016/0016-7037(95)00135-2

Deng, T.L., Zhou, H., Xia, C., 2013. Salt-Water System Phase Diagram and Its Application. Chemical Industry Press, Beijing.

Diakonov, I.I., Ragnarsdottir, K. V., Tagirov, B.R., 1998. Standard thermodynamic properties and heat capacity equations of rare earth hydroxides:: II. Ce(III)-, Pr-, Sm-, Eu(III)-, Gd-, Tb-, Dy-, Ho-, Er-, Tm-, Yb-, and Y-hydroxides. Comparison of thermochemical and solubility data. Chem. Geol. 151, 327–347. doi:10.1016/S0009-2541(98)00088-6

Dirkse, T.P. (Ed.), 1986. IUPAC Solubility Data Series Vol. 23. Pergamon Press.

Donnan, F.G., Harris, A.B., 1911. CLXXVII.—The osmotic pressure and conductivity of aqueous solutions of congo-red, and reversible membrane equilibria. J. Chem. Soc., Trans. 99, 1554–1577. doi:10.1039/CT9119901554

Duchesne, J., Reardon, E.J., 1995. Measurement and prediction of portlandite solubility in alkali solutions. Cem. Concr. Res. 25, 1043–1053. doi:10.1016/0008-8846(95)00099-X

Environmental Research Software, 2015. MINEQL+ Chemical Equilibrum Modeling System [WWW Document].

Eriksson, G., 1975. Thermodynamic studies of high-temperature equilibria. XII. SOLGASMIX, a computer-program for calculation of equilibrium compositions in multiphase systems. Chem. Scr. 8, 100–103.

Eriksson, G., Königsberger, E., 2008. FactSage and ChemApp: Two tools for the prediction of multiphase chemical equilibria in solutions. Pure Appl. Chem. 80, 1293–1302. doi:10.1351/pac200880061293

Ervin, G., Giorgi, A.L., McCarthy, C.E., 1944. The System Potassium Carbonate-Sodium Carbonate-Water at 100 and 150°. J. Am. Chem. Soc. 66, 384–387. doi:10.1021/ja01231a020

Felmy, A.R., Rai, D., 1999. Application of Pitzer's Equations for Modeling the

Aqueous Thermodynamics of Actinide Species in Natural Waters: A Review. J. Solution Chem. 28, 533–553. doi:10.1023/A:1022630931742

Filippov, V.K., Cheremnykh, L.M., 1983. No Title. Russ. J. Appl. Chem. 56, 1475.

Freeth, F.A., 1923. The System: Na2O-CO2-NaCl-H2O, Considered as Two Four-Component Systems. Philos. Trans. R. Soc. London. Ser. A, Contain. Pap. a Math. or Phys. Character 223, 35–87.

Freyer, D., Voigt, W., 2004. The measurement of sulfate mineral solubilities in the Na-K-Ca-Cl-SO4-H2O system at temperatures of 100, 150 and 200°C. Geochim. Cosmochim. Acta 68, 307–318. doi:10.1016/S0016-7037(03)00215-1

Geldenhuys, a. J., Maree, J.P., de Beer, M., Hlabela, P., 2003. An integrated limestone/lime process for partial sulphate removal. J. South Aafrican Institue Min. Metall. 345–354.

Gems Development Team, 2015. GEM Software Main Page.

GEOPIG - Arizona State University, 2015. slop15.dat; SUPCRT 2015 update.

Giffaut, E., Grivé, M., Blanc, P., Vieillard, P., Colàs, E., Gailhanou, H., Gaboreau, S., Marty, N., Madé, B., Duro, L., 2014. Andra thermodynamic database for performance assessment: ThermoChimie. Appl. Geochemistry 49, 225–236. doi:10.1016/j.apgeochem.2014.05.007

Gonçalves, B.C., Tran, H., Braz, S., Puig, F., Shenassa, R., 2008. Chlorine and potassium removal efficiency of an ash leaching system. Pulp Pap. Canada 3, 33–38.

Green, S.J., Frattali, F.J., 1946. The System Sodium Carbonate-Sodium Sulfate-Sodium Hydroxide-Water at 100 °C. J. Am. Chem. Soc. 68, 1789.

Greenberg, J.P., Møller, N., 1989. The prediction of mineral solubilities in natural waters: A chemical equilibrium model for the Na-K-Ca-Cl-SO4-H2O system to high concentration from 0 to 250°C. Geochim. Cosmochim. Acta 53, 2503–2518. doi:10.1016/0016-7037(89)90124-5

Grenthe, I., Fuger, J., Konings, R.J.M., Lemire, R.J., Muller, A.B., Nguyen-Trung, C., Wanner, H., Forest, I., Chairman, I.G., Fuger, J., Lemire, R.J., Canada, M., Muller, A.B., Wanner, H., Forest, I., 2004. CHEMICAL THERMODYNAMICS OF URANIUM Edited by 735.

Guillaumont, R., Fanghänel, T., Fuger, J., Grenthe, I., Palmer, D.A., Rand, M.H., 2003. Update on the chemical thermodynamics of uranium, neptunium, plutonium, americium and technetium. OECD Nuclear Energy Agency, Issyles-Moulineaux, France.

Hamer, W.J., Wu, Y.-C., 1972. Osmotic Coefficients and Mean Activity Coefficients of Uni-univalent Electrolytes in Water at 25°C. J. Phys. Chem. Ref. Data 1, 1047–1099. doi:10.1063/1.3253108

Harvie, C.E., Møller, N., Weare, J.H., 1984. The prediction of mineral solubilities in natural waters: The Na-K-Mg-Ca-H-Cl-SO4-OH-HCO3-CO3-CO2-H2O system to high ionic strengths at 25°C. Geochim. Cosmochim. Acta 48, 723–751. doi:10.1016/0016-7037(84)90098-X

Haynes, H.W., 2003. Thermodynamic solution model for trona brines. AIChE J. 49, 1883–1894. doi:10.1002/aic.690490724

Hernández-Luis, F., Fernández-Mérida, L., Esteso, M.A., Galleguillos-Castro, H.R., 1997. Thermodynamic study of the NaCl + MgCl2 + H2O mixed system by emf measurements at different temperatures. Berichte der Bunsengesellschaft für Phys. Chemie 101, 1136–1145. doi:10.1002/bbpc.19971010809

Hietala, J., Härmä, T., 2012. Talvivaaran kaivoksen toiminnan kuvaus.

Hill, A.E., Bacon, L.R., 1927. TERNARY SYSTEMS. VI. SODIUM CARBONATE, SODIUM BICARBONATE AND WATER. J. Am. Chem. Soc. 49, 2487–2495. doi:10.1021/ja01409a018

Hill, A.E., Miller, F.W., 1927. TERNARY SYSTEMS. IV. POTASSIUM CARBONATE, SODIUM CARBONATE AND WATER. J. Am. Chem. Soc. 49, 669–686. doi:10.1021/ja01402a010

Holmes, H.F., Mesmer, R.E., 1986. Thermodynamics of aqueous solutions of the alkali metal sulfates. J. Solution Chem. 15, 495–517. doi:10.1007/BF00644892

Holmes, H.F., Mesmer, R.E., 1994. An isopiestic study of {(1 - y)NaHSO4 + yNa2SO4}(aq) at elevated temperatures. J. Chem. Thermodyn. 26, 581–594. doi:10.1006/jcht.1994.1067

Holmes, H.F., Mesmer, R.E., 1996. An isopiestic study of aqueous solutions of the alkali metal hydrogensulfates at elevated temperatures. J. Chem. Thermodyn. 28, 67–81. doi:10.1006/jcht.1996.0007

Hovey, J.K., Pitzer, K.S., Rard, J.A., 1993. Thermodynamics of Na2SO4(aq) at temperatures T from 273 K to 373 K and of {(1-y)H2SO4+yNa2SO4}(aq) at T = 298.15 K. J. Chem. Thermodyn. 25, 173–192. doi:10.1006/jcht.1993.1016

HydroGeoLogic Inc, Allison Geoscience Consultants Inc., 1998.

MINTEQA2/PRODEFA2, A Geochemical Assessment Model for Environmental Systems: User Manual Supplement for Version 4.0 1998, 76.

Hämäläinen, M., Rannikko, H., Sippola, H., 1991. Vesiliuossysteemien termodynaaminen mallitus, Report TKK-V-C108. Otaniemi.

INAP, 2003. Treatment of Sulphate in Mine Effluents.

Itkina, L.S., Kokhova, V.F., 1953. Solubility isotherm of the system Na2SO4–Na2CO3–NaCl–NaOH–H2O at 25 °C. Izvest. Sekt. Fiz. Khim. Anal. Akad. Nauk S.S.S.R. 23, 20–54.

IVANTHERMO, 2004. IVANTHERMO DOWNLOADS.

Johnson, J.W., Oelkers, E.H., Helgeson, H.C., 1992. SUPCRT92: A software package for calculating the standard molal thermodynamic properties of minerals, gases, aqueous species, and reactions from 1 to 5000 bar and 0 to 1000°C. Comput. Geosci. 18, 899–947. doi:10.1016/0098-3004(92)90029-Q

Joint Expert Speciation System, 2015. JOINT EXPERT SPECIATION SYSTEM [WWW Document].

Kalliola, A., Pajarre, R., Koukkari, P., Hakala, J., Kukkamäki, E., 2012. Multi-phase thermodynamic modelling of pulp suspensions: Application to a papermaking process. Nord. Pulp Pap. Res. J. 27, 613–620. doi:10.3183/NPPRJ-2012-27-03-p613-620

Kangas, P., Pajarre, R., Nappa, M., Koukkari, P., 2012. Multi-phase thermodynamic modelling of pulp suspensions: Review of the methodology. Nord. Pulp Pap. Res. J. 27, 604–612. doi:10.3183/NPPRJ-2012-27-03-p604-612

Kim, H.T., Frederick, W.J., 1988. Evaluation of Pitzer ion interaction parameters of aqueous mixed electrolyte solutions at 25.degree.C. 2. Ternary mixing parameters. J. Chem. Eng. Data 33, 278–283. doi:10.1021/je00053a017

Konno, H., Nanri, Y., Kitamura, M., 2002. Crystallization of aragonite in the causticizing reaction. Powder Technol. 123, 33–39. doi:10.1016/S0032-5910(01)00424-7

Kosinski, J.J., Wang, P., Springer, R.D., Anderko, A., 2007. Modeling acid–base equilibria and phase behavior in mixed-solvent electrolyte systems. Fluid Phase Equilib. 256, 34–41. doi:10.1016/j.fluid.2006.11.018

Koukkari, P., Kalliola, A., Pajarre, R., Manninen, J., Hakala, J., Rimpinen, O., Nuortila-Jokinen, J., Kukkamäki, E., 2007. Control of pH and calcium chemistry with multiphase modelling, in: PTS Symposium Modelling and Simulation of the Wet End Processes. Munich, pp. 1–12.

Koukkari, P., Pajarre, R., Blomberg, P., 2011. Reaction rates as virtual constraints in Gibbs energy minimization. Pure Appl. Chem. 83, 1063–1074. doi:10.1351/PAC-CON-10-09-09

Koukkari, P., Pajarre, R., Pakarinen, H., Salminen, J., 2001. Practical Multiphase Models for Aqueous Process Solutions. Ind. Eng. Chem. Res. 40, 5014–5020. doi:10.1021/ie010236r

Koukkari, P., Penttilä, K., Hack, K., Petersen, S., 2005. CHEMSHEET – An Efficient Worksheet Tool for Thermodynamic Process Simulation, in: Bréchet, Y. (Ed.), Microstructures, Mechanical Properties and Processes, EUROMAT. Wiley-VCH Verlag GmbH & Co. KGaA, Weinheim, pp. 323–330. doi:10.1002/3527606157.ch51

Koukkari, P., Sippola, H., Sundquist, A., 1994. Multicomponent equilibrium calculations in process design: study of some acid digester reactors, in: Hydrometallurgy '94. Springer Netherlands, Dordrecht, pp. 139–157. doi:10.1007/978-94-011-1214-7_8

Koukkari, P.S., Liukkonen, S.S., 2002. Calculation of Entropy Production in Process Models. Ind. Eng. Chem. Res. 41, 2931–2940. doi:10.1021/ie010498t

Kulik, D. a., Wagner, T., Dmytrieva, S. V., Kosakowski, G., Hingerl, F.F., Chudnenko, K. V., Berner, U.R., 2013. GEM-Selektor geochemical modeling package: Revised algorithm and GEMS3K numerical kernel for coupled simulation codes. Comput. Geosci. 17, 1–24. doi:10.1007/s10596-012-9310-6

Königsberger, E., 2001. Prediction of electrolyte solubilities from minimal thermodynamic information. Monatshefte fur Chemie 132, 1363–1386. doi:10.1007/s007060170022

Königsberger, E., May, P.M., Hefter, G.T., 2006. Comprehensive model of synthetic bayer liquors. Part 3. Sodium aluminate solutions and the solubility of gibbsite and boehmite. Monatshefte fur Chemie 137, 1139–1149. doi:10.1007/s00706-006-0526-9

Larsson, M., 2012. Calculation tool for the treatment of electrostatic precipitator ash in Metso ' s ash leaching process (Master's thesis). Chalmers University of Technology.

Li, Z., Pitzer, K.S., 1996. Thermodynamics of aqueous KOH over the full range to saturation and to 573 K. J. Solution Chem. 25, 813–823. doi:10.1007/BF00972574

Lin, Y., Kate, A. ten, Mooijer, M., Delgado, J., FosbÃ¸l, P.L., Thomsen, K., 2009.

Comparison of activity coefficient models for electrolyte systems. AIChE J. 56, 1334–1351. doi:10.1002/aic.12040

Lindberg, D., Backman, R., Chartrand, P., 2006. Thermodynamic evaluation and optimization of the (Na2SO4+K2SO4+Na2S2O7+K2S2O7) system. J. Chem. Thermodyn. 38, 1568–1583. doi:10.1016/j.jct.2006.04.002

Lindberg, D., Backman, R., Chartrand, P., 2007. Thermodynamic evaluation and optimization of the (Na2CO3+Na2SO4+Na2S+K2CO3+K2SO4+K2S) system. J. Chem. Thermodyn. 39, 942–960. doi:10.1016/j.jct.2006.11.002

Lindberg, R., Runnells, D., 1984. Ground Water Redox Reactions: An Analysis of Equilibrium State Applied to Eh Measurements and Geochemical Modeling. Science (80-.). 225, 925–927. doi:10.1126/science.225.4665.925

Linke, W.F., 1965. Solubilities of Inorganic, and Metal Organic Compounds (vols 1 and 2), 4th ed. American Chemical Society, Washington D. C.

Lothenbach, B., Matschei, T., Möschner, G., Glasser, F.P., 2008. Thermodynamic modelling of the effect of temperature on the hydration and porosity of Portland cement. Cem. Concr. Res. 38, 1–18. doi:10.1016/j.cemconres.2007.08.017

Makarov, S.Z., Blidin, V.P., 1938. The polytherm of quaternary system Na2Co3 – Na2So4-NaCl-H2O and solid solutions of Berkeite type (in Russian). Bull. l'Académie des Sci. l'URSS. Cl. des Sci. mathématiques Nat. 865–892.

Mariner, P., 2003. In-Drift Precipitates/Salts Model. Las Vegas, Nevada. doi:10.2172/828239

Marion, G.M., 2001. Carbonate mineral solubility at low temperatures in the Na-K-Mg-Ca-H-Cl-SO4-OH-HCO3-CO3-CO2-H2O system. Geochim. Cosmochim. Acta 65, 1883–1896. doi:10.1016/S0016-7037(00)00588-3

Marion, G.M., Kargel, J.S., Catling, D.C., 2008. Modeling ferrous-ferric iron chemistry with application to martian surface geochemistry. Geochim. Cosmochim. Acta 72, 242–266. doi:10.1016/j.gca.2007.10.012

Marshall, W.L., Jones, E. V., 1966. Second Dissociation Constant of Sulfuric Acid from 25 to 350C Evaluated from Solubilities of Calcium Sulfate in Sulfuric Acid Solutions. J. Phys. Chem. 70, 4028–4040. doi:10.1021/j100884a045

Marshall, W.L., Slusher, R., Jones, E. V., 1964. Aqueous Systems at High Temperatures XIV. Solubility and Thermodynamic Relationships for CaSO 4 in NaCl-H 2 O Solutions from 40o to 200o C., 0 to 4 Molal NaCl. J. Chem. Eng. Data 9, 187–191. doi:10.1021/je60021a011

Martell, A.E., Smith, R.M., 1989. Critical stability constants: Second Supplement, Vol. 6. Plenum Press, New York.

Mashkovtsev, M., Botalov, M., Smyshlyaev, D., Pajarre, R., Kangas, P., Rychkov, V., Koukkari, P., 2016. Pilot-scale recovery of rare earths and scandium from phosphogypsum and uranium leachates, in: Mineral Engineering Conference. Swieradow-Zdroj, Poland.

Matschei, T., Lothenbach, B., Glasser, F.P., 2007. Thermodynamic properties of Portland cement hydrates in the system CaO-Al2O3-SiO2-CaSO4-CaCO3-H2O. Cem. Concr. Res. 37, 1379–1410. doi:10.1016/j.cemconres.2007.06.002

May, P.M., 2015. JESS at thirty: Strengths, weaknesses and future needs in the modelling of chemical speciation. Appl. Geochemistry 55, 3–16. doi:10.1016/j.apgeochem.2014.11.023

Moog, H.C., Bok, F., Marquardt, C.M., Brendler, V., 2015. Disposal of nuclear waste in host rock formations featuring high-saline solutions – Implementation of a thermodynamic reference database (THEREDA). Appl. Geochemistry 55, 72–84. doi:10.1016/j.apgeochem.2014.12.016

Mosgovykh, G. Ya.; Nurkeev, S. S.; Romanov, L. G.; Zaripova, A., 1984. No Title. Zhurnal Prikl. Khimii 57, 2104–2107.

Moshinskii, A.S., Chibizov, V.P., 1975. No Title. Zhurnal Prikl. Khimii 48, 2186–2190.

Moučka, F., Lísal, M., Smith, W.R., 2012. Molecular Simulation of Aqueous Electrolyte Solubility. 3. Alkali-Halide Salts and Their Mixtures in Water and in Hydrochloric Acid. J. Phys. Chem. B 116, 5468–5478. doi:10.1021/jp301447z

Møller, N., 1988. The prediction of mineral solubilities in natural waters: A chemical equilibrium model for the Na-Ca-Cl-SO4-H2O system, to high temperature and concentration. Geochim. Cosmochim. Acta 52, 821–837. doi:10.1016/0016-7037(88)90354-7

OECD, 2014. Thermochemical Database (TDB) Project [WWW Document].

OLI Systems Inc, 2015. OLI Systems home page [WWW Document].

OLI Systems Inc., 2016. OLI Engine + Alliance Partners [WWW Document].

Outokumpu Research, 1999. HSC Chemistry 4.0.

Outotec, 2015. HSC Chemistry [WWW Document].

Outotec Research, 2011. HSC Chemistry 7.1.

Outotec Research, 2015. HSC Chemistry 8.1.

Pabalan, R.T., Pitzer, K.S., 1987. Thermodynamics of concentrated electrolyte mixtures and the prediction of mineral solubilities to high temperatures for mixtures in the system Na-K-Mg-Cl-SO4-OH-H2O. Geochim. Cosmochim. Acta 51, 2429–2443. doi:10.1016/0016-7037(87)90295-X

Pajarre, R., Koukkari, P., Kangas, P., 2016. Constrained and extended free energy minimisation for modelling of processes and materials. Chem. Eng. Sci. 146, 244–258. doi:10.1016/j.ces.2016.02.033

Pajarre, R., Koukkari, P., Penttilä, K., Kangas, P., Penttilä, K., Koukkari, P., 2008. Industrial Applications of Multi-Phase Thermochemical Simulation. Comput. Aided Chem. Eng. 25, 883–888. doi:http://dx.doi.org/10.1016/S1570-7946(08)80153-8

Pajarre, R., Koukkari, P., Räsänen, E., 2006. Inclusion of the Donnan effect in Gibbs energy minimization. J. Mol. Liq. 125, 58–61. doi:10.1016/j.molliq.2005.11.016

Pallagi, A., Tasi, Á., Gácsi, A., Csáti, M., Pálinkó, I., Peintler, G., Sipos, P., 2011. The solubility of Ca(OH)2 in extremely concentrated NaOH solutions at 25°C. Cent. Eur. J. Chem. 10, 332–337. doi:10.2478/s11532-011-0145-0

Parkhurst, D.L., Appelo, C. a. J., 2013. Description of Input and Examples for PHREEQC Version 3 — A Computer Program for Speciation , Batch-Reaction , One-Dimensional Transport , and Inverse Geochemical Calculations. U.S. Geological Survey Techniques and Methods, book 6, chapter A43, U.S. Geological Survey Techniques and Methods, book 6, chapter A43. U.S. Geological Survey.

Peiper, J.C., Pitzer, K.S., 1982. Thermodynamics of aqueous carbonate solutions including mixtures of sodium carbonate, bicarbonate, and chloride. J. Chem. Thermodyn. 14, 613–638. doi:10.1016/0021-9614(82)90078-7

Petersen, S., Hack, K., 2007. The thermochemistry library ChemApp and its applications. Int. J. Mater. Res. 98, 935–945.

Phutela, R.C., Pitzer, K.S., 1986. Heat capacity and other thermodynamic properties of aqueous magnesium sulfate to 473 K. J. Phys. Chem. 90, 895–901. doi:10.1021/j100277a037

Picot, J.B., Mortha, G., Rueff, M., Nortier, P., 2012. A thermodynamically consistent model for burkeite solubility. Chem. Eng. Sci. 68, 383–391.

doi:10.1016/j.ces.2011.09.047

Pitzer, K.S., 1986. Theoretical considerations of solubility with emphasis on mixed aqueous electrolytes. Pure Appl. Chem. 58, 1599–1610. doi:10.1351/pac198658121599

Pitzer, K.S., 1995. Thermodynamics, 3rd ed. McGraw-Hill, Singapore.

Pitzer, K.S., Silvester, L.F., 1978. Thermodynamics of electrolytes. 11. Properties of 3:2, 4:2, and other high-valence types. J. Phys. Chem. 82, 1239–1242. doi:10.1021/j100500a009

Popović, D.Ž., Miladinović, J.M., Todorović, M.D., Miladinović, Z.P., 2013. Solubility in K+-Na+-Mg 4 2− aqueous solution at T = 298.15 K. Russ. J. Phys. Chem. A 87, 2181–2186. doi:10.1134/S0036024413130219

Rai, D., Felmy, A.R., Fulton, R.W., 1995. Nd3+ and Am3+ ion interactions with sulfate ion and their influence on NdPO4(c) solubility. J. Solution Chem. 24, 879–895. doi:10.1007/BF00973443

Rard, J.A., Archer, D.G., 1995. Isopiestic Investigation of the Osmotic and Activity Coefficients of Aqueous NaBr and the Solubility of NaBr□2H2O(cr) at 298.15 K: Thermodynamic Properties of the NaBr + H2O System over Wide Ranges of Temperature and Pressure. J. Chem. Eng. Data 40, 170–185. doi:10.1021/je00017a037

Rard, J.A., Clegg, S.L., 1997. Critical Evaluation of the Thermodynamic Properties of Aqueous Calcium Chloride. 1. Osmotic and Activity Coefficients of 0−10.77 mol·kg - 1 Aqueous Calcium Chloride Solutions at 298.15 K and Correlation with Extended Pitzer Ion-Interaction Models. J. Chem. Eng. Data 42, 819–849. doi:10.1021/je9700582

Reardon, E.J., 1988. Ion interaction parameters for aluminum sulfate and application to the prediction of metal sulfate solubility in binary salt systems. J. Phys. Chem. 92, 6426–6431. doi:10.1021/j100333a046

Reardon, E.J., 1990. An ion interaction model for the determination of chemical equilibria in cement/water systems. Cem. Concr. Res. 20, 175–192. doi:10.1016/0008-8846(90)90070-E

Russell, A.S., Edwards, J.D., Taylor, C.S., 1955. Solubility and density of hydrated aluminas in NaOH solution. Trans. Am. Inst. Min. Metall. Eng. 203, 1123–1128.

Räsänen, E., 2003. Modelling Ion Exchange and Flow in Pulp Suspensions. VTT Publ. TKK.

Salminen, J., Blomberg, P.B.A., Mäkinen, J., Räsänen, L., 2015. Environmental aspects of metals removal from waters and gold recovery. AIChE J. 61, 2739–2748. doi:10.1002/aic.14917

Sangster, J.M., Abraham, M.-C., Abraham, M., 1978. Vapour pressures of aqueous solutions of (Ag, Tl, Cd)NO 3 at 98.5 °C. I. Brunauer–Emmett–Teller isotherms. Can. J. Chem. 56, 348–351. doi:10.1139/v78-054

Šefčík, J., McCormick, A. V., 1997. Thermochemistry of aqueous silicate solution precursors to ceramics. AIChE J. 43, 2773–2784. doi:10.1002/aic.690431324

Seidell, A., Linke, W.F., Francis, A.W., Bates, R.G., 1952. Solubilities of inorganic and organic compounds: supplement to the third edition containing data published during the years 1939-1949 inclusive: a compilation of quantitative solubility data from the periodical literature. D. Van Nostrond Co., New York.

Shi, B., Rousseau, R.W., 2001. Crystal Properties and Nucleation Kinetics from Aqueous Solutions of Na2CO3 and Na2SO4. Ind. Eng. Chem. Res. 40, 1541–1547. doi:10.1021/ie0006559

Shock, E.L., Helgeson, H.C., 1988. Calculation of the thermodynamic and transport properties of aqueous species at high pressures and temperatures: Correlation algorithms for ionic species and equation of state predictions to 5 kb and 1000°C. Geochim. Cosmochim. Acta 52, 2009–2036. doi:10.1016/0016-7037(88)90181-0

Shock, E.L., Helgeson, H.C., Sverjensky, D.A., 1989. Calculation of the thermodynamic and transport properties of aqueous species at high pressures and temperatures: Standard partial molal properties of inorganic neutral species. Geochim. Cosmochim. Acta 53, 2157–2183. doi:10.1016/0016-7037(89)90341-4

Shock, E.L., Sassani, D.C., Willis, M., Sverjensky, D.A., 1997. Inorganic species in geologic fluids: Correlations among standard molal thermodynamic properties of aqueous ions and hydroxide complexes. Geochim. Cosmochim. Acta 61, 907–950. doi:10.1016/S0016-7037(96)00339-0

Shvarov, Y. V., 2008. HCh: New potentialities for the thermodynamic simulation of geochemical systems offered by windows. Geochemistry Int. 46, 834–839. doi:10.1134/S0016702908080089

Silvester, L.F., Pitzer, K.S., 1978. Thermodynamics of electrolytes. X. Enthalpy and the effect of temperature on the activity coefficients. J. Solution Chem. 7, 327–337. doi:10.1007/BF00662893

Simonson, J.M., Roy, R.N., Mrad, D., Lord, P., Roy, L.N., Johnson, D.A., 1988. The thermodynamics of aqueous borate solutions. II. Mixtures of boric acid with calcium or magnesium borate and chloride. J. Solution Chem. 17, 435–446. doi:10.1007/BF00647311

Sippola, H., 2012. Thermodynamic modelling of concentrated sulfuric acid solutions. Calphad 38, 168–176. doi:10.1016/j.calphad.2012.06.008

Sippola, H., 2015. Thermodynamic Modelling of Aqueous Sulfuric Acid (Dissertiation). Aalto University, Helsinki.

Stephen, H., Stephen, T., 1963. Solubilities of Inorganic and Organic Compounds. The MacMillian Co., New York.

Sterner, S.M., Felmy, A.R., Oakes, C.S., Pitzer, K.S., 1998. Correlation of Thermodynamic Data for Aqueous Electrolyte Solutions to Very High Ionic Strength Using INSIGHT: Vapor Saturated Water Activity in the System CaCl2-H2O to 250°C and Solid Saturation. Int. J. Thermophys. 19, 761–770. doi:10.1007/BF03356042

Stokes, R.H., Robinson, R. a, 1948. Ionic hydration and activity in electrolyte solutions. J. Am. Chem. Soc. 70, 1870–1878. doi:10.1021/ja01185a065

Sundman, O., Persson, P., Ohman, L.-O., 2008. A multitechnique study of the interactions between H+, Na+, Ca2+ and Cu2+, and two types of softwood Kraft fibre materials. J. Colloid Interface Sci. 328, 248–56. doi:10.1016/j.jcis.2008.09.027

Sundquist, A., 2016. Modelling the chemistry of metal cations in pulp and papermaking processes. Åbo Akademi University.

Sverjensky, D.A., Shock, E.L., Helgeson, H.C., 1997. Prediction of the thermodynamic properties of aqueous metal complexes to 1000 degrees C and 5 kb. Geochim. Cosmochim. Acta 61, 1359–1412. doi:10.1016/S0016-7037(97)00009-4

Teeple, J.E., 1929. The industrial development of Searles lake brines, with equilibrium data, American Chemical Society Monograph Series. The Chemical Catalog Company Inc., New York.

Thoenen, T., Hummel, W., Berner, U., Curti, E., 2014. The PSI / Nagra Chemical Thermodynamic Database 12 / 07. Villigen, Switzerland.

Thomsen, K., 2005. Modeling electrolyte solutions with the extended universal quasichemical (UNIQUAC) model*. Pure Appl. Chem 77, 531–542. doi:10.1351/pac200577030531

van der Lee, J., DeWindt, L., 2002. CHESS Tutorial and Cookbook Updated for version 3.0. Fontainebleau, France.

VISUAL MINTEQ, 2013. Visual MINTEQ | Visual MINTEQ – a free equilibrium speciation model [WWW Document].

Voigt, W., 1993. Calculation of salt activities in molten salt hydrates applying the modified BET equation, I: Binary systems. Monatshefte für Chemie Chem. Mon. 124, 839–848. doi:10.1007/BF00816406

VTT - Technical Research Centre of Finland, 2013. BALAS Process Simulation Software [WWW Document].

Waldeck, W.F., Lynn, G., Hill, A.E., 1934. Aqueous Solubility of Salts at High Temperatures. II. The Ternary System Na2CO3—NaHCO3 —H2O from 100 to 200°. J. Am. Chem. Soc. 56, 43–47. doi:10.1021/ja01316a013

Wang, P., Anderko, A., Young, R.D., 2002. A speciation-based model for mixed-solvent electrolyte systems. Fluid Phase Equilib. 203, 141–176. doi:10.1016/S0378-3812(02)00178-4

Wang, W., Zeng, D., Chen, Q., Yin, X., 2013. Experimental determination and modeling of gypsum and insoluble anhydrite solubility in the system CaSO4-H2SO4-H2O. Chem. Eng. Sci. 101, 120–129. doi:10.1016/j.ces.2013.06.023

Wesolowski, D.J., 1992. Aluminum speciation and equilibria in aqueous solution: I. The solubility of gibbsite in the system Na-K-Cl-OH-Al(OH)4 from 0 to 100°C. Geochim. Cosmochim. Acta 56, 1065–1091. doi:10.1016/0016-7037(92)90047-M

Windmaisser, F., Stöckl, F., 1950. Basische Alkalisulfate. Monatshefte für Chemie 81, 543–550. doi:10.1007/BF00906444

Wolery, T.J., 1992. EQ3NR, A Computer Program for Geochemical Aqueous Speciation-Solubility Calculations : Theoretical Manual, User ' s Guide, and Related Documentation (Version 7 . 0). Program 262. doi:10.2172/138643

Wolery, T.J., 1994. LLNL Yucca Mountain project - near-field environment characterization technical area: Letter report: EQ3/6 version 8: differences from version 7. Livermore, CA. doi:10.2172/331558

Wolery, T.J., Daveler, S.A., 1992. EQ6, a computer program for reaction path modeling of aqueous geochemical systems: Theoretical manual, user`s guide, and related documentation (Version 7.0); Part 4. Livermore, CA (United States). doi:10.2172/138820

Wolery, T.J., Sutton, M., 2013. Evaluation of Thermodynamic Data.

Wolery, T.W., Sutton, M., 2011. Generic Natural Systems Evaluation - Thermodynamic Database Development and Data Management.

Yanateva, O.K., T., O. V., C., K. V., 1963. On the nature of glaserite phase in the system K2SO4-Na2SO4-H2O. Zhurnal Neorg. Khimii 8, 1156–1165.

Zakir, T., 2012. Evaluation and Control of Pirssonite Scale Formation in Green Liquor Systems of the Kraft Process. University of Toronto.

Appendix A: Standard state thermodynamic values applied

The following gaseous, solid and aqueous species were selected for further thermochemical studies (Tables A.1-A.3). Listed are enthalpy of formation ($\Delta_f H^\circ$) and entropy (S°)at 298.15 K and coefficients for heat capacity according to equation

$$c_p \,/(J \cdot mol^{-1}) = a_1 + a_2(T/K) + a_3(T/K)^2 + a_4(T/K)^{-2} \tag{66}$$

The heat capacity is defined piecewise, whit the maximum temperature of each temperature interval given.

Table A.1. Gaseous species applied in the models. Data sources listed after Table A.4

	$\Delta_f H^\circ$	S°	$T_{\max}$	a_1	a_2	a_3	a_4	ref
CO2(g)	-393505.2	213.77	500	22.22616	0.05620048	-2.252E-05	10489.17	a
H2O(g)	-241826.8	188.83	600	33.56823	-0.0042007	1.4761E-05	0	a

Table A.2. Aqueous species applied in the models. Data sources listed after Table A.4

	$\Delta_f H^\circ$	S°	$T_{\max}$	a_1	a_2	a_3	a_4	ref
H2O	-285830	69.95	372.8	59.69	0.02301	2.4761E-05	5.8702E+05	a
			500	16.75	0.06212	9.0391E-05	3.2798E+06	
H(+aq)	0	0.00	473.15	0.00	0.00000	0	0.0000E+00	b
OH(-aq)	-230034	-10.71	338.15	21021.48	-83.22346	0.09233753	-4.0481E+08	c
			388.15	-128.93	2.16371	-0.0046564	-1.9741E+07	
Al(+3aq)	-530639	-325.10	338.15	18066.96	-71.10274	0.07792527	-3.4889E+08	d
			388.15	-2068.64	9.71536	-0.0133607	2.2178E+07	
Al(OH)4(-aq)	-1501088	109.69	385.15	3616.11	-11.70168	0.01044879	-8.4906E+07	d
AlO(+aq)	-715086	-112.97	338.15	17869.71	-70.96995	0.07912916	-3.4399E+08	d
			388.15	662.62	-1.31294	-0.0002043	-3.2509E+07	
AlO2H(aq)	-951869	20.92	338.15	24110.73	-96.40509	0.10849067	-4.6412E+08	d
			388.15	2883.66	-9.96018	0.00947458	-8.4742E+07	
AlOH(+2aq)	-767032	-184.93	338.15	2788.76	-10.19436	0.01017038	-5.3174E+07	d
			388.15	-2245.13	9.56967	-0.0116677	4.3762E+07	
Ca(+2aq)	-543018	-56.48	338.15	6118.47	-23.91671	0.02597756	-1.1809E+08	c
			388.15	-1155.86	5.17737	-0.0067714	1.6937E+07	
CaCO3(aq)	-1202449	10.46	338.15	16530.20	-66.02373	0.07431378	-3.1782E+08	d
			388.15	2020.86	-6.92861	0.00661672	-5.8569E+07	
CaSO4(aq)	-1425567	84.96	339.82	39079.64	-153.35449	0.16811097	-7.6452E+08	*e
			381.48	807.02	0.91130	-0.0067511	-6.6705E+07	
Cl(-aq)	-167109	56.74	338.15	12174.65	-48.20272	0.05313711	-2.3555E+08	c
			388.15	-813.49	4.06356	-0.0060488	2.5141E+06	

	$\Delta_f H^\circ$	S°	$T_{\max}$	a_1	a_2	a_3	a_4	ref
CO2(aq)	-413798	117.57	338.15	-15998.41	64.36728	-0.0724065	3.0997E+08	f
			388.15	-1760.84	6.40335	-0.0060317	5.5352E+07	
CO3(-2aq)	-675307	-50.00	338.15	35506.89	-140.62811	0.15566917	-6.8517E+08	c
			388.15	-1002.70	6.59016	-0.0113675	-1.8796E+07	
Cu(+2aq)	65722	-97.07	338.15	9874.43	-38.62684	0.04234728	-1.8949E+08	c
			388.15	-1034.16	5.16308	-0.0071213	1.1478E+07	
Cu(CO3)2(-2aq)	-1284892	-1.79	323.15	80887.89	-319.88162	0.35368387	-1.5598E+09	*g
Cu2(OH)2(+2aq)	-328625	117.56	323.15	61791.56	-243.69949	0.26936829	-1.1886E+09	*g
CuCl(+aq)	-98624	-27.24	338.15	-4531.05	18.68685	-0.0215128	8.8444E+07	*g,h
			388.15	-1451.82	5.87387	-0.0065395	3.5997E+07	
CuCl2(aq)	-273764	3.26	338.15	-14578.90	58.66973	-0.0659823	2.8259E+08	*g,h
			388.15	-1569.82	5.71565	-0.0053535	4.9855E+07	
CuCl4(-2aq)	-638288	-77.32	338.15	-21296.15	87.09639	-0.1006261	4.1109E+08	h
			388.15	-7712.44	30.30238	-0.0339682	1.8229E+08	
CuCO3(aq)	-609585	-17.46	323.15	45381.14	-179.25414	0.19801546	-8.7466E+08	*g
CuHCO3(+aq)	-624282	35.84	323.15	20153.05	-79.03458	0.08685168	-3.8707E+08	*g
CuHSO4(+aq)	-821178	79.43	323.15	20205.36	-81.05076	0.0913442	-3.6862E+08	*g
CuO(aq)	-135157	-51.88	338.15	7008.17	-27.52658	0.03041454	-1.3429E+08	*g
			388.15	-258.59	1.74839	-0.0027718	-1.4039E+06	
CuO2(-2aq)	-321758	-96.65	338.15	29779.56	-117.59771	0.12962644	-5.7469E+08	*g
			388.15	-1927.24	9.99095	-0.0148491	6.5171E+06	
CuO2H(-aq)	-361567	1.26	338.15	15421.97	-61.33299	0.06859574	-2.9662E+08	*g
			388.15	1004.46	-2.86008	0.00188132	-3.6658E+07	
CuOH(+aq)	-176319	-25.52	338.15	439.88	-1.23793	0.00090516	-7.4948E+06	*g
			388.15	-878.06	3.85344	-0.0046267	1.8672E+07	
Fe(+3aq)	-35522	-277.40	338.15	15631.60	-61.30745	0.06703376	-3.0132E+08	*d,g
			388.15	-2064.96	9.65241	-0.0130413	2.5453E+07	
FeO(+aq)	-246656	-46.44	338.15	24316.27	-96.91021	0.10849454	-4.6833E+08	*d,g
			388.15	1768.49	-5.40595	0.00403031	-6.2324E+07	
FeO2(-aq)	-429942	44.35	338.15	28267.62	-112.43035	0.12539373	-5.4483E+08	*d,g
			388.15	1088.71	-2.38659	4.21E-05	-5.3022E+07	
FeOH(+2aq)	-278754	-106.27	338.15	10382.41	-40.75364	0.04476936	-1.9964E+08	*d,g
HCO3(-aq)	-690004	98.45	338.15	10278.70	-40.40810	0.04450483	-1.9758E+08	c
			388.15	-694.34	3.73072	-0.0054574	3.7169E+06	
HSiO3(-aq)	-1145880	20.92	338.15	15270.31	-60.29759	0.06667373	-2.9401E+08	h
			388.15	-540.55	3.42178	-0.005585	-5.1009E+06	
HSiO4(-3aq)	-1431710	-470.08	330.65	15561.03	-61.27216	0.06790923	-2.9709E+08	*j
			363.15	1276.50	-3.10285	0.00129857	-4.1983E+07	
HSO4(-aq)	-888045	125.52	338.15	5052.30	-19.50123	0.02105615	-9.6684E+07	c
			388.15	-1147.82	5.24516	-0.0067421	1.8890E+07	
K(+aq)	-252139	101.04	338.15	3542.40	-13.93614	0.01553474	-6.7560E+07	c
			388.15	155.79	-0.22845	-7.514E-05	-6.2379E+06	
Mg(+2aq)	-467328	-138.07	338.15	12702.11	-49.86370	0.05494475	-2.4374E+08	*d,g
			388.15	-783.67	4.39435	-0.0064847	3.5475E+06	

	$\Delta_f H^\circ$	S°	$T_{\max}$	a_1	a_2	a_3	a_4	ref
MgCO3(aq)	-1132109	-100.42	338.15	15713.62	-62.75064	0.07063114	-3.0206E+08	h
			388.15	1926.61	-6.59671	0.00630251	-5.5723E+07	
MgOH(+aq)	-691556	-79.91	338.15	-4812.52	19.89917	-0.0230258	9.3813E+07	*d,g
			388.15	-1784.88	7.21225	-0.0081055	4.3084E+07	
Mn(+2aq)	-217982	-67.78	338.15	8815.22	-34.48792	0.03774795	-1.6938E+08	*d,g
			388.15	-1056.80	5.11368	-0.0069591	1.2749E+07	
Mn2(OH)3(+aq)	-1293454	-383.28	323.15	17809.42	-68.90648	0.07556981	-3.3700E+08	*i
Mn2OH(+3aq)	-721794	-267.78	323.15	17690.05	-68.95251	0.07552029	-3.3817E+08	*i
MnHCO3(+aq)	-907986	54.98	323.15	19093.83	-74.89567	0.08225238	-3.6696E+08	*g
MnHSO4(+aq)	-1104882	107.19	323.15	19146.15	-76.91185	0.0867449	-3.4851E+08	*g
MnO(aq)	-380858	-10.46	338.15	10267.78	-40.91891	0.04606162	-1.9695E+08	*d,i
			388.15	1285.88	-4.33373	0.00414807	-3.6495E+07	
MnO2(-2aq)	-554679	-63.60	338.15	36309.20	-143.82293	0.15922652	-7.0067E+08	*d,i
			388.15	-985.20	6.56991	-0.011423	-2.0067E+07	
MnO2H(-aq)	-623855	-38.07	338.15	8965.47	-34.93364	0.03797223	-1.7240E+08	*d,i
			388.15	-1598.79	7.33033	-0.009614	2.3587E+07	
MnOH(+aq)	-446045	1.26	338.15	3026.36	-11.64810	0.01269389	-5.7381E+07	*d,g
			388.15	-426.28	2.17810	-0.0028883	6.5442E+06	
Na(+aq)	-240253	58.41	338.15	5932.23	-23.23964	0.02589846	-1.1268E+08	c
			388.15	269.84	-0.32404	-0.0001932	-1.0120E+07	
SiO2(aq)	-877699	75.31	338.15	94172.34	-374.47411	0.42123402	-1.8034E+09	f
			388.15	11321.81	-37.17900	0.03500177	-3.2167E+08	
SiO3(-2aq)	-1145880	-227.96	330.65	15270.28	-60.29748	0.0666736	-2.9401E+08	*j
			363.15	1447.14	-4.00753	0.00222234	-4.7218E+07	
SiO4(-4aq)	-1431710	-845.32	330.65	15560.20	-61.27055	0.06790968	-2.9706E+08	*j
			363.15	1119.94	-2.50415	0.00065506	-3.8817E+07	
SO4(-2aq)	-909688	18.83	338.15	36717.87	-145.42634	0.16125247	-7.0769E+08	c
			388.15	-454.98	4.59674	-0.0091097	-3.0447E+07	

Table A.3. Solid stoichiometric pure phases applied in the model.

	$\Delta_f H^\circ$	S°	$T_{\max}$	a_1	a_2	a_3	a_4	ref
Al(OH)3	−1289000	70.00	373	36.00	0.191	0.00	0	k
Al(OH)3(amorphous)	−1293500	68.44	700	30.60	0.209786	0.00	0	l
Al(OH)3(mcr)	−1281000	70.00	373	36.00	0.191	0.00	0	m
Al2(SO4)3	−3440754	239.30	1100	366.31	0.0625926	0.00	−11162910	l
Al2(SO4)3*17H2O	−8649453	714.18	298	147548.33	−579.194	0.64	−2814514269	*n
AlCl3	−705632	109.29	465	62.74	0.0912196	0.00	99997.6	a
			373	301.41	0.2467641	0.00	−2065639.388	
C2AH8	−5433000	440.00	373	324.88	0.7835	0.00	0	k
C3.5AH12*0.5CaCO3	−8270000	713.00	373	558.38	1.1631	0.00	0	m
C3AH10*CaCl2	−7795105	117.80	323	73788.44	−287.0105	0.31	−1403137439	*p
C3AH11*0.5CaSO4*0.5CaCl	−8082666	99.61	323	97418.47	−387.0497	0.43	−1795858250	*p
C3AH11*CaCO3	−8250000	657.00	373	618.00	0.982	0.00	−2590000	m
C3AH12*CaSO4	−8750000	821.00	373	594.00	1.168	0.00	0	m
C3AH32*3CaCO3	−16792000	1858.00	373	2042.00	0.559	0.00	−7780000	m
C3AH32*3CaSO4	−17535000	1900.00	373	1939.00	0.789	0.00	0	m
C3AH6	−5540000	419.00	373	292.00	0.561	0.00	0	k
C4AH13	−8302000	700.00	373	576.75	1.1861	0.00	0	k
Ca(OH)2	−984620	83.39	700	105.29	0.0119453	0.00	−1896607	*a,o
CaCl2	−795797	104.60	1045	89.64	−0.03379	0.00	−841820.8	a
CaCO3	−1206921	92.90	1200	99.67	0.0269659	0.00	−2154342	a
CaO	−635089	38.07	3200	49.62	0.0045187	0.00	−694544	a
CaSO4	−1438963	91.98	340	46505.70	−166.4827	0.17	−1051084142	**
			381	8233.08	−12.2169	−0.01	−353274135	
			423	−10301.30	53.03461	−0.07	89977046.69	
CaSO4*0.5H2O	−1573122	145.10	340	45683.66	−164.9119	0.17	−1026293799	*e
			381	7319.30	−10.30929	−0.01	−326480602.4	
			423	−11144.82	54.624978	−0.07	116113836.5	
CaSO4*2H2O	−2022059	196.00	800	91.38	0.317984	0.00	0	
Cu(OH)2	−394347	252.54	323	51917.17	−205.0728	0.23	−999110850.9	*r
CuCl2	−217986	108.07	675	78.87	0.0057404	0.00	−774876.8	a
CuCO3	−596220	87.86	500	92.05	0.0389112	0.00	−1799120	a
CuO	−156063	42.59	1397	48.60	0.0074266	0.00	−761488	a
CuSO4*5H2O	−2276515	301.25	600	280.96	0.070877	0.00	−1857696	l
Fe(OH)2.7Cl0.3	−857396	−129.72	323	19445.08	−75.70579	0.08	−370394489.6	*s
Fe(OH)3	−822997	106.70	1000	85.51	0.1232397	0.00	−1512098	a
Fe2(SO4)3	−2582992	307.52	1500	287.66	0.192715	0.00	−6852555	a
FeCl3	−399405	142.34	577	62.34	0.11506	0.00	0	a
FeCl3*2KCl*H2O	−1402210	2788.00	323	83648.99	−324.3491	0.36	−1613588550	*t
FeCl3*6H2O	−2223796	352.33	300	0.00	0	0.00	0	u
H2SO4	−813989	156.76	610	75.99	0.2063088	0.00	184514.4	a
K2Ca(SO4)2*H2O	−3165394	348.97	340	79099.40	−309.5104	0.34	−1528305874	*e
			381	2991.97	−2.472543	−0.01	−143243547.1	
			423	−31599.39	119.24386	−0.13	685052465.4	

	$\Delta_f H^\circ$	S°	$T_{\max}$	a_1	a_2	a_3	a_4	ref
K2CO3	−1150182	155.52	1174	97.93	0.0920815	0.00	−990771.2	a
K2SO4	−1437710	175.54	857	368.28	−0.640801	0.00	−8716109	a
KAl(SO4)2*12H2O	−6061800	687.40	364	−640.99	4.336298	0.00	0	l
KCl	−436684	82.55	1044	40.02	0.025468	0.00	364844.8	a
KOH	−423400	81.25	298	−1.06	0.405521	0.00	−3500	a
			516	53.87	0.051411	0.00	−23500	
M4AH10	−7196000	549.00	373	−200.19	3.9259	0.00	0	m
Mg(OH)2	−924664	63.14	900	114.52	−0.017853	0.00	−3022940	a
Mg2(OH)2CO3*3H2O	−2920612	232.92	1000	296.52	0.1157294	0.00	−3108712	a
MgAl2(SO4)4*22H2O	−11455620	980.21	298	197349.80	−774.7403	0.86	−3764239346	*n
MgCl2	−641616	89.63	987	79.08	0.0059413	0.00	−861904	a
MgCO3	−1095798	65.70	700	77.91	0.0577392	0.00	−1740544	a
MgCO3*3H2O	−1977258	195.64	307	−6588.98	16.31414	0.00	−174608800	a
MgSO4	−1284869	91.60	1400	105.27	0.0469529	0.00	−2085306	a
MgSO4*7H2O	−3388162	371.30	550	68.41	1.04759	0.00	0	*a,n
Mn(OH)2	−695000	99.00	398	0.00	0	0.00	0	a
MnCl2	−481290	118.24	923	75.48	0.0132214	0.00	−573208	a
MnCO3	−894100	85.80	700	92.01	0.0389112	0.00	−1962296	a
MnSO4	−1065251	112.10	973	122.17	0.0373213	0.00	−2945536	l
MnSO4*4H2O	−2258105	271.96	550	76.00	0.6018265	0.00	−18409.6	l
MnSO4*5H2O	−2553441	313.80	550	101.11	0.7542999	0.00	−30961.6	l
MnSO4*7H2O	−3139000	393.30	550	81.69	1.003491	0.00	−12133.6	l
MnSO4*H2O	−1376536	154.81	550	25.60	0.3769533	0.00	−7531.2	l
Na2Ca(CO3)2*2H2O	−2658680	223.40	400	388.25	0	0.00	0	v
Na2Ca(SO4)2	−2813795	294.24	340	83318.87	−324.141	0.36	−1686628174	*e
			381	3516.60	−2.071766	−0.01	−235558983.9	*e
			423	−32654.07	125.36064	−0.13	628242052.9	
Na2CO3	−1129261	134.48	342	666.52	−1.956415	0.00	10773139.47	**
			386	666.52	−1.956417	0.00	10773129.46	
			429	666.52	−1.956419	0.00	10773108.09	
Na2CO3*10H2O	−4086581	538.64	336	47270.42	−186.6701	0.20	−893351804.6	**w
			373	9613.52	−32.26142	0.03	−231432726.5	
Na2CO3*7H2O	−3199036	423.11	336	47212.17	−183.9671	0.20	−895112855.5	*x
			373	8395.70	−25.11352	0.02	−209854068.8	
Na2CO3*H2O	−1428384	171.31	336	46131.00	−180.2234	0.20	−883891246.3	**
			373	6170.26	−17.33952	0.01	−172495630.2	
Na2CO3*NaHCO3*2H2O	−2682111	303.13	398	270.00	0	0.00	0	a
Na2O	−417982	75.04	1023	66.22	0.0438651	0.00	−813369.6	a
Na2SiO3	−1561511	113.76	1362	113.45	0.0752241	0.00	−2006646	a
Na2SO4	−1387816	149.60	458	105.57	0.1151813	0.00	−1046000	a
Na2SO4*10H2O	−4329275	587.69	336	48470.90	−188.6515	0.21	−915704301	**w
			373	10210.87	−31.66539	0.03	−244168625.5	
Na2SO4*2Na2CO3	−3566705	672.18	340	128833.09	−506.1858	0.56	−2503526534	*y
Na2SO4*Al2(SO4)3*24H2O	−12040458	1386.15	298.15	196630	−771.30	0.8550957	−3744673085.83	*n
NaCl	−411120	72.13	1074	57.26	−0.015485	0.00	−378233.6	a

NaOH	−425931	64.43	572	118.64	−0.250973	0.00	−1520047	a
SiO2(amorphous)	−903000	41	373	47	0.034	0.00	−1.13E6	m
NaHCO3	−950824	95.23	336	16087.54	−59.15744	0.07	−414333755.3	z
			373	1665.01	−0.454988	0.00	−156667697.5	
Na2CO3*NaHCO3*2H2O	−2682110	303.13	398	169.04	0.37293	0.00	0	*aa
Na2CO3*3NaHCO3	−3984030	435.33	398	199.33	0.59175	0.00	0	*aa
K2CO3*1.5H2O	−1606520	205.02	300	163.18	0	0.00	0	*l,o
KNaCO3*6H2O	−2930680	370.37	300	340.26	0	0.00	0	**
K2Ca5(SO4)6*H2O	−8886562	830.76	342	224742.71	−884.3297	0.96	−4072964154	*aa
			386	−2426.25	26.301182	−0.07	116917869.7	
			429	−105944.23	388.48169	−0.42	2623402205	

* Calculated based on equilibrium coefficient value and data values for other species
** Fitted in this study
In $M_qC_xA_yH_z$ notation M =MgO; C = CaO; A = Al_2O_3 and H = H_2O

References: a) Outokumpu Research (1999); b) definition; c) Shock and Helgeson (1988); d) Shock et al. (1997); e) Greenberg and Møller (1989); f) Shock et al. (1989); g) Martell and Smith (1989); h) Sverjensky et al. (1997); i) Baes and Mesmer (1986); j) Šefčík and McCormick (1997); k) Matschei et al. (2007); l) Outotec Research (2011); m) Lothenbach et al. (2008); n) Reardon (1988); o) Harvie et al. (1984); p) THEREDA (AF Colenco et al., 2011); r) Dirkse (1986); s) Biedermann and Chow (1966); t) Marion et al. (2008); u) Outotec Research (2015); v) Zakir (2012); w) Marion (2001); x) Königsberger (2001); y) Bialik et al. (2008); z) Carter et al. (2014); aa) Haynes (2003)

Appendix B: Pitzer parameters values applied

Given are the type of the interaction, interacting species and coefficients for the temperature-dependent parameter equation

$$X = a + b \cdot (T/K)^{-1} + c \cdot ln(T/K) + d \cdot (T/K) + e \cdot (T/K)^2 + f \cdot (T/K)^{-2} \tag{67}$$

The formalism applied is the one supported by the ChemApp 'PIMZ' model, where the $\alpha_{MX}^{(1)}$ and $\alpha_{MX}^{(2)}$ parameters (equations (15)-(17)) can be defined for each cation-anion pair separately.

Table B.1. Applied Pitzer parameters.

type	a	b	c	d	e	f	α	ref
H(+aq)	Al(OH)4(-aq)							
β(0)	0.2106	0.	0.	0.	0	0	0	a
H(+aq)	Al(OH)4(-aq)							
β(1)	0.5320	0.	0.	0.	0	0	2	a
H(+aq)	Al(OH)4(-aq)							
C(ϕ)	0.0000	0.	0.	0.	0	0	0	a
H(+aq)	Cl(-aq)							
β(0)	-1338.0300	27509.6	253.062	-0.774427	0.00039361	0	0	b
H(+aq)	Cl(-aq)							
β(1)	1.6355	-43.78	-0.2367	0.000589	-2.3946E-07	0	2	b
H(+aq)	Cl(-aq)							
C(ϕ)	0.4521	-12.9	-0.0815	0.000216	-9.4578E-08	0	0	b
H(+aq)	HSO4(-aq)							
β(0)	52.6981	-954.74	-10.1142	0.033388	-1.8144E-05	-20.377697	0	c
H(+aq)	HSO4(-aq)							
β(1)	0.2025	0.	0.	0.001601	-2.6846E-06	0	2	c
H(+aq)	HSO4(-aq)							
C(ϕ)	0.0000	0.	0.	0.	0	0	0	c
H(+aq)	SO4(-2aq)							
β(0)	-250.4766	4602.83	48.761	-0.173643	0.00010214	98.2414229	0	c
H(+aq)	SO4(-2aq)							
β(1)	0.0000	0.	0.	0.	0	0	2	c
H(+aq)	SO4(-2aq)							
C(ϕ)	-172.5807	3143.31	33.2993	-0.109299	5.573E-05	67.089763	0	c
Al(+3aq)	Cl(-aq)							
β(0)	-12.3369	2109.39	0.	0.020113	0	0	0	d
Al(+3aq)	Cl(-aq)							
β(1)	119.1351	-18415.86	0.	-0.173302	0	0	2	d
Al(+3aq)	Cl(-aq)							
C(ϕ)	2.9901	-474.57	0.	-0.004708	0	0	0	d
Al(+3aq)	SO4(-2aq)							
β(0)	0.8540	0.	0.	0.	0	0	0	e
Al(+3aq)	SO4(-2aq)							
β(1)	18.5300	0.	0.	0.	0	0	2	e
Al(+3aq)	SO4(-2aq)							
C(ϕ)	-0.0911	0.	0.	0.	0	0	0	e

type	a	B	c	d	e	f	α	ref
Al(+3aq)	SO4(-2aq)							
β(2)	-500.0000	0.	0.	0.	0	0	50	e
AlOH(+2aq)	SO4(-2aq)							
β(0)	0.8540	0.	0.	0.	0	0	0	e#
AlOH(+2aq)	SO4(-2aq)							
β(1)	18.5300	0.	0.	0.	0	0	2	e#
AlOH(+2aq)	SO4(-2aq)							
C(ϕ)	-0.0911	0.	0.	0.	0	0	0	e#
type	a	b	c	d	e	f	ω	ref
AlOH(+2aq)	SO4(-2aq)							
β(2)	-500.0000	0.	0.	0.	0	0	50	e#
Ca(+2aq)	Al(OH)4(-aq)							
β(0)	0.2145	0.	0.	0.	0	0	0	a
Ca(+2aq)	Al(OH)4(-aq)							
β(1)	2.5300	0.	0.	0.	0	0	2	a
Ca(+2aq)	Al(OH)4(-aq)							
C(ϕ)	0.0000	0.	0.	0.	0	0	0	a
Ca(+2aq)	Cl(-aq)							
β(0)	151.4553	-3666.18	-27.5312	0.069163	-2.9409E-05	-128.76947	0	f
Ca(+2aq)	Cl(-aq)							
β(1)	3.4787	0.	0.	-0.015417	3.1791E-05	0	2	f
Ca(+2aq)	Cl(-aq)							
C(ϕ)	56.8529	-1369.49	-10.3381	0.025306	-1.0133E-05	-45.711625	0	f
Ca(+2aq)	HCO3(-aq)							
β(0)	0.3998	0.	0.	0.	0	0	0	g
Ca(+2aq)	HCO3(-aq)							
β(1)	2.9775	0.	0.	0.	0	0	2	g
Ca(+2aq)	HCO3(-aq)							
C(ϕ)	0.0000	0.	0.	0.	0	0	0	g
Ca(+2aq)	HSO4(-aq)							
β(0)	0.2145	0.	0.	0.	0	0	0	g
Ca(+2aq)	HSO4(-aq)							
β(1)	-0.6014	775.75	0.	0.	0	0	2	**
Ca(+2aq)	HSO4(-aq)							
C(ϕ)	0.0782	-10.82	0.	0.	0	0	0	**
Ca(+2aq)	OH(-aq)							
β(0)	-0.1747	0.	0.	0.	0	0	0	g
Ca(+2aq)	OH(-aq)							
β(1)	-0.2303	0.	0.	0.	0	0	2	g
Ca(+2aq)	OH(-aq)							
C(ϕ)	0.0000	0.	0.	0.	0	0	0	g
Ca(+2aq)	OH(-aq)							
β(2)	-5.7200	0.	0.	0.	0	0	12	g
Ca(+2aq)	SO4(-2aq)							
β(0)	0.1500	0.	0.	0.	0	0	0	h
Ca(+2aq)	SO4(-2aq)							
β(1)	3.0000	0.	0.	0.	0	0	1.4	h
Ca(+2aq)	SO4(-2aq)							
C(ϕ)	0.0000	0.	0.	0.	0	0	0	h

type	a	b	c	d	e	f	α	ref
Ca(+2aq)	SO4(-2aq)							
β(2)	302335.0499	-13847355.79	-49258.4405	60.802794	-0.00529094	630742615	12	h
Cu(+2aq)	Cl(-aq)							
β(0)	1.1061	0.	0.	-0.002715	0	0	0	f,i
Cu(+2aq)	Cl(-aq)							
β(1)	-1.1356	0.	0.	0.008475	0	0	2	f,i
Cu(+2aq)	Cl(-aq)							
C(ϕ)	-0.0360	0.	0.	0.	0	0	0	f,i
type	a	b	c	d	e	f	ω	ref
Cu(+2aq)	SO4(-2aq)							
β(0)	1.5459	0.	0.	-0.0044	0	0	0	f,i
Cu(+2aq)	SO4(-2aq)							
β(1)	-4.5690	0.	0.	0.0238	0	0	1.4	f,i
Cu(+2aq)	SO4(-2aq)							
C(ϕ)	-1.4267	0.	0.	0.0048	0	0	0	f,i
Cu(+2aq)	SO4(-2aq)							
β(2)	92.6950	0.	0.	-0.473	0	0	12	f,i
Fe(+3aq)	Cl(-aq)							
β(0)	0.2362	0.	0.	0.	0	0	0	j
Fe(+3aq)	Cl(-aq)							
β(1)	-5.3975	0.	0.	0.	0	0	2	j
Fe(+3aq)	Cl(-aq)							
C(ϕ)	-0.0080	0.	0.	0.	0	0	0	j
K(+aq)	Al(OH)4(-aq)							
β(0)	-0.0003	0.	0.	0.	0	0	0	a
K(+aq)	Al(OH)4(-aq)							
β(1)	0.1735	0.	0.	0.	0	0	2	a
K(+aq)	Al(OH)4(-aq)							
C(ϕ)	0.0000	0.	0.	0.	0	0	0	a
K(+aq)	Cl(-aq)							
β(0)	26.7373	-758.48	-4.7062	0.010072	-3.7599E-06	0	0	f
K(+aq)	Cl(-aq)							
β(1)	113.7748	-2770.66	-20.7006	0.05204	-2.0645E-05	-65.85452	2	f
K(+aq)	Cl(-aq)							
C(ϕ)	-3.3052	91.27	0.5864	-0.001298	4.9567E-07	0	0	f
K(+aq)	CO3(-2aq)							
β(0)	0.4568	-97.78	0.	0.	0	0	0	*f
K(+aq)	CO3(-2aq)							
β(1)	2.7329	-387.58	0.	0.	0	0	2	*f
K(+aq)	CO3(-2aq)							
C(ϕ)	-0.9028	53.76	0.	0.	0	0	0	*f
K(+aq)	HCO3(-aq)							
β(0)	-0.0107	0.	0.	0.	0	0	0	f
K(+aq)	HCO3(-aq)							
β(1)	0.0478	0.	0.	0.	0	0	2	f
K(+aq)	HCO3(-aq)							
C(ϕ)	0.0000	0.	0.	0.	0	0	0	f
K(+aq)	HSO4(-aq)							
β(0)	-6.6383	123.08	1.3038	-0.005014	3.3965E-06	2.62687678	0	k

type	a	b	c	d	e	f	α	ref
K(+aq)	HSO4(-aq)							
β(1)	538.4625	-9822.46	-104.0563	0.347487	-0.00018278	-209.64766	2	k
K(+aq)	HSO4(-aq)							
C(ϕ)	-0.0093	0.	0.	0.000008	-1.32E-08	0	0	k
K(+aq)	OH(-aq)							
β(0)	0.2259	-34.15	0.	0.0006	-1.5113E-06	0	0	l
K(+aq)	OH(-aq)							
β(1)	1.1511	-430.34	0.	0.003917	-6.6888E-06	0	3	l
K(+aq)	OH(-aq)							
C(ϕ)	-0.0175	6.68	0.	-0.000057	1.3004E-07	0	0	l
K(+aq)	OH(-aq)							
β(2)	-7.6210	3298.61	0.	-0.026377	5.26E-05	0	12	l
K(+aq)	SO4(-2aq)							
β(0)	0.2401	147.17	-0.0168	-0.0014	2.0026E-06	-35409.072	0	m
K(+aq)	SO4(-2aq)							
β(1)	1.1986	2659.13	-0.1413	-0.018606	2.9102E-05	-509707.73	1.4	m
K(+aq)	SO4(-2aq)							
C(ϕ)	0.0354	-11.42	0.0127	-0.000191	-1.0272E-09	-279.41192	0	m
Mg(+2aq)	Al(OH)4(-aq)							
β(0)	0.4746	0.	0.	0.	0	0	0	a
Mg(+2aq)	Al(OH)4(-aq)							
β(1)	1.7290	0.	0.	0.	0	0	2	a
Mg(+2aq)	Al(OH)4(-aq)							
C(ϕ)	0.0000	0.	0.	0.	0	0	0	a
Mg(+2aq)	Cl(-aq)							
β(0)	0.5761	0.	0.	-0.000932	5.9392E-07	0	0	f
Mg(+2aq)	Cl(-aq)							
β(1)	2.6014	0.	0.	-0.010944	2.6017E-05	0	2	f
Mg(+2aq)	Cl(-aq)							
C(ϕ)	0.0595	0.	0.	-0.00025	2.4183E-07	0	0	f
Mg(+2aq)	HCO3(-aq)							
β(0)	0.0330	0.	0.	0.	0	0	0	f
Mg(+2aq)	HCO3(-aq)							
β(1)	0.8498	0.	0.	0.	0	0	2	f
Mg(+2aq)	HCO3(-aq)							
C(ϕ)	0.0000	0.	0.	0.	0	0	0	f
Mg(+2aq)	HSO4(-aq)							
β(0)	0.4746	0.	0.	0.	0	0	0	f
Mg(+2aq)	HSO4(-aq)							
β(1)	1.7288	0.	0.	0.	0	0	2	f
Mg(+2aq)	HSO4(-aq)							
C(ϕ)	0.0000	0.	0.	0.	0	0	0	f
Mg(+2aq)	SO4(-2aq)							
β(0)	5.5988	-625.91	-0.0001	-0.015672	1.5621E-05	-5.446E-09	0	n
Mg(+2aq)	SO4(-2aq)							
β(1)	52.6395	-5713.99	0.	-0.14798	0.00015761	0	1.4	n
Mg(+2aq)	SO4(-2aq)							
C(ϕ)	0.3428	-115.33	0.	0.	-9.7798E-07	14123.8466	0	n

type	a	b	c	d	e	f	α	ref
Mg(+2aq)	SO4(-2aq)							
β(2)	82313.3235	-1545667.29	-15958.3006	56.400009	-0.03434689	-32152.023	12	n
MgOH(+aq)	Cl(-aq)							
β(0)	-0.1000	0.	0.	0.	0	0	0	f
MgOH(+aq)	Cl(-aq)							
β(1)	1.6580	0.	0.	0.	0	0	2	f
MgOH(+aq)	Cl(-aq)							
C(ϕ)	0.0000	0.	0.	0.	0	0	0	f
type	a	b	c	d	e	f	ω	ref
Mn(+2aq)	Cl(-aq)							
β(0)	0.3322	0.	0.	0.	0	0	0	f
Mn(+2aq)	Cl(-aq)							
β(1)	1.5146	0.	0.	0.	0	0	2	f
Mn(+2aq)	Cl(-aq)							
C(ϕ)	-0.0227	0.	0.	0.	0	0	0	f
Mn(+2aq)	SO4(-2aq)							
β(0)	0.2130	0.	0.	0.	0	0	0	f
Mn(+2aq)	SO4(-2aq)							
β(1)	2.9380	0.	0.	0.	0	0	1.4	f
Mn(+2aq)	SO4(-2aq)							
C(ϕ)	0.0155	0.	0.	0.	0	0	0	f
Mn(+2aq)	SO4(-2aq)							
β(2)	-41.9100	0.	0.	0.	0	0	12	f
Na(+aq)	Al(OH)4(-aq)							
β(0)	-647.0273	15569.21	117.9626	-0.296671	0.00012605	290.032804	0	o,p
Na(+aq)	Al(OH)4(-aq)							
β(1)	2978.5015	-73326.1	-540.2536	1.322168	-0.000544	-1220.411	2	o,p
Na(+aq)	Al(OH)4(-aq)							
C(ϕ)	324.8952	-7784.98	-59.2547	0.149111	-6.3351E-05	-145.66092	0	o,p
Na(+aq)	Cl(-aq)							
β(0)	38.3261	-1080.87	-6.7522	0.014557	-5.5652E-06	-9.0812334	0	f
Na(+aq)	Cl(-aq)							
β(1)	79.6136	-1949.93	-14.4138	0.035231	-1.3237E-05	-44.320823	2	f
Na(+aq)	Cl(-aq)							
C(ϕ)	-6.1130	162.93	1.0958	-0.002577	1.0428E-06	3.62065527	0	f
Na(+aq)	CO3(-2aq)							
β(0)	46.1224	-2516.71	-6.5134	-0.007476	1.2146E-05	54714.9693	0	q,r,s #
Na(+aq)	CO3(-2aq)							
β(1)	5.8288	6801.35	-3.7068	0.019316	-3.7083E-06	-1017024	2	q,r,s #
Na(+aq)	CO3(-2aq)							
C(ϕ)	1.1205	-239.67	0.0309	-0.003316	3.0106E-06	20751.8813	0	q,r,s #
Na(+aq)	HCO3(-aq)							
β(0)	-37.2622	682.89	6.8996	-0.01446	0	0	0	s
Na(+aq)	HCO3(-aq)							
β(1)	-61.4627	1129.39	11.4109	-0.02447	0	0	2	s

type	a	b	c	d	e	f	α	ref
Na(+aq)	HCO3(-aq)							
C(ϕ)	0.0000	0.	0.	0.	0	0	0	s
Na(+aq)	HSO4(-aq)							
β(0)	0.0312	0.	0.	0.000284	-4.7599E-07	0	0	c
Na(+aq)	HSO4(-aq)							
β(1)	226.7599	-4135.64	-43.8117	0.148045	-7.9873E-05	-88.26976	2	c
Na(+aq)	HSO4(-aq)							
C(ϕ)	-0.0067	0.	0.	0.000007	0	0	0	c
Na(+aq)	OH(-aq)							
β(0)	168.1500	-4353.01	-30.0747	0.067359	-2.4673E-05	0	0	b
type	a	b	c	d	e	f	ω	ref
Na(+aq)	OH(-aq)							
β(1)	462.7600	-10292.1	-85.9397	0.238996	-0.00010793	0	2	b
Na(+aq)	OH(-aq)							
C(ϕ)	-11.9195	313.37	2.1328	-0.004831	1.8088E-06	6.19904	0	b
Na(+aq)	SO4(-2aq)							
β(0)	1.3104	215.52	0.0301	-0.005991	6.0014E-06	-86177.664	0	m
Na(+aq)	SO4(-2aq)							
β(1)	1.9604	1821.92	-0.0108	-0.01749	2.4768E-05	-377168.37	1.4	m
Na(+aq)	SO4(-2aq)							
C(ϕ)	-0.0121	-89.86	0.0033	0.000531	-7.2823E-07	18913.6192	0	m
H(+aq)	K(+aq)							
θ	0.0050	0.	0.	0.	0	0	0	f
H(+aq)	Mg(+2aq)							
θ	0.1000	0.	0.	0.	0	0	0	g
H(+aq)	Mn(+2aq)							
θ	0.0899	0.	0.	0.	0	0	0	t
H(+aq)	Na(+aq)							
θ	0.0360	0.	0.	0.	0	0	0	t
OH(-aq)	SO4(-2aq)							
θ	-0.0130	0.	0.	0.	0	0	0	g
Al(+3aq)	H(+aq)							
θ	0.1791	0.	0.	0.	0	0	0	d
Al(+3aq)	K(+aq)							
θ	-1.2691	0.	0.	0.	0	0	0	d
Al(+3aq)	Na(+aq)							
θ	0.1323	0.	0.	0.	0	0	0	d
Al(OH)4(-aq)	OH(-aq)							
θ	0.0140	0.	0.	0.	0	0	0	p
Ca(+2aq)	H(+aq)							
θ	0.0920	0.	0.	0.	0	0	0	g
Ca(+2aq)	K(+aq)							
θ	0.5752	-171.48	0.	0.	0	0	0	**
Ca(+2aq)	Mg(+2aq)							
θ	0.0070	0.	0.	0.	0	0	0	g
Ca(+2aq)	Na(+aq)							
θ	0.0962	0.	0.	0.	0	0	0	**
Cl(-aq)	CO3(-2aq)							
θ	-0.0200	0.	0.	0.	0	0	0	g

type	a	b	c	d	e	f	α	ref
Cl(-aq)	HCO3(-aq)							
θ	0.0359	0.	0.	0.	0	0	0	q
Cl(-aq)	HSO4(-aq)							
θ	-0.0060	0.	0.	0.	0	0	0	g
Cl(-aq)	OH(-aq)							
θ	-0.0500	0.	0.	0.	0	0	0	q
Cl(-aq)	SO4(-2aq)							
θ	0.0297	0.	0.	0.	0	0	0	**
CO3(-2aq)	HCO3(-aq)							
θ	-0.0400	0.	0.	0.	0	0	0	g

type	a	b	c	d	e	f	ω	ref
CO3(-2aq)	OH(-aq)							
θ	0.1000	0.	0.	0.	0	0	0	g
CO3(-2aq)	SO4(-2aq)							
θ	0.0200	0.	0.	0.	0	0	0	g
HCO3(-aq)	SO4(-2aq)							
θ	0.0100	0.	0.	0.	0	0	0	g
HSO4(-aq)	SO4(-2aq)							
θ	-228.3010	4126.9	43.7192	-0.135999	6.5139E-05	88.0832821	0	c
K(+aq)	Mg(+2aq)							
θ	0.0000	0.	0.	0.	0	0	0	b
K(+aq)	Na(+aq)							
θ	-0.0120	0.	0.	0.	0	0	0	b
Mg(+2aq)	Na(+aq)							
θ	0.3894	0.	0.	-0.00089	0	0	0	u
Mn(+2aq)	Na(+aq)							
θ	0.0907	0.	0.	0.	0	0	0	t
H(+aq)	K(+aq)	Cl(-aq)						
ψ	-0.0070	0.	0.	0.	0	0	1	b
H(+aq)	K(+aq)	HSO4(-aq)						
ψ	-0.0265	0.	0.	0.	0	0	1	g
H(+aq)	K(+aq)	SO4(-2aq)						
ψ	0.1970	0.	0.	0.	0	0	1	g
H(+aq)	Mg(+2aq)	Cl(-aq)						
ψ	-0.0006	0.	0.	0.	0	0	1	t
H(+aq)	Mn(+2aq)	Cl(-aq)						
ψ	-0.0092	0.	0.	0.	0	0	1	t
H(+aq)	Na(+aq)	Cl(-aq)						
ψ	-0.0040	0.	0.	0.	0	0	1	b
H(+aq)	Na(+aq)	HSO4(-aq)						
ψ	-0.0129	0.	0.	0.	0	0	1	g
OH(-aq)	SO4(-2aq)	K(+aq)						
ψ	-0.0500	0.	0.	0.	0	0	1	g
OH(-aq)	SO4(-2aq)	Na(+aq)						
ψ	-0.0090	0.	0.	0.	0	0	1	g
Al(+3aq)	Ca(+2aq)	SO4(-2aq)						
ψ	0.0300	0.	0.	0.	0	0	1	e
Al(+3aq)	Cu(+2aq)	SO4(-2aq)						
ψ	0.0350	0.	0.	0.	0	0	1	e

type	a	b	c	d	e	f	α	ref
Al(+3aq)	H(+aq)	Cl(-aq)						
ψ	-1.2691	183.33	0.	0.002172	0	0	1	d
Al(+3aq)	K(+aq)	Cl(-aq)						
ψ	29.8247	-667.12	-5.4357	0.010954	0	0	1	d
Al(+3aq)	Mg(+2aq)	SO4(-2aq)						
ψ	0.0300	0.	0.	0.	0	0	1	e
Al(+3aq)	Na(+aq)	Cl(-aq)						
ψ	-1.1059	157.98	0.	0.001714	0	0	1	d
Al(OH)4(-aq)	OH(-aq)	K(+aq)						
ψ	-0.0048	0.	0.	0.	0	0	1	p
type	a	b	c	d	e	f	ω	ref
Al(OH)4(-aq)	OH(-aq)	Na(+aq)						
ψ	-0.0048	0.	0.	0.	0	0	1	p
Ca(+2aq)	H(+aq)	Cl(-aq)						
ψ	-0.0150	0.	0.	0.	0	0	1	g
Ca(+2aq)	K(+aq)	Cl(-aq)						
ψ	0.0476	-27.08	0.	0.	0	0	1	h
Ca(+2aq)	K(+aq)	SO4(-2aq)						
ψ	0.0000	0.	0.	0.	0	0	1	b
Ca(+2aq)	Mg(+2aq)	Cl(-aq)						
ψ	-0.0120	0.	0.	0.	0	0	1	b
Ca(+2aq)	Mg(+2aq)	SO4(-2aq)						
ψ	0.0500	0.	0.	0.	0	0	1	b
Ca(+2aq)	Na(+aq)	Cl(-aq)						
ψ	-0.0030	0.	0.	0.	0	0	1	h
Ca(+2aq)	Na(+aq)	SO4(-2aq)						
ψ	0.0267	-23.45	0.	0.	0	0	1	**
Cl(-aq)	CO3(-2aq)	K(+aq)						
ψ	0.0040	0.	0.	0.	0	0	1	g
Cl(-aq)	CO3(-2aq)	Na(+aq)						
ψ	0.0085	0.	0.	0.	0	0	1	g
Cl(-aq)	HCO3(-aq)	Mg(+2aq)						
ψ	-0.0960	0.	0.	0.	0	0	1	g
Cl(-aq)	HCO3(-aq)	Na(+aq)						
ψ	-0.0143	0.	0.	0.	0	0	1	q
Cl(-aq)	HSO4(-aq)	H(+aq)						
ψ	0.0130	0.	0.	0.	0	0	1	g
Cl(-aq)	HSO4(-aq)	Na(+aq)						
ψ	-0.0060	0.	0.	0.	0	0	1	g
Cl(-aq)	OH(-aq)	Ca(+2aq)						
ψ	-0.0250	0.	0.	0.	0	0	1	g
Cl(-aq)	OH(-aq)	K(+aq)						
ψ	-0.0060	0.	0.	0.	0	0	1	g
Cl(-aq)	OH(-aq)	Na(+aq)						
ψ	-0.0060	0.	0.	0.	0	0	1	q
Cl(-aq)	SO4(-2aq)	Ca(+2aq)						
ψ	-0.0180	0.	0.	0.	0	0	1	h
Cl(-aq)	SO4(-2aq)	Cu(+2aq)						
ψ	0.0234	0.	0.	0.	0	0	1	t

type	a	b	c	d	e	f	α	ref
Cl(-aq)	SO4(-2aq)	K(+aq)						
ψ	0.0000	0.	0.	0.	0	0	1	b
Cl(-aq)	SO4(-2aq)	Mg(+2aq)						
ψ	-0.0040	0.	0.	0.	0	0	1	b
Cl(-aq)	SO4(-2aq)	Na(+aq)						
ψ	-0.0049	0.	0.	0.	0	0	1	h
CO3(-2aq)	HCO3(-aq)	K(+aq)						
ψ	0.0120	0.	0.	0.	0	0	1	g
CO3(-2aq)	HCO3(-aq)	Na(+aq)						
ψ	0.0020	0.	0.	0.	0	0	1	g
type	a	b	c	d	e	f	ω	ref
CO3(-2aq)	OH(-aq)	K(+aq)						
ψ	-0.0100	0.	0.	0.	0	0	1	g
CO3(-2aq)	OH(-aq)	Na(+aq)						
ψ	-0.0170	0.	0.	0.	0	0	1	g
CO3(-2aq)	SO4(-2aq)	K(+aq)						
ψ	-0.0090	0.	0.	0.	0	0	1	g
CO3(-2aq)	SO4(-2aq)	Na(+aq)						
ψ	-0.0050	0.	0.	0.	0	0	1	g
Cu(+2aq)	Na(+aq)	Cl(-aq)						
ψ	-0.0129	0.	0.	0.	0	0	1	t
Cu(+2aq)	Na(+aq)	SO4(-2aq)						
ψ	-0.0235	0.	0.	0.	0	0	1	t
HCO3(-aq)	SO4(-2aq)	Mg(+2aq)						
ψ	-0.1610	0.	0.	0.	0	0	1	g
HCO3(-aq)	SO4(-2aq)	Na(+aq)						
ψ	-0.0050	0.	0.	0.	0	0	1	g
HSO4(-aq)	SO4(-2aq)	K(+aq)						
ψ	-0.0677	0.	0.	0.	0	0	1	g
HSO4(-aq)	SO4(-2aq)	Mg(+2aq)						
ψ	-0.0425	0.	0.	0.	0	0	1	g
HSO4(-aq)	SO4(-2aq)	Na(+aq)						
ψ	19.1644	-346.41	-3.6698	0.011425	-5.4555E-06	-7.393723	1	c
K(+aq)	Mg(+2aq)	Cl(-aq)						
ψ	-0.0220	0.	0.	0.	0	0	1	b
K(+aq)	Mg(+2aq)	SO4(-2aq)						
ψ	-0.0480	0.	0.	0.	0	0	1	b
K(+aq)	Na(+aq)	Cl(-aq)						
ψ	-0.0018	0.	0.	0.	0	0	1	b
K(+aq)	Na(+aq)	CO3(-2aq)						
ψ	0.0048	0.	0.	0.	0	0	1	g
K(+aq)	Na(+aq)	HCO3(-aq)						
ψ	-0.0030	0.	0.	0.	0	0	1	g
K(+aq)	Na(+aq)	SO4(-2aq)						
ψ	-0.0100	0.	0.	0.	0	0	1	b
Mg(+2aq)	MgOH(+aq)	Cl(-aq)						
ψ	0.0280	0.	0.	0.	0	0	1	g
Mg(+2aq)	Na(+aq)	Cl(-aq)						
ψ	-0.0290	0.	0.	-0.00001	0	0	1	u

type	a	b	c	d	e	f	α	ref
Mg(+2aq)	Na(+aq)	SO4(-2aq)						
ψ	-0.0150	0.	0.	0.	0	0	1	b
Mn(+2aq)	Na(+aq)	Cl(-aq)						
ψ	-0.0190	0.	0.	0.	0	0	1	t
CO2(aq)	Ca(+2aq)							
λ	0.0510	0.	0.	0.	0	0	0	g
CO2(aq)	Cl(-aq)							
λ	-0.0050	0.	0.	0.	0	0	0	g
CO2(aq)	H(+aq)							
λ	0.0000	0.	0.	0.	0	0	0	g
type	a	b	c	d	e	f	ω	ref
CO2(aq)	HSO4(-aq)							
λ	-0.0030	0.	0.	0.	0	0	0	g
CO2(aq)	K(+aq)							
λ	0.0510	0.	0.	0.	0	0	0	g
CO2(aq)	Mg(+2aq)							
λ	0.1830	0.	0.	0.	0	0	0	g
CO2(aq)	Na(+aq)							
λ	0.1000	0.	0.	0.	0	0	0	g
CO2(aq)	SO4(-2aq)							
λ	0.0970	0.	0.	0.	0	0	0	g

* Calculated based on equilibrium coefficient value and data values for other species

** Fitted in this study

Fitted as a linear combination of the listed values

a) Reardon (1990); b) Pitzer (1986); c) Holmes and Mesmer (1994); d) Christov et al. (2007); e) Reardon (1988); f) Pitzer (1995); g) Harvie et al. (1984); h) Greenberg and Møller (1989); i) Silvester and Pitzer (1978); j) Hämäläinen et al. (1991); k) Holmes and Mesmer (1996); l) Li and Pitzer (1996); m) Holmes and Mesmer (1986); n) Phutela and Pitzer (1986); o) Caiani et al. (1989); p) Wesolowski (1992); q) Peiper and Pitzer (1982); r) Königsberger (2001): s) Carter et al. (2014); t) Kim and Frederick (1988); u) Hernández-Luis et al. (1997)

Appendix C: The data for non-stoichiometric burkeite phase

Table C.1. Data for non-stoichiometric burkeite phase.

	$\Delta_f H^\circ$	S°	$T_{\max}$	a_1	a_2	a_3	a_4	ref
Na2SO4	-1387599	150.16	600	99.10	0.138260096	0.00	-901906.7659	a
Na2CO3	-1129261	134.48	342	666.52	-1.956414919	0.00	10773139.47	**
			386	666.52	-1.956416818	0.00	10773129.46	
			429	666.52	-1.956419013	0.00	10773108.09	

** Fitted in this study

a) Outokumpu Research (1999)

The phase was modelled as a regular solution with an interaction energy $G^{ex} = -8300(J \cdot mol^{-1}) \cdot x_1 x_2$

Appendix D: A kinetically constrained $CaCO_3$ precipitation model

As an example of a kinetically controlled precipitation system a model for $CaCO_3$ formation in aqueous lime milk solution was constructed. The experimental system consists of a tubular reactor, to which CO_2-gas is first injected at ca 3 bar pressure, followed by the feed of lime milk as aqueous $Ca(OH)_2$ slurry, schematically illustrated in Figure D1 (left).

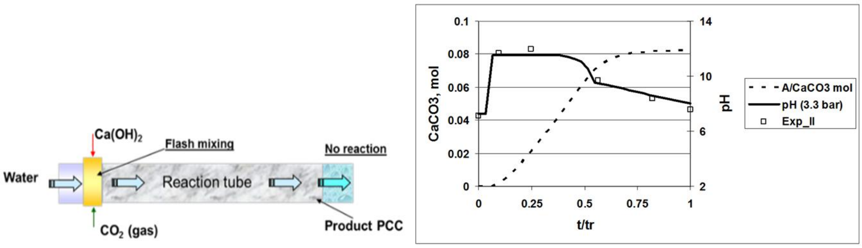

Figure D1. The schematic of in-line PCC reactor (left). Measured pH-values with model curves for pH and PCC formation in terms of dimensionless reaction time (right).

With a close to stoichiometric feed of CO_2 and $Ca(OH)_2$ the reaction is instantaneous producing precipitated calcium carbonate (PCC) and its progress can be followed in the reactor e.g. by direct pH-measurement, with pH transmitters situated in subsequent axial positions (experimental points shown in Figure D1 right). Assuming ideal mixing and plug flow a 1-dimensional model for the system was constructed and validated against the measured pH-values, which will vary from the original near neutral to pH ~ 12 at maximum and finally close to neutral again when all reactants have been consumed. The reaction sequence can be assumed as follows:

$$Ca(OH)_2 \leftrightarrow Ca^{2+}(aq) + 2OH^-(aq) \qquad \text{(DA)}$$

$$CO_2(g) \rightarrow CO_2(aq) \qquad \text{(DB)}$$

$$CO_2(aq) + 2OH^-(aq) \leftrightarrow CO_3^{2-}(aq) + H_2O \qquad \text{(DC)}$$

$$Ca^{2+}(aq) + CO_3^{2-}(aq) \leftrightarrow CaCO3(aq) \qquad \text{(DD)}$$

$$CaCO3(aq) \rightarrow CaCO_3(s) \qquad \text{(DE)}$$

It is a viable assumption that the reactions which involve phase change appear as rate determining, while the solvent-solute reactions often can be assumed to be in mutual (local) equilibrium. When reactions (DA) and (DE) are assumed to be the rate determining steps (denoted below as 1 and 2), it is necessary to define their rate equations which then are applicable in the respective kinetically constrained multiphase model. The formal rate equations are

$$r_1 = k_1 a\big(CO_2(g)\big)\left[1 - \frac{Q_1}{K_1}\right] = k_1 a\big(CO_2(g)\big)\left[1 - \frac{A_1/RT}{K_1}\right] \tag{D1}$$

$$r_2 = k_2 a(CaCO_3(aq)\left[1 - \frac{Q_1}{K_1}\right] = k_2 a(CaCO_3(aq)\left[1 - \frac{A_2/RT}{K_1}\right] \tag{D2}$$

with the two adjustable rate parameters k_1 and k_2, while all other terms on the right hand side can be received from the thermodynamic model. Then $a(\mathrm{CO_2}(g))$ and $a(\mathrm{CaCO_3}(aq))$ denote the activities of gaseous $\mathrm{CO_2}$ and aqueous $\mathrm{CaCO_3}$ complex, respectively and Q_i and K_i are the reaction quotients and equilibrium constants for reactions (b) and (e) as defined by their non-equilibrium and equilibrium activities in the system. The expressions on the right hand side are further written in terms of the affinities (A_1 and A_2) for the two reactions, respectively. As the affinities of the reactions can be received from the activities of the reactants and products by definition, the advantage of the thermodynamic method is then that the affinity of the non-equilibrium reactions can be followed during the course of the overall reaction path.

The constraining of these two reactions in the multicomponent Gibbs'ian model system is described in the stoichiometric **C**$^\mathrm{T}$ matrix below:

$$\begin{array}{l} \\ N_2(g) \\ O_2(g) \\ CO_2(g) \\ H_2O(g) \\ H_2O \\ H^+ \\ OH^- \\ CO_2 \\ HCO_3^- \\ CO_3^{2-} \\ Ca^{2+} \\ CaCO_3^{\circ} \\ Ca(OH)_2 \\ CaCO_3 \\ R(+1) \\ R(-1) \\ R(+2) \\ R(-2) \end{array} \begin{array}{cccccccc} N & O & C & H & Ca & EA & CO_2^* & CaCO_3^* \\ \hline 2 & 0 & 0 & 0 & 0 & 0 & 0 & 0 \\ 0 & 2 & 0 & 0 & 0 & 0 & 0 & 0 \\ 0 & 2 & 1 & 0 & 0 & 0 & 1 & 0 \\ 0 & 1 & 0 & 2 & 0 & 0 & 0 & 0 \\ 0 & 1 & 0 & 2 & 0 & 0 & 0 & 0 \\ 0 & 0 & 0 & 1 & 0 & -1 & 0 & 0 \\ 0 & 1 & 0 & 1 & 0 & 1 & 0 & 0 \\ 0 & 2 & 1 & 0 & 0 & 0 & 0 & 0 \\ 0 & 3 & 1 & 1 & 0 & 1 & 0 & 0 \\ 0 & 3 & 1 & 0 & 0 & 2 & 0 & 0 \\ 0 & 0 & 0 & 0 & 1 & -2 & 0 & 0 \\ 0 & 3 & 1 & 0 & 1 & 0 & 0 & 0 \\ 0 & 2 & 0 & 2 & 1 & 0 & 1 & 0 \\ 0 & 0 & 0 & 0 & 0 & 0 & -1 & 0 \\ 0 & 0 & 0 & 0 & 0 & 0 & 0 & 1 \\ 0 & 0 & 0 & 0 & 0 & 0 & 0 & -1 \end{array} = \mathbf{C}^\mathbf{T} \tag{D3}$$

Immaterial constraints have been set for the CO_2 in the gas phase as reactant and for the $CaCO_3$ precipitate as a product. The reaction advancements are then controlled by calculating incremental input (in molar units) for both the reactant and product and introducing these increments sequentially to the Gibbs energy minimisation calculation. The molar increments are given as $\Delta N[R(-1)] = r_1 \cdot \Delta t$ and as $\Delta N[R(+2)] = r_2 \cdot \Delta t$, respectively. The cumulative amount of consumed reactant and formed product is then straightforward to calculate from each increment.

It may be noted that the reaction rates and thus the increments themselves are dependent on the changing activities as function of time. As both constituents have been included in the thermodynamic system also as aqueous neutrals the activities of CO_2(*g*) and $CaCO_3$(*aq*) as well as the respective reaction quotients (Q_1 and Q_2) are calculated for each sequential step and thus the discretised model can be based on their subsequent values and the equilibrium constants (K_1 and K_2). All other reactions between the constituents defined in matrix (D3) are assumed to be in mutual equilibrium) in the multiphase model. These fast reactions then necessarily include the reactions between various solute species, which represent the key factors in the key observables, which are the axial pH change and formation of solid $CaCO_3$ in the reactor. The curves in figure X (right) have been received by fitting the two rate parameters (k_1 and k_2) to the multicomponent model by using the measured points shown. The 2-reaction plug flow model indicates both the pH 'hump' and $CaCO_3$ conversion rate in fair agreement with experiments. Then, these reaction rates can be used for further predictive studies with different reactant feed rates and reactor dimensions (Koukkari et al., 2011).

From Figure D2, it is evident that the overall precipitation reaction is all but finished at t/t_r ~1, i.e. when the allowed length of the reactor tube has been fully utilised. Yet, the as the pH has not stabilised fully, some reaction may further continue outside the reactor zone, which may cause undesired fouling of the downstream process equipment while operated in-line (http://www.wetend.com/admin/media/Newsletter_2013.pdfn). To prevent such malfunction, an additional feed of antiscalant can be used, as predicted by the affinity curve of Figure D2.

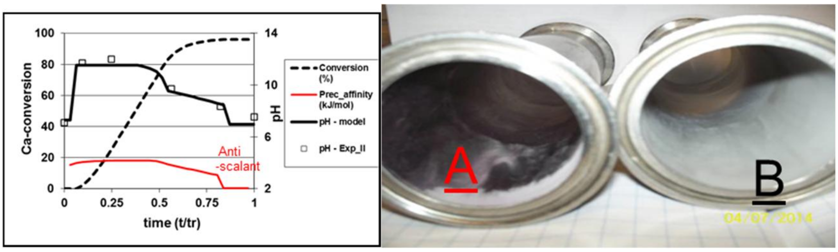

Figure D2. Calculated effect of added anti-scalant on precipitation conversion and pH-curve with equal inputs as in figure X (left). Results from a pilot experiment with and without anti-scalant (A and B, respectively, right[2]).

Assuming ideal mixing of the chemical used as an anti-scalant and added into the end section of the reactor tube (levelled range of the conversion curve) a set of

---

[2] Courtesy of WetEnd Technologies, http://www.wetend.com

calculations were made to support experimentation. A typical result is shown in Figure D2 (left). In the calculation an abrupt decrease of pH to a stable value of ca. 6.8 is received while the affinity of the precipitation reaction drops to zero (reaction rate $r_2 = 0$), due to the injection of the anti-scalant. The model prediction was then used to design pilot tests. The anti-scalant composition was added in the final section of the reactor tube with its feed positioned to the 'flat' area of the conversion curve with efficient flash mixing. The sampling tubes were positioned just outside the allowed reaction zone to follow formation of undesired precipitate. While the solvent-solute reactions of the anti-scaled system are very fast and allow the levelling of pH, they also lead to cessation of the precipitation reaction, which is also confirmed with the affinity calculation.

Series title and number

VTT Technology 321

Title	**Industrial and mine water chemistry** Advanced aqueous database for modelling industrial processes
Author(s)	Risto Pajarre, Pertti Koukkari & Petteri Kangas
Abstract	Within this report, the basic theory of modelling concentrated aqueous solutions based on thermodynamic approach is given. For complex industrial solutions, it is important to take into account the non-ideality of the solutions to gain reliable results with engineering calculations. The well-known Pitzer formalism for describing the activity coefficients in the concentrated aqueous solutions has been used with an extended database of Pitzer interaction parameters ranging from 25°C to 95°C. The database allows for reliable predictive simulations of the major metal cations (in particular Na , K , Ca^2 , Mg^2 ; Al^3 ,Fe^3 , Cu^2 , Mn^2) that most commonly occur in industrial sulphate, carbonate and chloride solutions. The database can also include solubility data of complex salts and mineral compounds from selected inter-national geochemical databases. The data is used in multicomponent reactor modules, which are connected to modular process modelling software typically used in chemical and process engineering. The application of data is given for selected examples, including • The leaching process for alkaline (soda) ash • Neutralisation treatment of acidic mine water (AMD) • Simulation of a mining water sulfate treatment cycle • Recovery of rare earth compounds from acidic leachate Alternative dosage for neutralisation, pH control and solubility controls as well as optional connections in a multi-stage hydrometallurgical plant or within a set of water treatment units can be simulated with fair accuracy. The models provide a fast and inexpensive tool for both troubleshooting and problem solving as well as for developing new economical and environmentally benign approaches for industrial and mine water management.
ISBN, ISSN, URN	ISBN 978-951-38-8622-6 (Soft back ed.) ISBN 978-951-38-8620-2 (URL: http://www.vttresearch.com/impact/publications) ISSN-L 2242-1211 ISSN 2242-1211 (Print) ISSN 2242-122X (Online) http://urn.fi/URN:ISBN:978-951-38-8620-2
Date	January 2018
Language	English
Pages	85 p. + app. 21 p.
Name of the project	Multirec
Commissioned by	
Keywords	industrial and mine waters, sulphate control, solubility, process simulation
Publisher	VTT Technical Research Centre of Finland Ltd P.O. Box 1000, FI-02044 VTT, Finland, Tel. 020 722 111

VTT TECHNOLOGY 321 Industrial and mine water chemistry

Industrial and mine water chemistry

Advanced aqueous database for modelling industrial processes

Solubility data and titration curves provide the basic instruments for hydrometallurgical practice and industrial water management. As a rule, the data is interpreted in terms of solubilities of stoichiometric electrolytes as well as in the form of pH – Eh-dependent stability diagrams for stoichiometric compounds.

While such predictions provide a practical tool for experimental and laboratory work, their accuracy is not good enough for such multicomponent solutions that one encounters in industrial practice. For complex industrial solutions appearing in a variety of pH ranges and in changing temperatures, it is important to take into account the non-ideality of the solutions to gain reliable results with engineering calculations. VTT has collected ionic interaction (activity) data for over 15 years. The database allows for reliable predictive simulations of the metal cations most commonly occurring in aqueous sulphate, carbonate and chloride systems, thus effectively serving industrial needs in mining and hydrometallurgy as well as in chemical and pulp-making processes.

The complex calculation is made easy in VTT's ChemSheet software, which can be used in Microsoft's Excel. The models then provide a fast and inexpensive tool for both troubleshooting and problem solving as well as for developing new economical and environmentally benign approaches for industrial and mine water management.

ISBN 978-951-38-8622-6 (Soft back ed.)
ISBN 978-951-38-8621-9 (URL: http://www.vttresearch.com/impact/publications)
ISSN-L 2242-1211
ISSN 2242-1211 (Print)
ISSN 2242-122X (Online)
http://urn.fi/URN:ISBN:978-951-38-8621-9